

Summer 2011

Modeling and control for heave dynamics of a flexible wing micro aerial vehicle distributed parameter system

Lisa M. Kuhn
Louisiana Tech University

Follow this and additional works at: <https://digitalcommons.latech.edu/dissertations>

 Part of the [Aerospace Engineering Commons](#), [Applied Mathematics Commons](#), and the [Mathematics Commons](#)

Recommended Citation

Kuhn, Lisa M., "" (2011). *Dissertation*. 355.
<https://digitalcommons.latech.edu/dissertations/355>

This Dissertation is brought to you for free and open access by the Graduate School at Louisiana Tech Digital Commons. It has been accepted for inclusion in Doctoral Dissertations by an authorized administrator of Louisiana Tech Digital Commons. For more information, please contact digitalcommons@latech.edu.

**MODELING AND CONTROL FOR HEAVE DYNAMICS
OF A FLEXIBLE WING MICRO AERIAL VEHICLE
DISTRIBUTED PARAMETER SYSTEM**

by

Lisa M. Kuhn, B.S., M.S.

A Dissertation Presented in Partial Fulfillment
of the Requirements for the Degree
Doctor of Philosophy

COLLEGE OF ENGINEERING AND SCIENCE
LOUISIANA TECH UNIVERSITY

August 2011

UMI Number: 3484620

All rights reserved

INFORMATION TO ALL USERS

The quality of this reproduction is dependent upon the quality of the copy submitted.

In the unlikely event that the author did not send a complete manuscript and there are missing pages, these will be noted. Also, if material had to be removed, a note will indicate the deletion.



UMI 3484620

Copyright 2011 by ProQuest LLC.

All rights reserved. This edition of the work is protected against unauthorized copying under Title 17, United States Code.



ProQuest LLC
789 East Eisenhower Parkway
P.O. Box 1346
Ann Arbor, MI 48106-1346

LOUISIANA TECH UNIVERSITY

THE GRADUATE SCHOOL

7/11/11
Date

We hereby recommend that the dissertation prepared under our supervision
by Lisa M. Kuhn

entitled Modeling and Control for Heave Dynamics of a Flexible Wing Micro Aerial
Vehicle Distributed Parameter System

be accepted in partial fulfillment of the requirements for the Degree of
Doctor of Philosophy

Kate A. Evans
Supervisor of Dissertation Research
W. Z. Dai
Head of Department
Computational Analysis and Modeling
Department

Recommendation concurred in:

Animesh Chakraborty (electronically present) / Kae

W. Z. Dai

Paul Whigg

Samuel D. Fox

Advisory Committee

Approved:

Paul E. Turner
Director of Graduate Studies

Approved:

Animesh Chakraborty
Dean of the Graduate School

Stanley
Dean of the College

ABSTRACT

In recent years, much research has been motivated by the idea of biologically-inspired flight. It is a conjecture of the United States Air Force that incorporating characteristics of biological flight into air vehicles will significantly improve the maneuverability and performance of modern aircraft. Although there are studies which involve the aerodynamics, structural dynamics, modeling, and control of flexible wing micro aerial vehicles (MAVs), issues of control and vehicular modeling as a whole are largely unexplored. Modeling with such dynamics lends itself to systems of partial differential equations (PDEs) with nonlinearities, and limited control theory is available for such systems.

In this work, a multiple component structure consisting of two Euler-Bernoulli beams connected to a rigid mass is used to model the heave dynamics of an aeroelastic wing MAV, which is acted upon by a nonlinear aerodynamic lift force. We seek to employ tools from distributed parameter modeling and linear control theory in an effort to achieve agile flight potential of flexible, morphable wing MAV airframes. Theoretical analysis of the model is conducted, which includes generating solutions to the eigenvalue problem for the system and determining well-posedness and the attainment of a C_0 -semigroup for the linearly approximated model. In order to test the model's ability to track to a desired state and to gain insight into optimal morphing

trajectories, two control objectives are employed on the model: target state tracking and morphing trajectory over time.

APPROVAL FOR SCHOLARLY DISSEMINATION

The author grants to the Prescott Memorial Library of Louisiana Tech University the right to reproduce, by appropriate methods, upon request, any or all portions of this Thesis. It is understood that "proper request" consists of the agreement, on the part of the requesting party, that said reproduction is for his personal use and that subsequent reproduction will not occur without written approval of the author of this Thesis. Further, any portions of the Thesis used in books, papers, and other works must be appropriately referenced to this Thesis.

Finally, the author of this Thesis reserves the right to publish freely, in the literature, at any time, any or all portions of this Thesis.

Author Livia M. Keuhn

Date August 4, 2011

DEDICATION

This dissertation is dedicated to Clay James, who has always encouraged me and stood by me.

TABLE OF CONTENTS

| | |
|---|------|
| ABSTRACT | ii |
| DEDICATION..... | v |
| LIST OF TABLES..... | viii |
| LIST OF FIGURES..... | ix |
| ACKNOWLEDGMENTS | xi |
| CHAPTER 1 INTRODUCTION..... | 1 |
| CHAPTER 2 BACKGROUND INFORMATION..... | 4 |
| 2.1 Linear Quadratic Regulator (LQR) Tracking..... | 5 |
| 2.2 Linear Quadratic Gaussian (LQG) Tracking..... | 6 |
| CHAPTER 3 FLEXIBLE WING AIRCRAFT MODEL..... | 9 |
| 3.1 Derivation of the Euler-Bernoulli Beam..... | 10 |
| 3.2 Beam-Mass-Beam (BMB) Model | 12 |
| 3.2.1 Model Description | 12 |
| 3.2.2 Linear Approximation of the BMB Model | 15 |
| 3.3 Beam-Mass-Beam Model with Piezoceramic Patch Actuators (BMB-PZT Model) | 17 |
| 3.3.1 Model Description | 17 |
| 3.3.2 Linear Approximation of the BMB-PZT Model..... | 20 |
| CHAPTER 4 THEORETICAL ANALYSIS..... | 21 |

| | | |
|---|---|----|
| 4.1 | Framework | 21 |
| 4.1.1 | Framework for Well-Posedness | 22 |
| 4.1.2 | Semigroup Discussion | 26 |
| 4.1.3 | Additional Theorems | 27 |
| 4.2 | Eigenvalue Analysis..... | 29 |
| 4.3 | Well-Posedness of the BMB System..... | 30 |
| CHAPTER 5 NUMERICAL RESULTS FOR THE BMB SYSTEM | | 51 |
| 5.1 | Weak Formulation of the BMB System | 51 |
| 5.1.1 | Variational Form | 51 |
| 5.1.2 | Discretization..... | 53 |
| 5.2 | Target Tracking Results..... | 58 |
| 5.3 | Wing Morphing Trajectory Results | 65 |
| CHAPTER 6 NUMERICAL RESULTS FOR THE BMB-PZT MODEL | | 70 |
| 6.1 | Weak Formulation of the BMB-PZT System..... | 70 |
| 6.2 | Discretization | 76 |
| 6.3 | Simulation..... | 80 |
| CHAPTER 7 CONCLUSIONS..... | | 84 |
| BIBLIOGRAPHY..... | | 87 |
| VITA..... | | 92 |

LIST OF TABLES

| | | |
|-----------|---------------------------------|----|
| Table 3.1 | Boundary Conditions..... | 15 |
| Table 5.1 | BMB System Parameters | 61 |
| Table 6.1 | BMB-PZT System Parameters | 81 |

LIST OF FIGURES

| | |
|---|----|
| Figure 1.1: Bat (left), Morphing gull wings (right)..... | 2 |
| Figure 3.1: Beam..... | 10 |
| Figure 3.2: Beam Segment | 11 |
| Figure 3.3: MAV model system..... | 14 |
| Figure 3.4: MAV model system with piezoceramic patches. | 18 |
| Figure 5.1: Desired State Target: Position (left), Slope (right) | 60 |
| Figure 5.2: Uncontrolled System: Position (top left), Slope (top right), Velocity (bottom left), Angular Velocity, (bottom right)..... | 62 |
| Figure 5.3: LQR Controlled System: Position (top left), Slope (top right), Velocity (bottom left), Angular Velocity (bottom right) | 63 |
| Figure 5.4: LQG Controlled System: Position (top left), Slope (top right), Velocity (bottom left), Angular Velocity (bottom right) | 64 |
| Figure 5.5: Control Effort: LQG (left), LQR (right) | 65 |
| Figure 5.6: Target Trajectory: Position (top left), Slope (top right), Velocity (bottom left), Angular Velocity, (bottom right)..... | 66 |
| Figure 5.7: LQR Controlled Morphing Trajectory System: Position (top left), Slope (top right), Velocity (bottom left), Angular Velocity (bottom right)..... | 67 |
| Figure 5.8: LQG Controlled Morphing Trajectory System: Position (top left), Slope (top right), Velocity (bottom left), Angular Velocity (bottom right)..... | 68 |
| Figure 5.9: Control Effort. Morphing Trajectory: LQG (left), LQR (right) | 68 |

Figure 6.1: Uncontrolled BMB-PZT System: Position (top left), Slope (top right), Velocity (bottom left), Angular Velocity, (bottom right)82

ACKNOWLEDGMENTS

It is impossible to articulate the gratitude I feel towards my advisor, Dr. Katie Evans, for her endless patience, support, guidance, and for allowing me the opportunity to learn from her. Our research conversations and her advice have had a substantial impact on my professional life. Dr. Animesh Chakravarthy also played an integral role in this work, and I appreciate his willingness to share his expertise. I also want to give a special thank you to my other committee members - Dr. Travis Atkison, Dr. Weizhong Dai, Dr. Sumeet Dua, and Dr. Bernd Schröder - for their time and input.

The faculty members in the Program of Mathematics and Statistics have gone out of their way to provide assistance to me and have been a pleasure to work with. I also want to thank Dr. Bernd Schröder for giving advice and providing me with teaching opportunities. Additionally, I am very grateful for Dr. David Mills and the National Science Foundation's GK-12 program for helping to prepare me for a career in academia.

Thank you to my parents, family, and friends for your support. Scarlett Bracey, James Elliott, and numerous others have helped me survive the graduate school experience. Most importantly I want to thank my husband, Clay James, for his unconditional support and patience. Without him none of this would have been possible.

CHAPTER 1

INTRODUCTION

Throughout the past century considerable improvement has been made in the development of aircraft, but much work remains to be done for modern aircraft to be comparable to the airborne capabilities of nature. In recent years, much research has been motivated by the notion of biologically-inspired flight, including aerodynamics, structural dynamics, flight mechanics, and control. The Air Force Office of Scientific Research Multidisciplinary University Research Initiative (MURI) project led by Kenny Breuer of Brown University involves studies of the aerodynamics and structural dynamics of bats in free-flight. Further information about this project can be found in [27] and [25]. The MURI project led by Wei Shyy of the University of Michigan consists of similar studies of bird and insect flight, which is elaborated upon in [23] and [24]. These studies, along with numerous others (see, for example, [2] and [14]), have inspired the Air Force Research Laboratory Munitions Directorate (AFRL/RW) to explore aeroelastic wing micro aerial vehicles (MAVs) for both military and civilian utilization.

While there are projects which involve control studies of biological flight, it is our goal to examine vehicular modeling as a whole while simultaneously ensuring that the model may be exploited for control design. Traditional controllers designed

using methods applicable to fixed wing aircraft are unlikely to realize the agile flight potential of flexible wing MAV airframes.

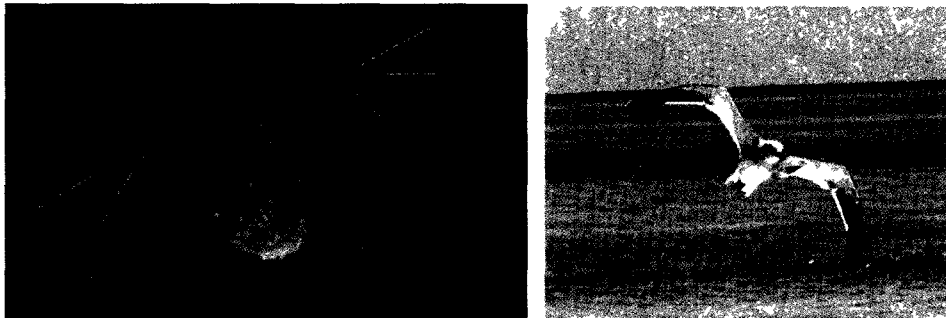


Figure 1.1: (Left) Bat flight is being studied as part of an Air Force Office of Scientific Research Multidisciplinary University Research Initiative project. Image credit: mime.oregonstate.edu/news/story/2103, (Right) Morphing gull wings.

In this dissertation we seek to provide an extension of the heave dynamics partial differential equation (PDE) model originally presented in [9], which consisted of two Euler-Bernoulli beams connected at a point mass. The modifications we make to this model consist of the inclusion of a finite mass, gravity, a nonlinear aerodynamic lift force, and realistic parameter values that reflect the material of the MAV system. We refer to this model as the beam-mass-beam (BMB) model.

The focus of this work is to apply tools from distributed parameter control theory in order to gain insight into exploiting wing flexibility for control design. We first begin by providing a theoretical analysis of the linearly approximated BMB model. This analysis includes examining the eigenvalue problem for this system and determining whether the model is well-posed and generates a C_0 -semigroup.

We then employ control design on the BMB system. Since limited theory is available for control of nonlinear PDE systems, we must obtain a linear approximation

of the system in order to design controllers. Two control mechanisms are analyzed here: target state tracking and morphing trajectory over time. Finally, we also present a MAV model with the presence of realistic controllers via piezoceramic patch actuators and point to future work involving this model. We refer to this model as the “BMB-PZT” model.

Chapter 2 contains background information of the control techniques considered in this dissertation. Chapter 3 provides a description of the two models. In Chapter 4 the framework for well-posedness is provided, along with a proof for well-posedness of the linearly approximated model and an extension to the model with piezoceramic patches. Numerical simulations of both systems, including controlled results for the BMB system can be found in Chapters 5 and 6. Finally, in Chapter 7 we conclude with observations and future work.

CHAPTER 2

BACKGROUND INFORMATION

Consider a time-invariant linear partial differential equation (PDE) system with dynamics given by

$$\dot{\xi}(t) = \mathcal{A}\xi(t) + \mathcal{B}u(t), \quad \xi(0) = \xi_0, \quad (2.1)$$

where the operator \mathcal{A} represents the dynamics of the system defined on $\mathbf{D}(\mathcal{A}) \subseteq X$ (with X a Hilbert space) that generates a C_0 -semigroup by assumption (see Chapter 4), \mathcal{B} describes how the control is applied to the system, and $u(t)$ is the control input, defined on a Hilbert space U , which is taken to be \mathbb{R}^m in this work.

Traditional linear quadratic control drives the state $\xi(t)$ to the zero state. For a tracking problem, the ideal state is not the zero state. Instead, the control objective is to steer $\xi(t)$ to some known, desired state $\tilde{\xi}(t)$. Two linear quadratic tracking approaches explored in this work are described below in an infinite dimensional setting, and the discussion presented here is summarized from [15]. It is important to note that theory is in place to guarantee convergence from a finite dimensional approximation to the infinite dimensional system, as stated in [17] and [16].

2.1 Linear Quadratic Regulator (LQR) Tracking

The aim of the Linear Quadratic Regulator (LQR) tracking problem is to minimize the cost function

$$V = \int_{t_0}^T (\langle x, \mathcal{Q}x \rangle_X + \langle u, Ru \rangle_U) dt, \quad (2.2)$$

where $\dot{x}(t) = \frac{d}{dt}x(t)$, $\mathcal{Q} : X \rightarrow X$ is a state weighting operator, taken to be $\mathcal{C}^*\mathcal{C}$ (see Equation (2.12)) and $R : U \rightarrow U$ is a control weighting operator taken to be of the form $R = \mathcal{I}$, with \mathcal{I} being the identity operator. Then for a chosen \mathcal{Q} and R , an optimal u is generated. The tracking problem under consideration is posed as a disturbance-rejection problem with the system dynamics given by

$$\dot{x}(t) = \mathcal{A}x(t) + \mathcal{B}u(t) + w(t), \quad x(0) = x_0, \quad (2.3)$$

where $x(t) = x(t, \cdot) = \xi(t, \cdot) - \tilde{\xi}(t, \cdot) \in X$ and $w(t)$ is represented by

$$w(t) = \mathcal{A}\tilde{\xi} - \dot{\tilde{\xi}} \neq 0. \quad (2.4)$$

The solution to the tracking problem involves integrating backwards in time to obtain the unique stabilizing solution of the Riccati differential equation

$$-\dot{\Pi}(t) = \mathcal{A}^*\Pi(t) + \Pi(t)\mathcal{A} + \mathcal{Q} - \Pi(t)\mathcal{B}R^{-1}\mathcal{B}^*\Pi(t), \quad (2.5)$$

with boundary condition $\Pi(T) = 0$. The feedback control gain is defined as

$$\mathcal{K} = R^{-1}\mathcal{B}^*\Pi(t). \quad (2.6)$$

The feed forward signal u_{fw} is

$$u_{fw}(t) = R^{-1}\mathcal{B}^*q(t). \quad (2.7)$$

where the solution $q(t)$ can be expressed in terms of the transition operator for the system:

$$\dot{q}(t) = -[\mathcal{A} - \mathcal{B}R^{-1}\mathcal{B}^*\Pi(t)]q(t), \quad (2.8)$$

with $q(T) = 0$. The control law for the LQR state tracking is

$$u(t) = -\mathcal{K}x(t) - u_{fw}. \quad (2.9)$$

Applying this control law to the original system in Equation (2.3), the following system is obtained

$$\dot{x}(t) = [\mathcal{A} - \mathcal{B}\mathcal{K}]x(t) - u_{fw}. \quad (2.10)$$

When considering the infinite-time case (steady state tracking), some simplifications may be made. Letting $T \rightarrow \infty$, Equation (2.5) reduces to the algebraic Riccati equation

$$\mathcal{A}^*\Pi + \Pi\mathcal{A} - \Pi\mathcal{B}R^{-1}\mathcal{B}^*\Pi + Q = 0. \quad (2.11)$$

and since $q(t)$ is bounded, a steady state solution can be obtained for Equation (2.8).

2.2 Linear Quadratic Gaussian (LQG) Tracking

While the LQR problem assumes full knowledge of the state is available for feedback, the Linear Quadratic Gaussian (LQG) problem assumes that only an estimate of the state from Equation (2.3) exists, based on a measurement

$$y = \mathcal{C}x(t), \quad (2.12)$$

where the measurement $y(t) : X \rightarrow Y$, with Y a Hilbert space, is taken to be in \mathbb{R}^p in this work, and a state estimate, $x_c(t) = x_c(t, \cdot) \in X$, is used in the control law in

Equation (2.9). The operator \mathcal{C} describes how the state is observed. Again, the state from Equation (2.3) is $\xi - \tilde{\xi}$, and it is assumed that the desired target of the state estimate is also $\tilde{\xi}$.

We next present the following definitions, which are necessary to understand the control theory presented in this section.

Definition 2.1. *An operator \mathcal{A} is exponentially stable if and only if \mathcal{A} generates an exponentially stable C_0 -semigroup.*

Definition 2.2. *The state linear system $\Sigma(\mathcal{A}, \mathcal{B}, \mathcal{C})$ is **exponentially stable** if \mathcal{A} is exponentially stable.*

Definition 2.3. *$\Sigma(\mathcal{A}, \mathcal{B}, \mathcal{C})$ is **stabilizable** if there exists a linear operator $\mathcal{F} : X \rightarrow U$ such that $\mathcal{A} + \mathcal{B}\mathcal{F}$ is exponentially stable. For convenience, we refer to the pair $(\mathcal{A}, \mathcal{B})$ as being stabilizable.*

Definition 2.4. *$\Sigma(\mathcal{A}, \mathcal{B}, \mathcal{C})$ is **detectable** if there exists a linear operator $\mathcal{L} : Y \rightarrow X$ such that $\mathcal{A} + \mathcal{L}\mathcal{C}$ is exponentially stable. For convenience, we refer to the pair $(\mathcal{A}, \mathcal{C})$ as being detectable.*

To provide a state estimate, a compensator is used that has the form

$$\dot{x}_c(t) = \mathcal{A}_c x_c(t) + \mathcal{F}_c y(t), \quad x_c(0) = x_{c_0}, \quad (2.13)$$

and the feedback control law is written

$$u(t) = -\mathcal{K}x_c(t) - u_{fw}, \quad (2.14)$$

where \mathcal{K} and u_{fw} are determined from the LQR tracking solution. Then by solving an additional filter Riccati equation

$$\dot{P}(t) = \mathcal{A}P(t) + P(t)\mathcal{A}^* - P(t)\mathcal{C}^*\mathcal{C}P(t) + \mathcal{B}\mathcal{B}^*, \quad (2.15)$$

one can obtain the operators \mathcal{F}_c , and \mathcal{A}_c via

$$\mathcal{F}_c = P(t)\mathcal{C}^*, \quad (2.16)$$

$$\mathcal{A}_c = \mathcal{A} - \mathcal{B}\mathcal{K} - \mathcal{F}_c\mathcal{C}.$$

When considering the steady state case, Equation (2.15) reduces to the filter algebraic Riccati equation

$$\mathcal{A}P + P\mathcal{A}^* - P\mathcal{C}^*\mathcal{C}P + \mathcal{B}\mathcal{B}^* = 0. \quad (2.17)$$

Under standard assumptions of stabilizability of $(\mathcal{A}, \mathcal{B})$ and detectability of $(\mathcal{A}, \mathcal{C})$, there are guaranteed unique solutions Π and P to Equation (2.11) and Equation (2.17), respectively, such that the linear system given by

$$\frac{d}{dt} \begin{bmatrix} x(t) \\ x_c(t) \end{bmatrix} = \begin{bmatrix} \mathcal{A} & -\mathcal{B}\mathcal{K} \\ \mathcal{F}_c\mathcal{C} & \mathcal{A}_c \end{bmatrix} \begin{bmatrix} x(t) \\ x_c(t) \end{bmatrix} - \begin{bmatrix} u_{fw} \\ 0 \end{bmatrix} \quad (2.18)$$

is stable.

CHAPTER 3

FLEXIBLE WING AIRCRAFT MODEL

Over time, morphable wing MAVs exhibit dynamics that are neither fast nor slow enough to be considered in a steady state (constant). Furthermore, since the bending moments of each wing are related to the mass moment of inertia of the fuselage, this moment varies with time as the vehicle morphs. Consequently, modeling with such dynamics lends itself to PDEs with time-varying coefficients. In this work a simplified model with constant coefficients is considered to gain insight into the more challenging time-varying model.

Two Euler-Bernoulli beams connected to a rigid mass are used to model the heave dynamics of a flexible wing MAV. Each beam represents a wing with the rigid mass at the center representing a fuselage. An initial model with a point mass was presented in [9], and the model is elaborated upon here. In this work we consider two versions of this system. The first model, hereinafter referred to as the “BMB” model, assumes that controllers act over the entire beam structure. The second, more realistic model assumes piezoceramic actuators are present on each beam, and we refer to this model as the “BMB-PZT” model. In this chapter we first provide a derivation of the standard beam equation, followed by a description of the two systems.

3.1 Derivation of the Euler-Bernoulli Beam

Consider the linear, undamped model with no axial forces. The Euler-Bernoulli beam is a special case of the Timoshenko beam that does not take into account shear deformation or rotary inertia. The derivation presented here is taken primarily from [19] and [28], although one should note the sign conventions we adopt here. A diagram of the beam can be seen in Figure 3.1. The following notation will be used in this discussion: t represents time, s, y, z are the position coordinates, $w(t, s)$ denotes the vertical displacement at time t and position s , ℓ is the length of the beam, ds is the length of a beam element, ρ is the density of the beam material, A is the cross-sectional area of the beam, I is the area moment of inertia, M represents the bending moment about the z -axis (the beam's tendency to bend in the plane of the loads), and V denotes the shear force (internal force acting in right angles to the neutral axis, or equilibrium position, of the beam).

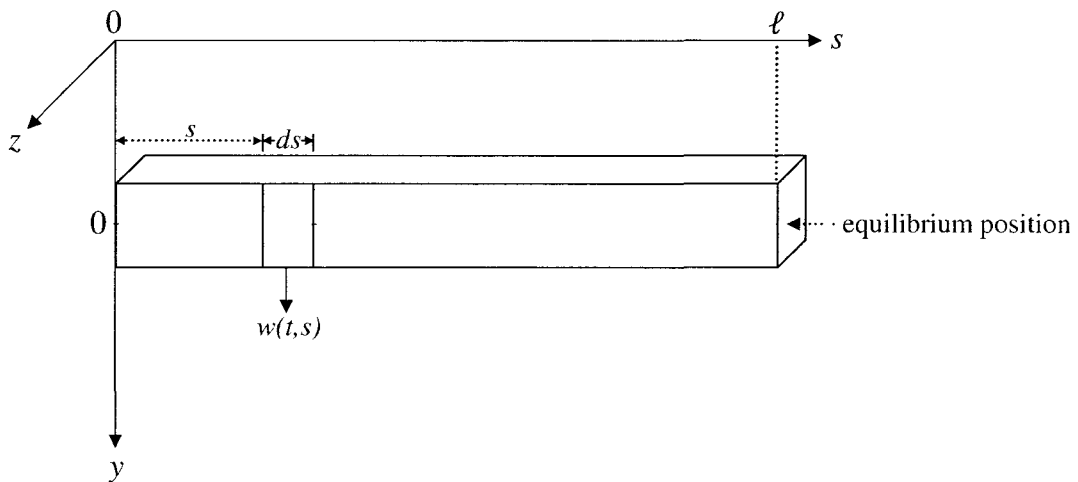


Figure 3.1: Beam

Consider a small segment of the beam shown in Figure 3.2. For the segment to be in equilibrium, the vertical forces are summed about an equilibrium position which results in the following relationship

$$V + \frac{\partial V}{\partial s} ds - V + \rho A ds \frac{\partial^2 w}{\partial t^2} = 0, \quad (3.1)$$

which implies

$$-\frac{\partial V}{\partial s} = \rho A \frac{\partial^2 w}{\partial t^2} \quad (3.2)$$

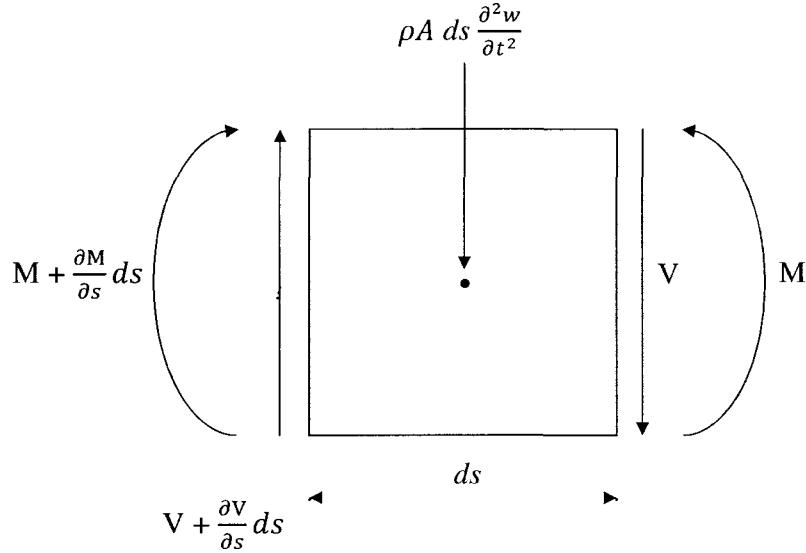


Figure 3.2 Beam Segment

Similarly, a moment equilibrium relationship is obtained (with counter clockwise being the positive direction)

$$M + \frac{\partial M}{\partial s} ds - M - V \frac{ds}{2} - \left(V + \frac{\partial V}{\partial s} ds \right) \frac{ds}{2} = 0 \quad (3.3)$$

Since ds is small $(ds)^2 \approx 0$, and the following relationship holds

$$\frac{\partial M}{\partial s} \approx V \quad (3.4)$$

Differentiating Equation (3.4) and substituting into Equation (3.2) yields

$$-\frac{\partial^2 M}{\partial s^2} = \rho A \frac{\partial^2 w}{\partial t^2}. \quad (3.5)$$

Furthermore, from elementary flexural theory the following moment-curvature relationship is obtained:

$$M = EI \frac{\partial^2 w}{\partial s^2}. \quad (3.6)$$

Substituting Equation (3.6) into Equation (3.5) yields the partial differential equation for the Euler-Bernoulli beam:

$$\rho A \frac{\partial^2 w}{\partial t^2} + EI \frac{\partial^4 w}{\partial s^4} = 0. \quad (3.7)$$

3.2 Beam-Mass-Beam (BMB) Model

3.2.1 Model Description

A graphical representation of the system can be seen in Figure 3.3. It is assumed that the material properties of both beams are uniform, identical, and composed of latex and carbon-graphite fiber with epoxy. Since one goal of this project is to gain insight into optimal morphing trajectories (wing deformations which optimize the vehicle's performance), it is assumed that the vehicle is initially in flight, gliding with morphable wings as opposed to performing a flapping movement. (See [25] and [24] for projects on flapping flight.) We denote the displacement (which is a combination of the vertical air position, or rigid body motions, and small flexible displacements in beam motion) of the left beam from its initial equilibrium position at time t and position s_L by $w_L(t, s_L)$ and the corresponding displacement of the right beam at time t and position s_R by $w_R(t, s_R)$. Including viscous and structural

damping, control, and aerodynamics in the beam equation yields the following model

$$\begin{aligned} \rho A \ddot{w}_L(t, s_L) + \gamma_1 \dot{w}_L(t, s_L) + \gamma_2 I \dot{w}_L'''(t, s_L) + EI w_L''''(t, s_L) \\ = b(s_L) u_L(t) + \frac{m_b g}{\ell_1} - \frac{0.5 \rho_a v^2 c}{\ell_1} C_\ell, \end{aligned} \quad (3.8)$$

for $0 \leq s_L \leq \ell_1$, $t > 0$, and

$$\begin{aligned} \rho A \ddot{w}_R(t, s_R) + \gamma_1 \dot{w}_R(t, s_R) + \gamma_2 I \dot{w}_R'''(t, s_R) + EI w_R''''(t, s_R) \\ = b(s_R) u_R(t) + \frac{m_b g}{\ell_2} - \frac{0.5 \rho_a v^2 c}{\ell_2} C_\ell. \end{aligned} \quad (3.9)$$

Since this model is designed for flight, it is important that neither beam be given favorability. Thus, cantilevering one beam off of the other and using two coordinate systems is not applicable here. Therefore, we let $\ell_1 + \ell_M \leq s_R \leq \ell_1 + \ell_M + \ell_2$, $t > 0$. Here $\dot{w}_i(t, s_i) = \frac{\partial}{\partial t} w_i(t, s_i)$ and $w_i'(t, s_i) = \frac{\partial}{\partial s_i} w_i(t, s_i)$ with $i = L, R$ for the left or right beam, respectively, ρ is the density of the beam material, A is the cross-sectional area of the beam, E is Young's modulus, I is the area moment of inertia of the beam, γ_1 is the coefficient of viscous damping, γ_2 is the coefficient of Kelvin-Voigt damping, g is gravity, m_b is the mass of each beam, $b_L(s_L)$ is the control input function for the left beam, $b_R(s_R)$ is the control input function for the right beam, $u_L(t)$ is the controller for the left beam, $u_R(t)$ is the controller for the right beam, ρ_a is the density of air, v is the forward vehicle velocity, c is the chord length of each wing (beam width), and C_ℓ is the aerodynamic lift coefficient.

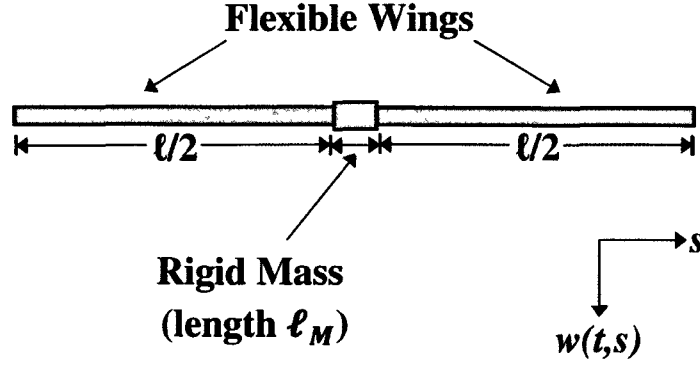


Figure 3.3: MAV model system.

The aerodynamic lift coefficient applied to this model is the same one derived in [14] for a fruit fly model. Although it was derived for a flapping flight insect, it should be noted that its relevance also holds in this framework due to the dimensionlessness of the lift coefficient and the flexibility of the wings of the fruit fly. The lift coefficient model is scaled to the size of the MAV under consideration here by the parameters of the dynamic pressure, $0.5\rho_a v^2$. Together the lift coefficient and the dynamic pressure make up the aerodynamic lift force, $0.5\rho_a v^2 c C_\ell$. The lift coefficient is given by

$$C_\ell = \left[k_1 + k_2 \sin \left(k_3 \arctan \left(\frac{\dot{w}(t, s) + k_5}{u} \right) + k_4 \right) \right], \quad (3.10)$$

where k_1, k_2, k_3, k_4 are the best fit parameters determined from the experimental analysis in [14]. By equating the lift and weight functions so that the two forces balance, some modifications were made to C_ℓ . To obtain real solutions and to accommodate atmospheric conditions, it has been assumed that $k_4 = 0$, and a new parameter, k_5 , has been included in the model to reflect the vertical wind velocity.

The boundary conditions applied to these elastic equations arise from standard beam theory and are presented in Table 3.1.

Table 3.1: Boundary Conditions

| Boundary Condition | Physical Interpretation |
|---|---|
| $EIw_L''(t, 0) + \gamma_2 I \dot{w}_L''(t, 0) = 0$ | No bending moment at free end, $w_L''(t, 0)$ |
| $EIw_L'''(t, 0) + \gamma_2 I \dot{w}_L'''(t, 0) = 0$ | No shear force at free end, $w_L'''(t, 0)$ |
| $EIw_R''(t, \ell_1 + \ell_M + \ell_2) + \gamma_2 I \dot{w}_R''(t, \ell_1 + \ell_M + \ell_2) = 0$ | No bending moment at free end, $w_R''(t, \ell_1 + \ell_M + \ell_2)$ |
| $EIw_R'''(t, \ell_1 + \ell_M + \ell_2) + \gamma_2 I \dot{w}_R'''(t, \ell_1 + \ell_M + \ell_2) = 0$ | No shear force at free end, $w_R'''(t, \ell_1 + \ell_M + \ell_2)$ |
| $-EIw_L''(t, \ell_1) - \gamma_2 I \dot{w}_L''(t, \ell_1) + EIw_R''(t, \ell_1 + \ell_M) + \gamma_2 I \dot{w}_R''(t, \ell_1 + \ell_M) = I_z \ddot{w}'_L(t, \ell_1)$ | Difference of bending moments at the mass location equals the mass moment of inertia (I_z) multiplied by the angular acceleration of the mass |
| $EIw_L'''(t, \ell_1) + \gamma_2 I \dot{w}_L'''(t, \ell_1) - EIw_R'''(t, \ell_1 + \ell_M) - \gamma_2 I \dot{w}_R'''(t, \ell_1 + \ell_M) = m \ddot{w}_L(t, \ell_1)$ | Difference of shear forces at the mass location equals the mass (m) multiplied by the acceleration of the mass |
| $w_L(t, \ell_1) - w_R(t, \ell_1 + \ell_M) = 0$ | Continuity of deflection at the mass location |
| $w'_L(t, \ell_1) - w'_R(t, \ell_1 + \ell_M) = 0$ | Continuity of slope at the mass location |

3.2.2 Linear Approximation of the BMB Model

As is common for nonlinear PDE systems, one may perform a linearization about an equilibrium position of the PDE model (by dropping the nonlinear terms) and apply tools from distributed parameter system (DPS) control theory (see, for example, [30] and [8]). However, results from the eigenvalue analysis presented in Section 4.2 indicate that such a linearization is not reasonable for Equation (3.8) and Equation (3.9), because a mathematical representation of a linearized system sees

free boundary conditions for displacement and slope at the free end of each beam, resulting in two zero eigenvalues for the system. Although mathematically these free end conditions exist, physically there are two external loads, lift and gravity, acting in equal and opposite directions across each beam. As a result, lift and gravity provide support for the beams. Designing control on only the linear dynamics of the BMB model showed that stability was still an issue. Therefore, it is necessary to communicate the existence of these external loads to the linear dynamics of the system. The mechanisms used to make this communication are introduced here because the upcoming theoretical analysis in Chapter 4 is conducted on the linearly approximated system.

To make the system \mathcal{A} operator from Equation (2.1) aware of a weight force in the system, $m_b g$ is approximated by the following

$$m_b g \approx m_b \ddot{w}(t, s). \quad (3.11)$$

Further, to provide the \mathcal{A} operator with knowledge of the aerodynamic lift force, a linear approximation of C_ℓ is calculated using a Taylor series expansion about a zero angle of attack. Consequently, it is important to note that this approximation is only sufficient for low angles of attack. Then for small angles of attack, the following approximation is reasonable and applied here:

$$\arctan\left(\frac{\dot{w}(t, s) + k_5}{v}\right) \approx \frac{\dot{w}(t, s) + k_5}{v}. \quad (3.12)$$

Making this substitution into Equation (3.10) yields the following Taylor expansion:

$$C_\ell = k_1 + k_2 k_3 \sum_{n=0}^{\infty} \frac{(-1)^n \delta^{2n+1}}{(2n+1)!}, \quad (3.13)$$

$$\text{where } \delta = \frac{\dot{w}(t, s) + k_5}{v}.$$

Keeping only the linear term from the expansion yields

$$C_\ell = \frac{k_2 k_3}{v} \dot{w}(t, s). \quad (3.14)$$

Note that the constant term from the Taylor expansion has been excluded since it would not be absorbed into the \mathcal{A} operator.

Substituting Equation (3.11) and Equation (3.14) into Equation (3.8) and Equation (3.9) yields the following linear system:

$$\begin{aligned} \rho A \ddot{w}_L(t, s_L) + \gamma_1 \dot{w}_L(t, s_L) + \gamma_2 I \dot{w}_L''''(t, s_L) + EI w_L''''(t, s_L) \\ = b(s_L) u_L(t) + \frac{m_b}{\ell_1} \ddot{w}_L(t, s_L) - \frac{0.5}{\ell_1 v} \rho_a v^2 c k_2 k_3 \dot{w}_L(t, s_L), \end{aligned} \quad (3.15)$$

for $0 \leq s_L \leq \ell_1$, $t > 0$, and

$$\begin{aligned} \rho A \ddot{w}_R(t, s_R) + \gamma_1 \dot{w}_R(t, s_R) + \gamma_2 I \dot{w}_R''''(t, s_R) + EI w_R''''(t, s_R) \\ = b(s_R) u_R(t) + \frac{m_b}{\ell_2} \ddot{w}_R(t, s_R) - \frac{0.5}{\ell_2 v} \rho_a v^2 c k_2 k_3 \dot{w}_R(t, s_R), \end{aligned} \quad (3.16)$$

for $\ell_1 + \ell_M \leq s_R \leq \ell_1 + \ell_M + \ell_2$, $t > 0$.

3.3 Beam-Mass-Beam Model with Piezoceramic Patch Actuators (BMB-PZT Model)

3.3.1 Model Description

We now make the more realistic assumption that controllers are available via piezoceramic patch actuators (alternatively referred to as piezoelectric transducers, or PZTs), and we refer to this system as the ‘‘BMB-PZT’’ system. When excited by an electric field, the actuators induce a bending moment on the beam. We assume all

parameter values and notation are the same as those of the BMB model in Section 3.2. A graphical representation of the BMB-PZT model can be seen in Figure 3.4. It is assumed the patches included on this system are the DuraAct P-876.A15 patch transducers, and all patch parameter values included in the BMB-PZT model reflect this composition. Additional information about these transducers can be found in [1]. This particular patch was chosen due to work done in [6], where it was shown that patches requiring high voltages may be employed on small air vehicles without compromising weight.

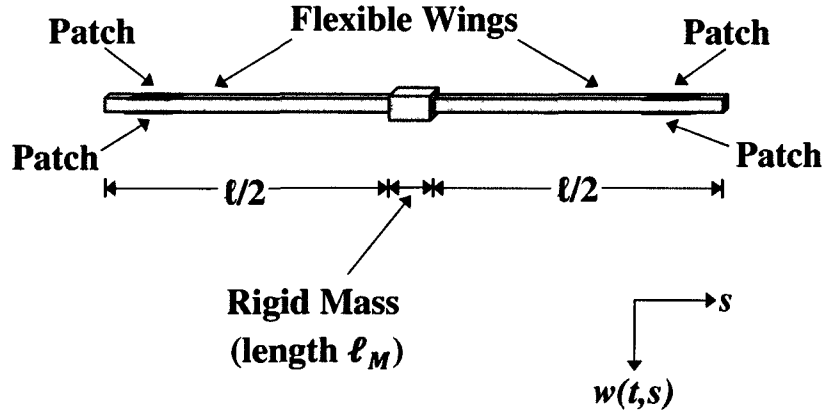


Figure 3.4: MAV model system with piezoceramic patches.

The model is described as follows:

$$\begin{aligned}
& [\rho A + 2c\rho_{pe}h_{pe}\chi_{pe}(s_L)] \ddot{w}_L(t, s_L) \\
& + \left[EI + \frac{2}{3}cE_{pe} \left(\frac{3}{4}h^2h_{pe} + \frac{3}{2}hh_{pe}^2 + h_{pe}^3 \right) \chi_{pe}(s_L) \right] w_L''''(t, s_L) \\
& + \gamma \dot{w}_L(t, s_L) + \left[\gamma_2 I + \frac{2}{3}cC_{Dpe} \left(\frac{3}{4}h^2h_{pe} + \frac{3}{2}hh_{pe}^2 + h_{pe}^3 \right) \chi_{pe}(s_L) \right] \dot{w}_L''''(t, s_L) \\
& = \frac{\partial^2}{\partial s_L^2} \left[-\frac{1}{2}E_{pe}cd_{31}(h + h_{pe})\chi_{pe}(s_L) \right] u(t) + \frac{m_b g}{\ell_1} - \frac{0.5\rho_a v^2 c}{\ell_1} C_\ell,
\end{aligned} \tag{3.17}$$

for $0 \leq s_L \leq \ell_1$, $t > 0$, with the left beam piezoceramic patch actuator located on $[s_1, s_2]$, where $0 \leq s_1 < s_2$. The characteristic function is given by

$$\chi_{pe}(s) = \begin{cases} 1 & , \quad s_1 \leq s \leq s_2 \\ 0 & , \quad \text{otherwise} \end{cases} . \quad (3.18)$$

The equation for the right beam follows similarly:

$$\begin{aligned} & [\rho A + 2c\rho_{pe}h_{pe}\chi_{pe}(s_R)] \ddot{w}_R(t, s_R) \\ & + \left[EI + \frac{2}{3}cE_{pe} \left(\frac{3}{4}h^2h_{pe} + \frac{3}{2}hh_{pe}^2 + h_{pe}^3 \right) \chi_{pe}(s_R) \right] w_R''''(t, s_R) \\ & + \gamma \dot{w}_R(t, s_R) + \left[\gamma_2 I + \frac{2}{3}c c_{Dpe} \left(\frac{3}{4}h^2h_{pe} + \frac{3}{2}hh_{pe}^2 + h_{pe}^3 \right) \chi_{pe}(s_R) \right] \dot{w}_R''''(t, s_R) \\ & = \frac{\partial^2}{\partial s_R^2} \left[-\frac{1}{2}E_{pe}cd_{31}(h + h_{pe})\chi_{pe}(s_R) \right] u(t) + \frac{m_b g}{\ell_2} - \frac{0.5\rho_a v^2 c}{\ell_2} C_\ell. \end{aligned} \quad (3.19)$$

for $\ell_1 + \ell_M \leq s_R \leq \ell_1 + \ell_M + \ell_2$, $t > 0$, with the right beam piezoceramic patch actuator located symmetrically on $[\ell_1 + \ell_M + \ell_2 - s_2, \ell_1 + \ell_M + \ell_2 - s_1]$. Here, E_{pe} refers to Young's modulus of the patch, ρ_{pe} is the linear density of the patch material, c_{Dpe} is the Kelvin-Voigt damping coefficient for the patch, h_{pe} is the patch thickness, d_{31} is the piezoceramic strain constant, $V_1(t)$ is the applied voltage to the outer (top) patch, and $V_2(t)$ is the applied voltage to the inner (bottom) patch. It is assumed that the patches are excited out-of-phase, i.e. $V_1(t) = -V_2(t)$.

The boundary conditions applied to these elastic equations are the same as those in the BMB model presented in Table 3.1.

3.3.2 Linear Approximation of the BMB-PZT Model

Applying the same linearization from Section 3.2.2, the linearized BMB-PZT is described as

$$\begin{aligned}
& [\rho A + 2c\rho_{pe}h_{pe}\chi_{pe}(s_L)] \ddot{w}_L(t, s_L) \\
& + \left[EI + \frac{2}{3}cE_{pe} \left(\frac{3}{4}h^2h_{pe} + \frac{3}{2}hh_{pe}^2 + h_{pe}^3 \right) \chi_{pe}(s_L) \right] w_L''''(t, s_L) \\
& + \gamma_1 \dot{w}_L(t, s_L) + \left[\gamma_2 I + \frac{2}{3}c c_{Dpe} \left(\frac{3}{4}h^2h_{pe} + \frac{3}{2}hh_{pe}^2 + h_{pe}^3 \right) \chi_{pe}(s_L) \right] \dot{w}_L''''(t, s_L) \quad (3.20) \\
& = \frac{\partial^2}{\partial s_L^2} \left[-\frac{1}{2}E_{pe}c d_{31}(h + h_{pe})\chi_{pe}(s_L) \right] u(t) + \frac{m_b}{\ell_1} \ddot{w}_L(t, s_L) \\
& - \frac{0.5}{\ell_1 v} \rho_a v^2 c k_2 k_3 \dot{w}_L(t, s_L),
\end{aligned}$$

for $0 \leq s_L \leq \ell_1$, $t > 0$, and

$$\begin{aligned}
& [\rho A + 2c\rho_{pe}h_{pe}\chi_{pe}(s_R)] \dot{w}_R(t, s_R) \\
& + \left[EI + \frac{2}{3}cE_{pe} \left(\frac{3}{4}h^2h_{pe} + \frac{3}{2}hh_{pe}^2 + h_{pe}^3 \right) \chi_{pe}(s_R) \right] w_R''''(t, s_R) \\
& + \gamma_1 \dot{w}_R(t, s_R) + \left[\gamma_2 I + \frac{2}{3}c c_{Dpe} \left(\frac{3}{4}h^2h_{pe} + \frac{3}{2}hh_{pe}^2 + h_{pe}^3 \right) \chi_{pe}(s_R) \right] \dot{w}_R''''(t, s_R) \quad (3.21) \\
& = \frac{\partial^2}{\partial s_R^2} \left[-\frac{1}{2}E_{pe}c d_{31}(h + h_{pe})\chi_{pe}(s_R) \right] u(t) + \frac{m_b}{\ell_2} \ddot{w}_R(t, s_R) \\
& - \frac{0.5}{\ell_2 v} \rho_a v^2 c k_2 k_3 \dot{w}_R(t, s_R),
\end{aligned}$$

for $\ell_1 + \ell_M \leq s_R \leq \ell_1 + \ell_M + \ell_2$, $t > 0$.

CHAPTER 4

THEORETICAL ANALYSIS

In this chapter we perform a theoretical analysis of the linearly approximated BMB system in order to gain insight into well-posedness of the system and the attainment of a C_0 -semigroup. The framework for well-posedness and background information for semigroups is provided in Section 4.1. Eigenvalue analysis for this problem is shown in Section 4.2. Section 4.3 provides a proof for well-posedness and concluding remarks regarding semigroup analysis.

4.1 Framework

The approach taken here is motivated by [19] where the well-posedness of two multiple component structures (MCS) was validated. One model consisted of two beams with an angular connection, cantilevered at the left end, and the second MCS consisted of a hub-beam-mass-beam-mass model. Additional work which exploits portions of this framework for MCS models can be found in [17], where an Euler-Bernoulli beam attached to a rotating hub at one end and a mass at the other was considered. In [26] a proof for well-posedness is provided for a similar model with a Timoshenko beam.

Much of the general theory for well-posedness can be found in [22] and [20]. A summary of the existing theory, including appropriate extensions to damped second

order (in time) systems is given in [4], and it is from this work that the general framework presented here is abridged. Necessary supplements have been included to accommodate the BMB model under consideration.

4.1.1 Framework for Well-Posedness

Let H and V be complex Hilbert spaces with norms $\|\cdot\|_H$ and $\|\cdot\|_V$ and inner products $\langle \cdot, \cdot \rangle_H$ and $\langle \cdot, \cdot \rangle_V$. Moreover, assume V and H form a Gelfand triple, which is denoted by $V \hookrightarrow H \cong H^* \hookrightarrow V^*$ with duality pairing $\langle \cdot, \cdot \rangle_{V^*, V}$. Here, H is known as the pivot space. By these assumptions V is a dense subset of H and there exists a positive constant c such that $\|\phi\|_H \leq c \|\phi\|_V$ for $\phi \in V$. That is, V is densely and continuously embedded in H . By the Riesz Representation Theorem, H is identified with H^* , where V^* and H^* denote the corresponding conjugate dual spaces. Note that $\langle \cdot, \cdot \rangle_{V^*, V}$ is the extension by continuity of $\langle \cdot, \cdot \rangle_H$ from $V \times H$ to $V^* \times H$. Therefore, for each $v^* \in V^*$ we have the representation $v^*(v) = \langle v^*, v \rangle_{V^*, V}$.

Since this framework approaches the weak formulation in the context of sesquilinear forms, we next define a sesquilinear form

Definition 4.1. *Let H and V be vector spaces over the same field K , where $K = \mathbb{R}$ or \mathbb{C} . A **sesquilinear form** \mathbf{a} on $H \times V$ is a mapping $\mathbf{a} : H \times V \rightarrow K$ such that for all $h, h_1, h_2 \in H$ and $v, v_1, v_2 \in V$ and all scalars α, β ,*

$$(1) \quad \mathbf{a}(h_1 + h_2, v) = \mathbf{a}(h_1, v) + \mathbf{a}(h_2, v)$$

$$(2) \quad \mathbf{a}(h, v_1 + v_2) = \mathbf{a}(h, v_1) + \mathbf{a}(h, v_2)$$

$$(3) \mathbf{a}(\alpha h, v) = \alpha \mathbf{a}(h, v)$$

$$(4) \mathbf{a}(h, \beta v) = \bar{\beta} \mathbf{a}(h, v)$$

That is, \mathbf{a} is linear in the first argument and conjugate linear in the second argument

Consider the abstract form of a second order (in time) system

$$z(t) + \mathcal{D}z(t) + \mathcal{A}z(t) = f(t) \text{ in } V^*, \quad (4.1)$$

$$z(0) = z_0, z(1) = z_1$$

It was noted in [17] and [19] that to make the appropriate identifications needed to exploit this framework, \mathcal{A} must be coercive in S . First we consider the definition of a self-adjoint operator, which is needed to appropriately define coercivity

Definition 4.2. A densely defined linear operator $\mathcal{A} : \mathbf{D}(\mathcal{A}) \rightarrow H$, with H a Hilbert space is said to be **self-adjoint** iff $\mathbf{D}(\mathcal{A}) = \mathbf{D}(\mathcal{A}^*)$ and $\mathcal{A} = \mathcal{A}^*$, where \mathcal{A}^* denotes the adjoint of \mathcal{A}

Definition 4.3. A self-adjoint operator \mathcal{A} on a real Hilbert space H is **coercive** in H if there exists a constant $\epsilon > 0$ such that

$$\langle \mathcal{A}\phi, \phi \rangle_H \geq \epsilon \|\phi\|_H^2, \quad (4.2)$$

for all $\phi \in H$

If \mathcal{A} is not H -coercive, a bounded self-adjoint linear operator \mathcal{A}_1 on H may be chosen so that $\tilde{\mathcal{A}} = \mathcal{A} + \mathcal{A}_1$ is coercive, an operator \mathcal{A}_1 that generates coercivity is nonunique and, in fact, there are an infinite number of possibilities for such an operator. Since $\tilde{\mathcal{A}}$ is a bounded perturbation of \mathcal{A} , well-posedness of $\tilde{\mathcal{A}}$ implies that $\mathcal{A} = \tilde{\mathcal{A}} - \mathcal{A}_1$ is also well-posed. Further discussion of this involves semigroups and thus is provided later on in Section 4.1.2

It is assumed the operators \mathcal{D} and \mathcal{A} are generated via sesquilinear forms \mathbf{d} and \mathbf{a} . That is,

$$\mathbf{d}(z, \phi) = (\mathcal{D}z)(\phi) = \langle \mathcal{D}z, \phi \rangle_{V^* V}, \quad (4.3)$$

and

$$\mathbf{a}(z, \phi) = (\mathcal{A}z)(\phi) = \langle \mathcal{A}z, \phi \rangle_{V^* V} \quad (4.4)$$

Furthermore, we assume $\mathbf{a} : V \times V \rightarrow \mathbb{C}$ is a sesquilinear form on V and satisfies the following hypotheses

(H1) For all $\phi, \psi \in V$, $\mathbf{a}(\phi, \psi) = \overline{\mathbf{a}(\psi, \phi)}$. That is, \mathbf{a} is symmetric

(H2) There exists a constant k_1 such that for all $\phi, \psi \in V$

$$\|\mathbf{a}(\phi, \psi)\| \leq k_1 \|\phi\|_V \|\psi\|_V \quad (4.5)$$

That is, \mathbf{a} is continuous

(H3) There exists a constant $c > 0$ such that for all $\phi \in V$

$$\operatorname{Re} \mathbf{a}(\phi, \phi) \geq c \|\phi\|_V^2 \quad (4.6)$$

That is, \mathbf{a} is elliptic in V

The sesquilinear form \mathbf{d} is defined to be on a complex Hilbert space V_2 , where $V \subseteq V_2 \subseteq H$. Again it is assumed V_2 and H form a Gelfand triple with duality pairing $\langle \cdot, \cdot \rangle_{V_2^* V_2}$, and $V \hookrightarrow V_2 \hookrightarrow H \cong H^* \hookrightarrow V_2^* \hookrightarrow V^*$. In this work, however, V_2 is taken to be V so that solutions may be obtained and the damped model may be appropriately considered. We assume that $\mathbf{d} : V_2 \times V_2$ satisfies the following hypotheses

(H4) There exists a constant k_2 such that for all $\phi, \psi \in V_2$

$$\|\mathbf{d}(\phi, \psi)\| \leq k_2 \|\phi\|_{V_2} \|\psi\|_{V_2}. \quad (4.7)$$

That is, \mathbf{d} is continuous.

(H5) There exists constants $c > 0$ and $\lambda \geq 0$ such that for all $\phi \in V_2$

$$\operatorname{Re} \mathbf{d}(\phi, \phi) \geq c \|\phi\|_{V_2}^2 - \lambda \|\phi\|_H^2. \quad (4.8)$$

That is, \mathbf{d} is coercive in V_2 .

Finally, we make the following assumption on $f(t)$.

(H6) The function f satisfies $f \in L_2[(0, T), V_2^*]$.

Then a weak formulation of the system is given by

$$\begin{aligned} \langle \ddot{z}(t), \phi \rangle + \mathbf{d}(\dot{z}(t), \phi) + \mathbf{a}(z(t), \phi) &= \langle f(t), \phi \rangle \text{ for all } \phi \in V, \\ z(0) = z_0, \dot{z}(0) &= z_1. \end{aligned} \quad (4.9)$$

We can note that Equation (4.1) and Equation (4.9) are the same if $\langle \cdot, \cdot \rangle$ is taken to be $\langle \cdot, \cdot \rangle_{V^*, V}$, and we note that $\langle f, \phi \rangle_{V^*, V} = \langle f, \phi \rangle_{V_2^*, V_2}$ since $f \in L_2[(0, T), V_2^*]$.

Well-posedness is then established by an application of the following theorem.

Theorem 4.4 (from [4]). *If $z_0 \in V$, $z_1 \in H$, and \mathbf{a} , \mathbf{d} , and f satisfy **(H1)**-**(H6)** then there exists a unique solution z to Equation (4.9) (or equivalently Equation (4.1)) with $z \in L_2[(0, T), V]$, $\dot{z} \in L_2[(0, T), V_2]$, and $\ddot{z} \in L_2[(0, T), V^*]$. Furthermore, the solutions of Equation (4.9) have continuous dependence on the data (z_0, z_1, f) in that the map $(z_0, z_1, f) \rightarrow (z, \dot{z})$ is continuous from $V \times H \times L_2[(0, T), V_2^*]$ to $L_2[(0, T), V] \times L_2[(0, T), V_2]$.*

4.1.2 Semigroup Discussion

Now we consider a semigroup formulation of the system under consideration, which is needed to guarantee a solution exists to the control problem described in Equation (2.1). We begin by considering the following definitions from [21].

Definition 4.5. *Let X be a Hilbert space. A family $T(t)$, $0 \leq t < \infty$, of bounded linear operators from X into X is a **semigroup** of bounded linear operators on X if*

1. $T(0) = \mathcal{I}$, where \mathcal{I} is the identity operator on X .
2. $T(t + s) = T(t)T(s)$ for every $t, s > 0$.

Definition 4.6. *A linear operator \mathcal{A} defined by*

$$\mathbf{D}(\mathcal{A}) = \left\{ x \in X : \lim_{t \rightarrow 0^+} \frac{T(t)x - x}{t} \text{ exists} \right\}$$

and

$$\mathcal{A}x = \lim_{t \rightarrow 0^+} \frac{T(t)x - x}{t} = \left. \frac{d^+ T(t)x}{dt} \right|_{t=0} \text{ for } x \in \mathbf{D}(\mathcal{A})$$

is the **infinitesimal generator** of the semigroup $T(t)$, where $\mathbf{D}(\mathcal{A})$ is the domain of \mathcal{A} .

Definition 4.7. *A semigroup $T(t)$, $0 \leq t < \infty$, of bounded linear operators on a Hilbert space X is a **strongly continuous** semigroup of bounded linear operators if*

$$\lim_{t \rightarrow 0^+} T(t)x = x \text{ for every } x \in X.$$

A strongly continuous semigroup of bounded linear operators on X will be called a **semigroup of class C_0** or a **C_0 -semigroup**.

For additional discussion of semigroup theory and applications to control systems beyond the scope of this work, one should consult [21] and [11]. To consider

a semigroup formulation. we must consider the first order form of Equation (4.1) or Equation (4.9) which is

$$\begin{aligned}\hat{z}(t) &= \hat{\mathcal{A}}\hat{z}(t) + F(t) \\ \hat{z}(0) &= \hat{z}_0,\end{aligned}\tag{4.10}$$

and we cite the following theorem.

Theorem 4.8 (from [4]). *Under hypotheses (H1)-(H5) on \mathbf{a} and \mathbf{d} , the operator $\hat{\mathcal{A}}$ generates a C_0 -semigroup $\mathcal{T}(t)$ on $V \times H$ and satisfies $\|\mathcal{T}(t)\|_{\mathcal{H}_1} \leq e^{\lambda t}$ for any $\lambda \geq \lambda_0$.*

Finally, we revisit the case in which \mathcal{A} is not coercive in H . We note a converse argument can be made that if \mathcal{A} is the infinitesimal generator of a C_0 -semigroup then Equation (4.10) is well-posed, and the same can be said for Equation (4.1). (See pages 86 - 90 of [29].) By applying the following theorem, we can infer that if $\tilde{\mathcal{A}}$ is well-posed then so is $\mathcal{A} = \tilde{\mathcal{A}} - \mathcal{A}_1$.

Theorem 4.9 (from [21]). *Let X be a Banach space and let \mathcal{A} be the infinitesimal generator of a C_0 -semigroup $\mathcal{T}(t)$ on X satisfying $\|\mathcal{T}(t)\| \leq Me^{\omega t}$. If \mathcal{B} is a bounded linear operator on X , then $\mathcal{A} + \mathcal{B}$ is the infinitesimal generator of a C_0 -semigroup $\mathcal{S}(t)$ on X satisfying $\|\mathcal{S}(t)\| \leq Me^{(\omega + M\|\mathcal{B}\|)t}$.*

4.1.3 Additional Theorems

Here we cite some additional theorems which are useful for conducting the analysis described in Section 4.1.1.

Lemma 4.10 (from [7]). (*Fundamental Lemma of the Calculus of Variations*).

Part A. If $\alpha(\cdot)$ is piecewise continuous on $[a, b]$ and

$$\int_a^b \alpha(x)\eta'(x)dx = 0, \quad (4.11)$$

for all $\eta(\cdot) \in V_0 = \{\eta(\cdot) \text{ piecewise smooth on } (a, b) : \eta(a) = 0, \eta(b) = 0\}$ then there is a constant c and a finite number of points $a < \hat{x}_1, \hat{x}_2, \dots, \hat{x}_p < b$ in (a, b) such that for all $x \in (a, b)$ with $x \neq \hat{x}_i, i = 1, 2, \dots, p$

$$\alpha(x) = c \quad (4.12)$$

Part B. Conversely, if $\alpha(\cdot)$ and $\beta(\cdot)$ are piecewise continuous on $[a, b]$ and

$$\int_a^b (\alpha(x)\gamma(x) + \beta(x)\gamma'(x))dx = 0, \quad (4.13)$$

for all $\gamma \in V_0$, then there is a constant c such that for all $x \in (a, b)$

$$\beta(x) = c + \int_a^x \alpha(s)ds. \quad (4.14)$$

The converse also holds. In particular, $\beta(\cdot)$ is piecewise smooth and at points x where $\alpha(\cdot)$ is continuous

$$\beta'(x) = \alpha(x) \quad (4.15)$$

Theorem 4.11 (from [22]). *If \mathbf{a} is a continuous, V -elliptic sesquilinear form on V then $\mathbf{D}(\mathbf{A})$ is dense in V and hence dense in H*

Theorem 4.12 (from [3]). *Let \mathbf{A} and \mathbf{B} be self-adjoint operators on $\mathbf{D} \rightarrow H$. Then $\mathbf{A} + \mathbf{B}$ is self-adjoint.*

4.2 Eigenvalue Analysis

To obtain solutions to the eigenvalue problem of the linearized BMB model, some simplifications were made. Both a single free-free beam model and a model which consists of two beams connected at a point mass were examined. The beam-point mass-beam analysis is presented here. It is important to note that the dynamics of the beam-point mass-beam system are the exact same as the beam-rigid mass-beam system, with a rigid mass merely creating a spatial separation for the two beams. Furthermore, since damping ultimately has no influence over the eigenvalues of the system, it is reasonable to analyze the undamped model here.

Consider the uncontrolled, undamped abstract form of (3.8) and (3.9) connected at a point mass. Written in second order form, we analyze the following:

$$\ddot{w}_L(t) + \frac{EI}{\rho A} w_L''''(t) = \frac{m_b g}{\ell_1 \rho A} - \frac{0.5 \rho_a v^2 c C_\ell}{\ell_1 \rho A}, \quad (4.16)$$

for $0 \leq s_L \leq \ell/2$ and

$$\ddot{w}_R(t) + \frac{EI}{\rho A} w_R''''(t) = \frac{m_b g}{\ell_2 \rho A} - \frac{0.5 \rho_a v^2 c C_\ell}{\ell_2 \rho A}, \quad (4.17)$$

for $\ell/2 \leq s_R \leq \ell$. The eigenvalue problem under consideration for this system is

$$\frac{EI}{\rho A} \varphi_L''''(s_L) = \lambda \varphi_L(s_L) \quad \text{and} \quad \frac{EI}{\rho A} \varphi_R''''(s_R) = \lambda \varphi_R(s_R), \quad (4.18)$$

where λ represents the eigenvalues and φ_i with $i = L, R$ corresponds to the natural modes, or eigenvectors of the system. Due to the complexities in obtaining solutions to the eigenvalue problem, the cases when $\lambda > 0$ and $\lambda < 0$ are not considered here.

Let $\lambda = 0$ for both beams. We seek to determine any nontrivial solutions to φ_i if any such solutions exist. This system is subject to the following boundary

conditions, as obtained from Table 3.1. (Note for a point mass $I_z, \ell_M = 0$.)

$$\begin{aligned}
\varphi_L''(0) &= 0, & \varphi_R''(\ell) &= 0, \\
\varphi_L'''(0) &= 0, & \varphi_R'''(\ell) &= 0, \\
\varphi_L(\ell/2) &= \varphi_R(\ell/2), & \varphi_L'(\ell/2) &= \varphi_R'(\ell/2), \\
\varphi_L''(\ell/2) &= \varphi_R''(\ell/2), & \varphi_L'''(\ell/2) &= \varphi_R'''(\ell/2).
\end{aligned} \tag{4.19}$$

The general solutions to (4.18) are

$$\varphi_L(s_L) = c_1 + c_2 s_L + c_3 s_L^2 + c_4 s_L^3 \tag{4.20}$$

and

$$\varphi_R(s_R) = d_1 + d_2 s_R + d_3 s_R^2 + d_4 s_R^3. \tag{4.21}$$

Applying boundary conditions, we see that $c_3 = d_3 = c_4 = d_4 = 0$ and $c_1 = d_1 = c_2 = d_2 = \text{free}$. Thus, the system contains two zero modes. These zero modes result from the free end conditions (or, more clearly, the lack of any cantilevered conditions) for displacement and slope.

4.3 Well-Posedness of the BMB System

In this section we use the results of Section 4.2 to investigate issues of well-posedness of the linearly approximated BMB system with a rigid mass.

Given real Hilbert spaces V and S , we choose the state space S to be $S = L_2[0, \ell_1] \times L_2[\ell_1 + \ell_M, \ell_1 + \ell_M + \ell_2] \times \mathbb{R} \times \mathbb{R}$. The strong form of Equation (3.15) and Equation (3.16) with boundary conditions from Table 3.1 is listed below; equations containing acceleration terms are written first

$$\begin{aligned}
& \rho A \ddot{w}_L(t, s_L) + \gamma_1 \dot{w}_L(t, s_L) + \gamma_2 I \dot{w}_L''''(t, s_L) + EI w_L''''(t, s_L) \\
&= b_L(s_L) u_L(t) + \frac{m_b}{\ell_1} \ddot{w}_L(t, s_L) - \frac{0.5 \rho_a v^2 c k_2 k_3}{\ell_1 v} \dot{w}_L(t, s_L). \\
& \rho A \ddot{w}_R(t, s_R) + \gamma_1 \dot{w}_R(t, s_R) + \gamma_2 I \dot{w}_R''''(t, s_R) + EI w_R''''(t, s_R) \\
&= b_R(s_R) u_R(t) + \frac{m_b}{\ell_2} \ddot{w}_R(t, s_R) - \frac{0.5 \rho_a v^2 c k_2 k_3}{\ell_2 v} \dot{w}_R(t, s_R), \\
& EI w_L''''(t, \ell_1) + \gamma_2 I \dot{w}_L''''(t, \ell_1) - EI w_R''''(t, \ell_1 + \ell_M) - \gamma_2 I \dot{w}_R''''(t, \ell_1 + \ell_M) = m \ddot{w}_L(t, \ell_1), \\
& -EI w_L''(t, \ell_1) - \gamma_2 I \dot{w}_L''(t, \ell_1) + EI w_R''(t, \ell_1 + \ell_M) + \gamma_2 I \dot{w}_R''(t, \ell_1 + \ell_M) = I_z \dot{w}'_L(t, \ell_1), \\
& EI w_L''(t, 0) + \gamma_2 I \dot{w}_L''(t, 0) = 0, \\
& EI w_L'''(t, 0) + \gamma_2 I \dot{w}_L'''(t, 0) = 0, \\
& EI w_R''(t, \ell_1 + \ell_M + \ell_2) + \gamma_2 I \dot{w}_R''(t, \ell_1 + \ell_M + \ell_2) = 0, \\
& EI w_R'''(t, \ell_1 + \ell_M + \ell_2) + \gamma_2 I \dot{w}_R'''(t, \ell_1 + \ell_M + \ell_2) = 0, \\
& w_L(t, \ell_1) - w_R(t, \ell_1 + \ell_M) = 0, \\
& w'_L(t, \ell_1) - w'_R(t, \ell_1 + \ell_M) = 0,
\end{aligned} \tag{4.22}$$

for $0 \leq s_L \leq \ell_1$, $t > 0$, for $\ell_1 + \ell_M \leq s_R \leq \ell_1 + \ell_M + \ell_2$, and $t > 0$. These equations can be written as:

$$\begin{aligned}
& \left(\rho A - \frac{m_b}{\ell_1} \right) \ddot{w}_L(t, s_L) + \left(\gamma_1 + \frac{0.5 \rho_a v c k_2 k_3}{\ell_1} + \gamma_2 I \frac{\partial^4}{\partial s_L^4} \right) \dot{w}_L(t, s_L) + EI \frac{\partial^4}{\partial s_L^4} w_L(t, s_L) \\
&= b_L(s_L) u_L(t), \\
& \left(\rho A - \frac{m_b}{\ell_2} \right) \ddot{w}_R(t, s_R) + \left(\gamma_1 + \frac{0.5 \rho_a v c k_2 k_3}{\ell_2} + \gamma_2 I \frac{\partial^4}{\partial s_R^4} \right) \dot{w}_R(t, s_R) + EI \frac{\partial^4}{\partial s_R^4} w_R(t, s_R) \\
&= b_R(s_R) u_R(t),
\end{aligned}$$

$$\begin{aligned}
& m\ddot{w}_L(t, \ell_1) - EI \frac{\partial^3}{\partial s_L^3} w_L(t, \ell_1) - \gamma_2 I \frac{\partial^3}{\partial s_L^3} \dot{w}_L(t, \ell_1) \\
& + EI \frac{\partial^3}{\partial s_R^3} w_R(t, \ell_1 + \ell_M) + \gamma_2 I \frac{\partial^3}{\partial s_R^3} \dot{w}_R(t, \ell_1 + \ell_M) = 0,
\end{aligned}$$

$$\begin{aligned}
& I_z \frac{\partial}{\partial s_L} \ddot{w}_L(t, \ell_1) + EI \frac{\partial^2}{\partial s_L^2} w_L(t, \ell_1) + \gamma_2 I \frac{\partial^2}{\partial s_L^2} \dot{w}_L(t, \ell_1) \\
& - EI \frac{\partial^2}{\partial s_R^2} w_R(t, \ell_1 + \ell_M) - \gamma_2 I \frac{\partial^2}{\partial s_R^2} \dot{w}_R(t, \ell_1 + \ell_M) = 0.
\end{aligned}$$

$$EI \frac{\partial^2}{\partial s_L^2} w_L(t, 0) + \gamma_2 I \frac{\partial^2}{\partial s_L^2} \dot{w}_L(t, 0) = 0,$$

(4.23)

$$EI \frac{\partial^3}{\partial s_L^3} w_L(t, 0) + \gamma_2 I \frac{\partial^3}{\partial s_L^3} \dot{w}_L(t, 0) = 0,$$

$$EI \frac{\partial^2}{\partial s_R^2} w_R(t, \ell_1 + \ell_M + \ell_2) + \gamma_2 I \frac{\partial^2}{\partial s_R^2} \dot{w}_R(t, \ell_1 + \ell_M + \ell_2) = 0.$$

$$EI \frac{\partial^3}{\partial s_R^3} w_R(t, \ell_1 + \ell_M + \ell_2) + \gamma_2 I \frac{\partial^3}{\partial s_R^3} \dot{w}_R(t, \ell_1 + \ell_M + \ell_2) = 0.$$

$$w_L(t, \ell_1) - w_R(t, \ell_1 + \ell_M) = 0.$$

$$\frac{\partial}{\partial s_L} w_L(t, \ell_1) - \frac{\partial}{\partial s_R} w_R(t, \ell_1 + \ell_M) = 0.$$

We now rewrite as

$$\begin{aligned}
\dot{w}_L(t, s_L) + \left(\frac{\gamma_1}{\left(\rho A - \frac{m_b}{\ell_1}\right)} + \frac{0.5 \rho_a v c k_2 k_3}{(\ell_1 \rho A - m_b)} + \frac{\gamma_2 I}{\left(\rho A - \frac{m_b}{\ell_1}\right)} \frac{\partial^4}{\partial s_L^4} \right) \dot{w}_L(t, s_L) \\
+ \frac{EI}{\left(\rho A - \frac{m_b}{\ell_1}\right)} \frac{\partial^4}{\partial s_L^4} w_L(t, s_L) = \frac{1}{\left(\rho A - \frac{m_b}{\ell_1}\right)} b_L(s_L) u_L(t),
\end{aligned}$$

(4.24)

$$\begin{aligned}
\dot{w}_R(t, s_R) + \left(\frac{\gamma_1}{\left(\rho A - \frac{m_b}{\ell_2}\right)} + \frac{0.5 \rho_a v c k_2 k_3}{(\ell_2 \rho A - m_b)} + \frac{\gamma_2 I}{\left(\rho A - \frac{m_b}{\ell_2}\right)} \frac{\partial^4}{\partial s_R^4} \right) \dot{w}_R(t, s_R) \\
+ \frac{EI}{\left(\rho A - \frac{m_b}{\ell_2}\right)} \frac{\partial^4}{\partial s_R^4} w_R(t, s_R) = \frac{1}{\left(\rho A - \frac{m_b}{\ell_2}\right)} b_R(s_R) u_R(t),
\end{aligned}$$

$$\begin{aligned}
& \ddot{w}_L(t, \ell_1) - \frac{\gamma_2 I}{m} \frac{\partial^3}{\partial s_L^3} \dot{w}_L(t, \ell_1) + \frac{\gamma_2 I}{m} \frac{\partial^3}{\partial s_R^3} \dot{w}_R(t, \ell_1 + \ell_M) \\
& - \frac{EI}{m} \frac{\partial^3}{\partial s_L^3} w_L(t, \ell_1) + \frac{EI}{m} \frac{\partial^3}{\partial s_R^3} w_R(t, \ell_1 + \ell_M) = 0, \\
& \frac{\partial}{\partial s_L} \ddot{w}_L(t, \ell_1) + \frac{\gamma_2 I}{I_z} \frac{\partial^2}{\partial s_L^2} \dot{w}_L(t, \ell_1) - \frac{\gamma_2 I}{I_z} \frac{\partial^2}{\partial s_R^2} \dot{w}_R(t, \ell_1 + \ell_M) \\
& + \frac{EI}{I_z} \frac{\partial^2}{\partial s_L^2} w_L(t, \ell_1) - \frac{EI}{I_z} \frac{\partial^2}{\partial s_R^2} w_R(t, \ell_1 + \ell_M) = 0, \\
& \gamma_2 I \frac{\partial^2}{\partial s_L^2} \dot{w}_L(t, 0) + EI \frac{\partial^2}{\partial s_L^2} w_L(t, 0) = 0, \\
& \gamma_2 I \frac{\partial^3}{\partial s_L^3} \dot{w}_L(t, 0) + EI \frac{\partial^3}{\partial s_L^3} w_L(t, 0) = 0, \\
& \gamma_2 I \frac{\partial^2}{\partial s_R^2} \dot{w}_R(t, \ell_1 + \ell_M + \ell_2) + EI \frac{\partial^2}{\partial s_R^2} w_R(t, \ell_1 + \ell_M + \ell_2) = 0, \\
& \gamma_2 I \frac{\partial^3}{\partial s_R^3} \dot{w}_R(t, \ell_1 + \ell_M + \ell_2) + EI \frac{\partial^3}{\partial s_R^3} w_R(t, \ell_1 + \ell_M + \ell_2) = 0, \\
& w_L(t, \ell_1) - w_R(t, \ell_1 + \ell_M) = 0, \\
& \frac{\partial}{\partial s_L} w_L(t, \ell_1) - \frac{\partial}{\partial s_R} w_R(t, \ell_1 + \ell_M) = 0.
\end{aligned}$$

The state is $z(t) = (z_1(t), z_2(t), z_3(t), z_4(t))$ in S , with $z_1(t) = w_L(t, \cdot)$, $z_2(t) = w_R(t, \cdot)$, $z_3(t) = w_L(t, \ell_1)$, and $z_4(t) = w'_L(t, \ell_1)$. The inner product on S is

$$\begin{aligned}
\langle z, \tilde{z} \rangle_S &= \left\langle \left(\rho A - \frac{m_b}{\ell_1} \right) z_1, \tilde{z}_1 \right\rangle_{L_2[0, \ell_1]} + \left\langle \left(\rho A - \frac{m_b}{\ell_2} \right) z_2, \tilde{z}_2 \right\rangle_{L_2[\ell_1 + \ell_M, \ell_1 + \ell_M + \ell_2]} \\
&+ m z_3 \tilde{z}_3 + I_z z_4 \tilde{z}_4.
\end{aligned} \tag{4.25}$$

Taking an inner product of the first four equations in Equation (4.24) with a sufficiently smooth $\Phi = (\phi_1, \phi_2, \phi_3, \phi_4)$ yields the abstract form

$$\ddot{z}(t) + \mathcal{D}_{\ell_0} \dot{z}(t) + \mathcal{A}_{\ell_0} z(t) = \mathcal{B}u(t), \tag{4.26}$$

with

$$\mathcal{D}_{\ell_0} z = \begin{bmatrix} \left(\frac{\gamma_1}{\left(\rho A - \frac{m_b}{\ell_1}\right)} + \frac{0.5\rho_a v c k_2 k_3}{(\ell_1 \rho A - m_b)} + \frac{\gamma_2 I}{\left(\rho A - \frac{m_b}{\ell_1}\right)} \frac{\partial^4}{\partial s_L^4} \right) z_1(\cdot) \\ \left(\frac{\gamma_1}{\left(\rho A - \frac{m_b}{\ell_2}\right)} + \frac{0.5\rho_a v c k_2 k_3}{(\ell_2 \rho A - m_b)} + \frac{\gamma_2 I}{\left(\rho A - \frac{m_b}{\ell_2}\right)} \frac{\partial^4}{\partial s_R^4} \right) z_2(\cdot) \\ -\frac{\gamma_2 I}{m} \frac{\partial^3}{\partial s_L^3} z_1(\ell_1) + \frac{\gamma_2 I}{m} \frac{\partial^3}{\partial s_R^3} z_2(\ell_1 + \ell_M) \\ \frac{\gamma_2 I}{I_z} \frac{\partial^2}{\partial s_L^2} z_1(\ell_1) - \frac{\gamma_2 I}{I_z} \frac{\partial^2}{\partial s_R^2} z_2(\ell_1 + \ell_M) \end{bmatrix}, \quad (4.27)$$

and

$$\mathcal{A}_{\ell_0} z = \begin{bmatrix} \frac{EI}{\left(\rho A - \frac{m_b}{\ell_1}\right)} \frac{\partial^4}{\partial s_L^4} z_1(\cdot) \\ \frac{EI}{\left(\rho A - \frac{m_b}{\ell_2}\right)} \frac{\partial^4}{\partial s_R^4} z_2(\cdot) \\ -\frac{EI}{m} \frac{\partial^3}{\partial s_L^3} z_1(\ell_1) + \frac{EI}{m} \frac{\partial^3}{\partial s_R^3} z_2(\ell_1 + \ell_M) \\ \frac{EI}{I_z} \frac{\partial^2}{\partial s_L^2} z_1(\ell_1) - \frac{EI}{I_z} \frac{\partial^2}{\partial s_R^2} z_2(\ell_1 + \ell_M) \end{bmatrix}, \quad (4.28)$$

and $\mathbf{D}(\mathcal{A}_{\ell_0}) = \{z \in S : z_1 \in H^4[0, \ell_1], z_2 \in H^4[\ell_1 + \ell_M, \ell_1 + \ell_M + \ell_2],$

$$z_1(\ell_1) - z_3 = 0, z_4 - z_1'(\ell_1) = 0, z_3 - z_2(\ell_1 + \ell_M) = 0, z_2'(\ell_1 + \ell_M) - z_4 = 0\}$$

Due to the eigenvalue analysis presented in Section 4.2, $\mathcal{A}_{\ell_0} z = 0$ has a nontrivial solution and $\langle \mathcal{A}_{\ell_0} z, z \rangle_S = \langle 0, z \rangle_S = 0 \not\geq \epsilon \|z\|_S^2$ for $\epsilon > 0$. Therefore, \mathcal{A}_{ℓ_0} is not coercive in S . Consequently, we seek to choose a bounded, self-adjoint linear operator \mathcal{A}_1 so that $\tilde{\mathcal{A}} = \mathcal{A}_{\ell_0} + \mathcal{A}_1$ is coercive in S . According to [17] it is natural to choose an operator whose null space is the orthogonal complement (in S) of the eigenspace of \mathcal{A}_{ℓ_0} corresponding to nonpositive eigenvalues. That is, it is natural to choose an operator that corresponds to one's mode problem, and in [17], [19], [26] this

was the motivation for choosing \mathcal{A}_1 . However, such an approach is not natural for the BMB model under consideration due to the fact that the mode problem occurs at the essential boundary conditions, and only natural boundary conditions can be included in the \mathcal{A}_{ℓ_0} operator via the finite element method.

Let $\mathcal{A}_1 = \mathcal{I}$, where \mathcal{I} is the identity operator. Note that there is no physical significance to this chosen operator. Clearly \mathcal{I} is linear, bounded, and self-adjoint. Furthermore, \mathcal{I} is positive definite for any $z \in S$. Then $V = V_2 = \mathbf{D}(\tilde{\mathcal{A}}_{\ell_0}^{1/2}) = \mathbf{D}(\mathcal{A}_{\ell_0}^{1/2})$ which is contained in the set $\{z \in S : z_1 \in H^2[0, \ell_1], z_2 \in H^2[\ell_1 + \ell_M, \ell_1 + \ell_M + \ell_2], z_1(\ell_1) - z_3 = 0, z_4 - z'_1(\ell_1) = 0, z_3 - z_2(\ell_1 + \ell_M) = 0, z'_2(\ell_1 + \ell_M) - z_4 = 0\}$, and $\mathbf{D}(\mathcal{D}_{\ell_0}) = \mathbf{D}(\mathcal{A}_{\ell_0})$. The inner product on V can be taken to be

$$\begin{aligned} \langle z, \tilde{z} \rangle_V &= \left\langle \tilde{\mathcal{A}}^{\frac{1}{2}} z, \tilde{\mathcal{A}}^{\frac{1}{2}} \tilde{z} \right\rangle_S \\ &= \left\langle \tilde{\mathcal{A}} z, \tilde{z} \right\rangle_S \\ &= \langle EI z''_1, \tilde{z}'_1 \rangle_{L_2[0, \ell_1]} + \langle EI z''_2, \tilde{z}''_2 \rangle_{L_2[\ell_1 + \ell_M, \ell_1 + \ell_M + \ell_2]} + \langle \mathcal{A}_1 z, \tilde{z} \rangle_S. \end{aligned} \tag{4.29}$$

To verify coercivity, we must first verify that $\tilde{\mathcal{A}}$ is self-adjoint.

Theorem 4.13. *$\tilde{\mathcal{A}}$ is self-adjoint with respect to the inner product on S .*

Proof. We begin by first showing that \mathcal{A}_{ℓ_0} is self-adjoint. The density of the domain of \mathcal{A}_{ℓ_0} is verified later on. This proof follows similarly to the self-adjointness proofs provided in [19], [26], and [18]. We must determine $\mathcal{A}_{\ell_0}^*$ and $\mathbf{D}(\mathcal{A}_{\ell_0}^*)$. Assume there exists a $\tilde{\Phi} \in S$ such that

$$\langle \mathcal{A}_{\ell_0} z, \tilde{\Phi} \rangle_S - \langle z, \tilde{\Phi} \rangle_S = 0 \text{ for all } z \in \mathbf{D}(\mathcal{A}_{\ell_0}). \tag{4.30}$$

Note that Φ belongs to $\mathbf{D}(\mathcal{A}_{\ell_0}^*)$ if there exists a $\tilde{\Phi} \in S$ so that Equation (4.30) holds

(see [13]). Expanding this in terms of the inner product on S yields

$$\begin{aligned}
& EI \int_0^{\ell_1} z_1''''(s_L) \phi_1(s_L) ds_L + EI \int_{\ell_1+\ell_M}^{\ell_1+\ell_M+\ell_2} z_2''''(s_R) \phi_2(s_R) ds_R \\
& - EI z_1'''(\ell_1) \phi_3 + EI z_2'''(\ell_1 + \ell_M) \phi_3 + EI z_1''(\ell_1) \phi_4 - EI z_2''(\ell_1 + \ell_M) \phi_4 \\
& - \left[\left(\rho A - \frac{m_b}{\ell_1} \right) \int_0^{\ell_1} z_1(s_L) \tilde{\phi}_1(s_L) ds_L \right. \\
& \left. + \left(\rho A - \frac{m_b}{\ell_2} \right) \int_{\ell_1+\ell_M}^{\ell_1+\ell_M+\ell_2} z_2(s_R) \tilde{\phi}_2(s_R) ds_R + m z_3 \tilde{\phi}_3 + I_z z_4 \tilde{\phi}_4 \right] = 0.
\end{aligned} \tag{4.31}$$

Next integration by parts (coupled with the Fundamental Theorem of Calculus) is applied four times to the last two integrals in Equation (4.31). Note the parameters used below are the same for both the left and right beams, although due to the separate spacial domains this is not necessarily the case, but provides an ease of notation.

$$\begin{aligned}
& EI \int_0^{\ell_1} z_1''''(s_L) \phi_1(s_L) ds_L + EI \int_{\ell_1+\ell_M}^{\ell_1+\ell_M+\ell_2} z_2''''(s_R) \phi_2(s_R) ds_R \\
& - EI z_1'''(\ell_1) \phi_3 + EI z_2'''(\ell_1 + \ell_M) \phi_3 + EI z_1''(\ell_1) \phi_4 - EI z_2''(\ell_1 + \ell_M) \phi_4 \\
& - \left[\left(\rho A - \frac{m_b}{\ell_1} \right) \left[z_1(s_L) \int_0^{s_L} \tilde{\phi}_1(\iota) d\iota \Big|_0^{\ell_1} - z_1'(s_L) \int_0^{s_L} \int_0^\iota \tilde{\phi}_1(\varsigma) d\varsigma d\iota \Big|_0^{\ell_1} \right. \right. \\
& \quad \left. \left. + z_1''(s_L) \int_0^{s_L} \int_0^\iota \int_0^\varsigma \tilde{\phi}_1(\chi) d\chi d\varsigma d\iota \Big|_0^{\ell_1} \right. \right. \\
& \quad \left. \left. - z_1'''(s_L) \int_0^{s_L} \int_0^\iota \int_0^\varsigma \int_0^\chi \tilde{\phi}_1(\tau) d\tau d\chi d\varsigma d\iota \Big|_0^{\ell_1} \right] \tag{4.32} \\
& + \int_0^{\ell_1} \int_0^{s_L} \int_0^\iota \int_0^\varsigma \int_0^\chi \tilde{\phi}_1(\tau) d\tau d\chi d\varsigma d\iota z_1''''(s_L) ds_L \\
& + \left(\rho A - \frac{m_b}{\ell_2} \right) \left[z_2(s_R) \int_{\ell_1+\ell_M}^{s_R} \tilde{\phi}_2(\iota) d\iota \Big|_{\ell_1+\ell_M}^{\ell_1+\ell_M+\ell_2} \right. \\
& \quad \left. - z_2'(s_R) \int_{\ell_1+\ell_M}^{s_R} \int_{\ell_1+\ell_M}^\iota \tilde{\phi}_2(\varsigma) d\varsigma d\iota \Big|_{\ell_1+\ell_M}^{\ell_1+\ell_M+\ell_2} \right]
\end{aligned}$$

$$\begin{aligned}
& + z_2''(s_R) \int_{\ell_1+\ell_M}^{s_R} \int_{\ell_1+\ell_M}^{\iota} \int_{\ell_1+\ell_M}^{\varsigma} \tilde{\phi}_2(\chi) d\chi d\varsigma d\iota \Big|_{\ell_1+\ell_M}^{\ell_1+\ell_M+\ell_2} \\
& - z_2'''(s_R) \int_{\ell_1+\ell_M}^{s_R} \int_{\ell_1+\ell_M}^{\iota} \int_{\ell_1+\ell_M}^{\varsigma} \int_{\ell_1+\ell_M}^{\chi} \tilde{\phi}_2(\tau) d\tau d\chi d\varsigma d\iota \Big|_{\ell_1+\ell_M}^{\ell_1+\ell_M+\ell_2} \\
& + \int_{\ell_1+\ell_M}^{\ell_1+\ell_M+\ell_2} \int_{\ell_1+\ell_M}^{s_R} \int_{\ell_1+\ell_M}^{\iota} \int_{\ell_1+\ell_M}^{\varsigma} \int_{\ell_1+\ell_M}^{\chi} \tilde{\phi}_2(\tau) d\tau d\chi d\varsigma d\iota z_2''''(s_R) ds_R \\
& \quad + m z_3 \tilde{\phi}_3 + I_z z_4 \tilde{\phi}_4 \Big] = 0.
\end{aligned}$$

Rearranging terms yields:

$$\begin{aligned}
& \int_0^{\ell_1} [EI z_1''''(s_L) \phi_1(s_L) \\
& - \left(\rho A - \frac{m_b}{\ell_1} \right) \int_0^{s_L} \int_0^{\iota} \int_0^{\varsigma} \int_0^{\chi} \tilde{\phi}_1(\tau) d\tau d\chi d\varsigma d\iota z_1''''(s_L)] ds_L \\
& \quad + \int_{\ell_1+\ell_M}^{\ell_1+\ell_M+\ell_2} [EI z_2''''(s_R) \phi_2(s_R) \\
& - \left(\rho A - \frac{m_b}{\ell_2} \right) \int_{\ell_1+\ell_M}^{s_R} \int_{\ell_1+\ell_M}^{\iota} \int_{\ell_1+\ell_M}^{\varsigma} \int_{\ell_1+\ell_M}^{\chi} \tilde{\phi}_2(\tau) d\tau d\chi d\varsigma d\iota z_2''''(s_R)] ds_R \\
& - \left(\rho A - \frac{m_b}{\ell_1} \right) \left[z_1(s_L) \int_0^{s_L} \tilde{\phi}_1(\iota) d\iota \Big|_0^{\ell_1} - z_1'(s_L) \int_0^{s_L} \int_0^{\iota} \tilde{\phi}_1(\varsigma) d\varsigma d\iota \Big|_0^{\ell_1} \right. \\
& \quad + z_1''(s_L) \int_0^{s_L} \int_0^{\iota} \int_0^{\varsigma} \tilde{\phi}_1(\chi) d\chi d\varsigma d\iota \Big|_0^{\ell_1} \\
& \quad \left. - z_1'''(s_L) \int_0^{s_L} \int_0^{\iota} \int_0^{\varsigma} \int_0^{\chi} \tilde{\phi}_1(\tau) d\tau d\chi d\varsigma d\iota \Big|_0^{\ell_1} \right] \tag{4.33} \\
& - \left(\rho A - \frac{m_b}{\ell_2} \right) \left[z_2(s_R) \int_{\ell_1+\ell_M}^{s_R} \tilde{\phi}_2(\iota) d\iota \Big|_{\ell_1+\ell_M}^{\ell_1+\ell_M+\ell_2} \right. \\
& \quad - z_2'(s_R) \int_{\ell_1+\ell_M}^{s_R} \int_{\ell_1+\ell_M}^{\iota} \tilde{\phi}_2(\varsigma) d\varsigma d\iota \Big|_{\ell_1+\ell_M}^{\ell_1+\ell_M+\ell_2} \\
& \quad + z_2''(s_R) \int_{\ell_1+\ell_M}^{s_R} \int_{\ell_1+\ell_M}^{\iota} \int_{\ell_1+\ell_M}^{\varsigma} \tilde{\phi}_2(\chi) d\chi d\varsigma d\iota \Big|_{\ell_1+\ell_M}^{\ell_1+\ell_M+\ell_2} \\
& \quad \left. - z_2'''(s_R) \int_{\ell_1+\ell_M}^{s_R} \int_{\ell_1+\ell_M}^{\iota} \int_{\ell_1+\ell_M}^{\varsigma} \int_{\ell_1+\ell_M}^{\chi} \tilde{\phi}_2(\tau) d\tau d\chi d\varsigma d\iota \Big|_{\ell_1+\ell_M}^{\ell_1+\ell_M+\ell_2} \right] \\
& + [-EI z_1''''(\ell_1) + EI z_2''''(\ell_1 + \ell_M)] \phi_3 + [EI z_1''(\ell_1) - EI z_2''(\ell_1 + \ell_M)] \phi_4 \\
& \quad - [m z_3 \tilde{\phi}_3 + I_z z_4 \tilde{\phi}_4] = 0.
\end{aligned}$$

Next we consider the set $D_1 = \{z \in S : z_1 \in H_0^4[0, \ell_1], z_2 = z_3 = z_4 = 0\} \subset \mathbf{D}(\mathcal{A}_{\ell_0})$.

Then Equation (4.33) holds for all $z \in D_1$, and

$$\int_0^{\ell_1} z_1''''(s_L) \left[EI\phi_1(s_L) - \left(\rho A - \frac{m_b}{\ell_1} \right) \int_0^{s_L} \int_0^\iota \int_0^\varsigma \int_0^\chi \tilde{\phi}_1(\tau) d\tau d\chi d\varsigma d\iota \right] ds_L = 0. \quad (4.34)$$

Applying Lemma 4.10, we conclude

$$EI\phi_1(s_L) - \left(\rho A - \frac{m_b}{\ell_1} \right) \int_0^{s_L} \int_0^\iota \int_0^\varsigma \int_0^\chi \tilde{\phi}_1(\tau) d\tau d\chi d\varsigma d\iota = as_L^3 + bs_L^2 + cs_L + d, \quad (4.35)$$

for some constants a, b, c , and d . Consequently,

$$\phi_1(s_L) = \frac{\left(\rho A - \frac{m_b}{\ell_1} \right)}{EI} \int_0^{s_L} \int_0^\iota \int_0^\varsigma \int_0^\chi \tilde{\phi}_1(\tau) d\tau d\chi d\varsigma d\iota + as_L^3 + bs_L^2 + cs_L + d. \quad (4.36)$$

This implies that $\phi_1 \in H^4$, and ϕ_1 can be differentiated four times to obtain

$$\phi_1''''(s_L) = \frac{\left(\rho A - \frac{m_b}{\ell_1} \right)}{EI} \tilde{\phi}_1 \quad (4.37)$$

or

$$\tilde{\phi}_1 = \frac{EI}{\left(\rho A - \frac{m_b}{\ell_1} \right)} \phi_1''''(s_L). \quad (4.38)$$

Similarly, $\mathbf{D}(\mathcal{A}_{\ell_0})$ includes the set $D_2 = \{z \in S : z_2 \in H_0^4[\ell_1 + \ell_M, \ell_1 + \ell_M + \ell_2],$

$z_1 = z_3 = z_4 = 0\}$. Therefore,

$$\int_{\ell_1 + \ell_M}^{\ell_1 + \ell_M + \ell_2} z_2''''(s_R) \left[EI\phi_2(s_R) - \left(\rho A - \frac{m_b}{\ell_2} \right) \int_{\ell_1 + \ell_M}^{s_R} \int_{\ell_1 + \ell_M}^\iota \int_{\ell_1 + \ell_M}^\varsigma \int_{\ell_1 + \ell_M}^\chi \tilde{\phi}_2(\tau) d\tau d\chi d\varsigma d\iota \right] ds_R = 0. \quad (4.39)$$

Again we apply Lemma 4.10.

$$\begin{aligned} EI\phi_2(s_R) - \left(\rho A - \frac{m_b}{\ell_2} \right) \int_{\ell_1 + \ell_M}^{s_R} \int_{\ell_1 + \ell_M}^\iota \int_{\ell_1 + \ell_M}^\varsigma \int_{\ell_1 + \ell_M}^\chi \tilde{\phi}_2(\tau) d\tau d\chi d\varsigma d\iota \\ = a_0 s_R^3 + b_0 s_R^2 + c_0 s_R + d_0, \end{aligned} \quad (4.40)$$

for constants a_0, b_0, c_0 , and d_0 . Then the following holds:

$$\begin{aligned} \phi_2(s_R) = & \frac{\left(\rho A - \frac{m_b}{\ell_2}\right)}{EI} \int_{\ell_1+\ell_M}^{s_R} \int_{\ell_1+\ell_M}^{\iota} \int_{\ell_1+\ell_M}^{\varsigma} \int_{\ell_1+\ell_M}^{\chi} \tilde{\phi}_2(\tau) d\tau d\chi d\varsigma d\iota \\ & + a_0 s_R^3 + b_0 s_R^2 + c_0 s_R + d_0. \end{aligned} \quad (4.41)$$

Thus $\phi_2 \in H^4$ and ϕ_2 can be differentiated four times to yield

$$\phi_2''''(s_R) = \frac{\left(\rho A - \frac{m_b}{\ell_2}\right)}{EI} \tilde{\phi}_2 \quad (4.42)$$

or

$$\tilde{\phi}_2 = \frac{EI}{\left(\rho A - \frac{m_b}{\ell_2}\right)} \phi_2''''(s_R). \quad (4.43)$$

We now substitute Equation (4.38) and Equation (4.43) into Equation (4.31).

$$\begin{aligned} & EI \int_0^{\ell_1} z_1''''(s_L) \phi_1(s_L) ds_L + EI \int_{\ell_1+\ell_M}^{\ell_1+\ell_M+\ell_2} z_2''''(s_R) \phi_2(s_R) ds_R \\ & - EI z_1'''(\ell_1) \phi_3 + EI z_2'''(\ell_1 + \ell_M) \phi_3 + EI z_1''(\ell_1) \phi_4 - EI z_2''(\ell_1 + \ell_M) \phi_4 \\ & - \left[\left(\rho A - \frac{m_b}{\ell_1}\right) \int_0^{\ell_1} z_1(s_L) \frac{EI}{\left(\rho A - \frac{m_b}{\ell_1}\right)} \phi_1''''(s_L) ds_L \right. \\ & \left. + \left(\rho A - \frac{m_b}{\ell_2}\right) \int_{\ell_1+\ell_M}^{\ell_1+\ell_M+\ell_2} z_2(s_R) \frac{EI}{\left(\rho A - \frac{m_b}{\ell_2}\right)} \phi_2''''(s_R) ds_R \right] \\ & - m z_3 \tilde{\phi}_3 - I_z z_4 \tilde{\phi}_4 = 0. \end{aligned} \quad (4.44)$$

Integration by parts is applied four times to the first two integrals in Equation (4.44).

$$\begin{aligned} & EI \int_0^{\ell_1} z_1(s_L) \phi_1''''(s_L) ds_L + EI \int_{\ell_1+\ell_M}^{\ell_1+\ell_M+\ell_2} z_2(s_R) \phi_2''''(s_R) ds_R \\ & - \left(\rho A - \frac{m_b}{\ell_1}\right) \int_0^{\ell_1} z_1(s_L) \frac{EI}{\rho A - \frac{m_b}{\ell_1}} \phi_1''''(s_L) ds_L \\ & - \left(\rho A - \frac{m_b}{\ell_2}\right) \int_{\ell_1+\ell_M}^{\ell_1+\ell_M+\ell_2} z_2(s_R) \frac{EI}{\rho A - \frac{m_b}{\ell_2}} \phi_2''''(s_R) ds_R \\ & + EI \left[z_1'''(s_L) \phi_1(s_L) \Big|_0^{\ell_1} - z_1''(s_L) \phi_1'(s_L) \Big|_0^{\ell_1} + z_1'(s_L) \phi_1''(s_L) \Big|_0^{\ell_1} \right. \end{aligned} \quad (4.45)$$

$$\begin{aligned}
& -z_1(s_L)\phi_1'''(s_L)\Big|_0^{\ell_1} + EI \left[z_2'''(s_R)\phi_2(s_R)\Big|_{\ell_1+\ell_M}^{\ell_1+\ell_M+\ell_2} - z_2''(s_R)\phi_2'(s_R)\Big|_{\ell_1+\ell_M}^{\ell_1+\ell_M+\ell_2} \right. \\
& \quad \left. + z_2'(s_R)\phi_2''(s_R)\Big|_{\ell_1+\ell_M}^{\ell_1+\ell_M+\ell_2} - z_2(s_R)\phi_2'''(s_R)\Big|_{\ell_1+\ell_M}^{\ell_1+\ell_M+\ell_2} \right] - EI z_1'''(\ell_1)\phi_3 \\
& + EI z_2'''(\ell_1 + \ell_M)\phi_3 + EI z_1''(\ell_1)\phi_4 - EI z_2''(\ell_1 + \ell_M)\phi_4 - mz_3\tilde{\phi}_3 - I_z z_4\tilde{\phi}_4 \\
& = 0.
\end{aligned}$$

The first four terms in Equation (4.45) cancel. Applying properties of $\mathbf{D}(\mathcal{A}_{\ell_0})$ to ϕ cancels additional terms, and Equation (4.45) can be regrouped to become

$$\begin{aligned}
& -EI z_1'''(0)\phi_1(0) + EI z_1''(0)\phi_1'(0) - EI z_1'(0)\phi_1''(0) + EI z_1(0)\phi_1'''(0) \\
& \quad + EI z_2'''(\ell_1 + \ell_M + \ell_2)\phi_2(\ell_1 + \ell_M + \ell_2) \\
& \quad - EI z_2''(\ell_1 + \ell_M + \ell_2)\phi_2'(\ell_1 + \ell_M + \ell_2) \\
& \quad + EI z_2'(\ell_1 + \ell_M + \ell_2)\phi_2''(\ell_1 + \ell_M + \ell_2) \\
& \quad - EI z_2(\ell_1 + \ell_M + \ell_2)\phi_2'''(\ell_1 + \ell_M + \ell_2) \\
& \quad + z_3 \left[EI\phi_2'''(\ell_1 + \ell_M) - EI\phi_1'''(\ell_1) - m\tilde{\phi}_3 \right] \\
& \quad + z_4 \left[EI\phi_1''(\ell_1) - EI\phi_2''(\ell_1 + \ell_M) - I_z\tilde{\phi}_4 \right] \\
& = 0
\end{aligned} \tag{4.46}$$

Since Equation (4.46) must hold for all $z \in S$, we can infer that

$$z_3 \left[EI\phi_2'''(\ell_1 + \ell_M) - EI\phi_1'''(\ell_1) - m\tilde{\phi}_3 \right] = 0 \tag{4.47}$$

and

$$z_4 \left[EI\phi_1''(\ell_1) - EI\phi_2''(\ell_1 + \ell_M) - I_z\tilde{\phi}_4 \right] = 0, \tag{4.48}$$

and the remaining terms in Equation (4.46) sum to zero. This implies

$$\tilde{\phi}_3 = \frac{EI}{m} [\phi_2'''(\ell_1 + \ell_M) - \phi_1'''(\ell_1)] \quad (4.49)$$

and

$$\tilde{\phi}_4 = \frac{EI}{I_z} [\phi_2''(\ell_1) - \phi_1''(\ell_1 + \ell_M)]. \quad (4.50)$$

We consider subsets of the domain of \mathcal{A}_{ℓ_0} from which terms of z cancel, and infer that

$$\begin{aligned} \mathbf{D}(\mathcal{A}_{\ell_0}^*) &\subseteq \{ \Phi \in S : \phi_1 \in H^4[0, \ell_1], \phi_2 \in H^4[\ell_1 + \ell_M, \ell_1 + \ell_M + \ell_2], \\ &\phi_1(\ell_1) - \phi_3 = 0, \phi_4 - \phi_1'(\ell_1) = 0, \\ &\phi_3 - \phi_2(\ell_1 + \ell_M) = 0, \phi_2'(\ell_1 + \ell_M) - \phi_4 = 0 \} \\ &= \mathbf{D}(\mathcal{A}_{\ell_0}), \end{aligned} \quad (4.51)$$

and the reverse containment is clear. Thus,

$$\mathcal{A}_{\ell_0}^* \Phi = \tilde{\Phi} = \begin{bmatrix} \frac{EI}{\left(\rho A - \frac{m_b}{\ell_1}\right)} \phi_1'''(s_L) \\ \frac{EI}{\left(\rho A - \frac{m_b}{\ell_2}\right)} \phi_2'''(s_R) \\ -\frac{EI}{m} \phi_1'''(\ell_1) + \frac{EI}{m} \phi_2'''(\ell_1 + \ell_M) \\ \frac{EI}{I_z} \phi_1''(\ell_1) - \frac{EI}{I_z} \phi_2''(\ell_1 + \ell_M) \end{bmatrix} = \mathcal{A}_{\ell_0} \Phi. \quad (4.52)$$

Therefore, $\mathbf{D}(\mathcal{A}_{\ell_0}^*) = \mathbf{D}(\mathcal{A}_{\ell_0})$, $\mathcal{A}_{\ell_0}^* \Phi = \mathcal{A}_{\ell_0} \Phi$ for all $\Phi \in \mathbf{D}(\mathcal{A}_{\ell_0})$ and \mathcal{A}_{ℓ_0} is self-adjoint.

By applying Theorem 4.12, $\tilde{\mathcal{A}}$ is self-adjoint. \square

Theorem 4.14. $\tilde{\mathcal{A}}$ is coercive in S .

Proof.

$$\begin{aligned} \langle \tilde{\mathcal{A}}z, z \rangle_S &= \langle z, z \rangle_V \\ &= \langle EI z_1'', z_1'' \rangle_{L_2[0, \ell_1]} + \langle EI z_2'', z_2'' \rangle_{L_2[\ell_1 + \ell_M, \ell_1 + \ell_M + \ell_2]} + \langle \mathcal{A}_1 z, z \rangle_S \\ &= \langle EI z_1'', z_1'' \rangle_{L_2[0, \ell_1]} + \langle EI z_2'', z_2'' \rangle_{L_2[\ell_1 + \ell_M, \ell_1 + \ell_M + \ell_2]} + \langle \mathcal{I}z, z \rangle_S \end{aligned} \quad (4.53)$$

$$\begin{aligned}
&= \langle EIZ_1'', z_1'' \rangle_{L_2[0, \ell_1]} + \langle EIZ_2'', z_2'' \rangle_{L_2[\ell_1 + \ell_M, \ell_1 + \ell_M + \ell_2]} \\
&\quad + \left\langle \left(\rho A - \frac{m_b}{\ell_1} \right) z_1, z_1 \right\rangle_{L_2[0, \ell_1]} \\
&\quad + \left\langle \left(\rho A - \frac{m_b}{\ell_2} \right) z_2, z_2 \right\rangle_{L_2[\ell_1 + \ell_M, \ell_1 + \ell_M + \ell_2]} + mz_3z_3 + I_z z_4 z_4 \\
&\geq \epsilon \left\langle \left(\rho A - \frac{m_b}{\ell_1} \right) z_1, z_1 \right\rangle_{L_2[0, \ell_1]} \\
&\quad + \epsilon \left\langle \left(\rho A - \frac{m_b}{\ell_2} \right) z_2, z_2 \right\rangle_{L_2[\ell_1 + \ell_M, \ell_1 + \ell_M + \ell_2]} + \epsilon m z_3 z_3 + \epsilon I_z z_4 z_4 \\
&= \epsilon \langle z, z \rangle_S \\
&= \epsilon \|z\|_S^2 \text{ for } 0 < \epsilon \leq 1.
\end{aligned}$$

□

Let $\Phi \in V$ and $z \in \mathbf{D}(\mathcal{A}_{\ell_0})$. Next we determine the sesquilinear forms associated with $\tilde{\mathcal{A}}$ and $\tilde{\mathcal{D}} = \mathcal{D}_{\ell_0} + \mathcal{A}_1$. First consider

$$\begin{aligned}
\langle \mathcal{A}_{\ell_0} z, \Phi \rangle_S &= \langle EIZ_1''', \phi_1 \rangle_{L_2[0, \ell_1]} + \langle EIZ_2''', \phi_2 \rangle_{L_2[\ell_1 + \ell_M, \ell_1 + \ell_M + \ell_2]} \\
&\quad - EIZ_1'''(\ell_1)\phi_3 + EIZ_2'''(\ell_1 + \ell_M)\phi_3 + EIZ_1''(\ell_1)\phi_4 \\
&\quad - EIZ_2''(\ell_1 + \ell_M)\phi_4.
\end{aligned} \tag{4.54}$$

Integrating by parts twice results in

$$\begin{aligned}
\langle \mathcal{A}_{\ell_0} z, \Phi \rangle_S &= \langle EIZ_1'', \phi_1'' \rangle_{L_2[0, \ell_1]} + \langle EIZ_2'', \phi_2'' \rangle_{L_2[\ell_1 + \ell_M, \ell_1 + \ell_M + \ell_2]} \\
&\quad + EIZ_1'''(s_L)\phi_1(s_L) \Big|_0^{\ell_1} - EIZ_1''(s_L)\phi_1'(s_L) \Big|_0^{\ell_1} \\
&\quad + EIZ_2'''(s_R)\phi_2(s_R) \Big|_{\ell_1 + \ell_M}^{\ell_1 + \ell_M + \ell_2} - EIZ_2''(s_R)\phi_2'(s_R) \Big|_{\ell_1 + \ell_M}^{\ell_1 + \ell_M + \ell_2} \\
&\quad - EIZ_1'''(\ell_1)\phi_3 + EIZ_2'''(\ell_1 + \ell_M)\phi_3 + EIZ_1''(\ell_1)\phi_4 \\
&\quad - EIZ_2''(\ell_1 + \ell_M)\phi_4.
\end{aligned} \tag{4.55}$$

This is equivalent to

$$\begin{aligned}
\langle \mathcal{A}_{\ell_0} z, \Phi \rangle_S &= \langle EI z_1'', \phi_1'' \rangle_{L_2[0, \ell_1]} + \langle EI z_2'', \phi_2'' \rangle_{L_2[\ell_1 + \ell_M, \ell_1 + \ell_M + \ell_2]} \\
&\quad + EI z_1'''(\ell_1) \phi_1(\ell_1) - EI z_1'''(0) \phi_1(0) - EI z_1''(\ell_1) \phi_1'(\ell_1) \\
&\quad + EI z_1''(0) \phi_1'(0) + EI z_2'''(\ell_1 + \ell_M + \ell_2) \phi_2(\ell_1 + \ell_M + \ell_2) \\
&\quad - EI z_2'''(\ell_1 + \ell_M) \phi_2(\ell_1 + \ell_M) \\
&\quad - EI z_2''(\ell_1 + \ell_M + \ell_2) \phi_2'(\ell_1 + \ell_M + \ell_2) \\
&\quad + EI z_2''(\ell_1 + \ell_M) \phi_2'(\ell_1 + \ell_M) - EI z_1'''(\ell_1) \phi_3 \\
&\quad + EI z_2'''(\ell_1 + \ell_M) \phi_3 + EI z_1''(\ell_1) \phi_4 - EI z_2''(\ell_1 + \ell_M) \phi_4.
\end{aligned} \tag{4.56}$$

Regrouping terms yields

$$\begin{aligned}
\langle \mathcal{A}_{\ell_0} z, \Phi \rangle_S &= \langle EI z_1'', \phi_1'' \rangle_{L_2[0, \ell_1]} + \langle EI z_2'', \phi_2'' \rangle_{L_2[\ell_1 + \ell_M, \ell_1 + \ell_M + \ell_2]} \\
&\quad + EI [z_1'''(\ell_1) \phi_1(\ell_1) - z_1'''(0) \phi_1(0) \\
&\quad - z_1''(\ell_1) \phi_1'(\ell_1) + z_1''(0) \phi_1'(0) - z_1'''(\ell_1) \phi_3 + z_1''(\ell_1) \phi_4] \\
&\quad + EI [z_2'''(\ell_1 + \ell_M + \ell_2) \phi_2(\ell_1 + \ell_M + \ell_2) \\
&\quad - z_2'''(\ell_1 + \ell_M) \phi_2(\ell_1 + \ell_M) \\
&\quad - z_2''(\ell_1 + \ell_M + \ell_2) \phi_2'(\ell_1 + \ell_M + \ell_2) \\
&\quad + z_2''(\ell_1 + \ell_M) \phi_2'(\ell_1 + \ell_M) \\
&\quad + z_2'''(\ell_1 + \ell_M) \phi_3 - z_2''(\ell_1 + \ell_M) \phi_4].
\end{aligned} \tag{4.57}$$

Regrouping further we obtain

$$\begin{aligned}
\langle \mathcal{A}_{\ell_0} z, \Phi \rangle_S &= \langle EI z_1'', \phi_1'' \rangle_{L_2[0, \ell_1]} + \langle EI z_2'', \phi_2'' \rangle_{L_2[\ell_1 + \ell_M, \ell_1 + \ell_M + \ell_2]} \\
&\quad + EI [z_1'''(\ell_1) (\phi_1(\ell_1) - \phi_3) - z_1'''(0) \phi_1(0) \\
&\quad + z_1''(\ell_1) (\phi_4 - \phi_1'(\ell_1)) + z_1''(0) \phi_1'(0)] \\
&\quad + EI [z_2'''(\ell_1 + \ell_M + \ell_2) \phi_2(\ell_1 + \ell_M + \ell_2) \\
&\quad - z_2''(\ell_1 + \ell_M + \ell_2) \phi_2'(\ell_1 + \ell_M + \ell_2)
\end{aligned} \tag{4.58}$$

$$\begin{aligned}
& +z_2'''(\ell_1 + \ell_M) (\phi_3 - \phi_2(\ell_1 + \ell_M)) \\
& +z_2''(\ell_1 + \ell_M) (\phi_2'(\ell_1 + \ell_M) - \phi_4)].
\end{aligned}$$

Since $\Phi \in V$ substitutions are made into the boundary terms arising from the definition of the state z and the boundary conditions for displacement and slope at the mass location, resulting in

$$\begin{aligned}
\langle \mathcal{A}_{\ell_0} z, \Phi \rangle_S &= \langle EI z_1'', \phi_1'' \rangle_{L_2[0, \ell_1]} + \langle EI z_2'', \phi_2'' \rangle_{L_2[\ell_1 + \ell_M, \ell_1 + \ell_M + \ell_2]} \\
& - EI z_1'''(0) \phi_1(0) + EI z_1''(0) \phi_1'(0) \\
& + EI z_2'''(\ell_1 + \ell_M + \ell_2) \phi_2(\ell_1 + \ell_M + \ell_2) \\
& - EI z_2''(\ell_1 + \ell_M + \ell_2) \phi_2'(\ell_1 + \ell_M + \ell_2).
\end{aligned} \tag{4.59}$$

Now consider

$$\begin{aligned}
\langle \mathcal{D}_{\ell_0} z, \Phi \rangle_S &= \langle \gamma_1 z_1, \phi_1 \rangle_{L_2[0, \ell_1]} + \left\langle \frac{0.5 \rho_a v c k_2 k_3}{\ell_1} z_1, \phi_1 \right\rangle_{L_2[0, \ell_1]} \\
& + \langle \gamma_2 I z_1'''' , \phi_1 \rangle_{L_2[0, \ell_1]} + \langle \gamma_1 z_2, \phi_2 \rangle_{L_2[\ell_1 + \ell_M, \ell_1 + \ell_M + \ell_2]} \\
& + \left\langle \frac{0.5 \rho_a v c k_2 k_3}{\ell_2} z_2, \phi_2 \right\rangle_{L_2[\ell_1 + \ell_M, \ell_1 + \ell_M + \ell_2]} \\
& + \langle \gamma_2 I z_2'''' , \phi_2 \rangle_{L_2[\ell_1 + \ell_M, \ell_1 + \ell_M + \ell_2]} - \gamma_2 I z_1'''(\ell_1) \phi_3 \\
& + \gamma_2 I z_2'''(\ell_1 + \ell_M) \phi_3 + \gamma_2 I z_1''(\ell_1) \phi_4 - \gamma_2 I z_2''(\ell_1 + \ell_M) \phi_4.
\end{aligned} \tag{4.60}$$

Integrating by parts twice results in

$$\begin{aligned}
\langle \mathcal{D}_{\ell_0} z, \Phi \rangle_S &= \langle \gamma_1 z_1, \phi_1 \rangle_{L_2[0, \ell_1]} + \left\langle \frac{0.5 \rho_a v c k_2 k_3}{\ell_1} z_1, \phi_1 \right\rangle_{L_2[0, \ell_1]} \\
& + \langle \gamma_1 z_2, \phi_2 \rangle_{L_2[\ell_1 + \ell_M, \ell_1 + \ell_M + \ell_2]} \\
& + \left\langle \frac{0.5 \rho_a v c k_2 k_3}{\ell_2} z_2, \phi_2 \right\rangle_{L_2[\ell_1 + \ell_M, \ell_1 + \ell_M + \ell_2]} \\
& - \gamma_2 I z_1'''(\ell_1) \phi_3 + \gamma_2 I z_2'''(\ell_1 + \ell_M) \phi_3 + \gamma_2 I z_1''(\ell_1) \phi_4 \\
& - \gamma_2 I z_2''(\ell_1 + \ell_M) \phi_4 + \langle \gamma_2 I z_1'', \phi_1'' \rangle_{L_2[0, \ell_1]}
\end{aligned} \tag{4.61}$$

$$\begin{aligned}
& + \langle \gamma_2 I z_2'', \phi_2'' \rangle_{L_2[\ell_1+\ell_M, \ell_1+\ell_M+\ell_2]} + \gamma_2 I z_1'''(\ell_1) \phi_1(\ell_1) \\
& - \gamma_2 I z_1'''(0) \phi_1(0) - \gamma_2 I z_1''(\ell_1) \phi_1'(\ell_1) + \gamma_2 I z_1''(0) \phi_1'(0) \\
& + \gamma_2 I z_2'''(\ell_1 + \ell_M + \ell_2) \phi_2(\ell_1 + \ell_M + \ell_2) \\
& - \gamma_2 I z_2'''(\ell_1 + \ell_M) \phi_2(\ell_1 + \ell_M) \\
& - \gamma_2 I z_2''(\ell_1 + \ell_M + \ell_2) \phi_2'(\ell_1 + \ell_M + \ell_2) \\
& + \gamma_2 I z_2''(\ell_1 + \ell_M) \phi_2'(\ell_1 + \ell_M).
\end{aligned}$$

Regrouping terms yields

$$\begin{aligned}
\langle \mathcal{D}_{\ell_0} z, \Phi \rangle_S & = \langle \gamma_1 z_1, \phi_1 \rangle_{L_2[0, \ell_1]} + \langle \gamma_1 z_2, \phi_2 \rangle_{L_2[\ell_1+\ell_M, \ell_1+\ell_M+\ell_2]} \\
& + \left\langle \frac{0.5 \rho_a v c k_2 k_3}{\ell_1} z_1, \phi_1 \right\rangle_{L_2[0, \ell_1]} \\
& + \left\langle \frac{0.5 \rho_a v c k_2 k_3}{\ell_2} z_2, \phi_2 \right\rangle_{L_2[\ell_1+\ell_M, \ell_1+\ell_M+\ell_2]} \\
& + \langle \gamma_2 I z_1'', \phi_1'' \rangle_{L_2[0, \ell_1]} + \langle \gamma_2 I z_2'', \phi_2'' \rangle_{L_2[\ell_1+\ell_M, \ell_1+\ell_M+\ell_2]} \\
& + \gamma_2 I [-z_1'''(\ell_1) \phi_3 + z_2'''(\ell_1 + \ell_M) \phi_3 + z_1''(\ell_1) \phi_4 \\
& - z_2''(\ell_1 + \ell_M) \phi_4 + z_1'''(\ell_1) \phi_1(\ell_1) - z_1'''(0) \phi_1(0) \\
& - z_1''(\ell_1) \phi_1'(\ell_1) + z_1''(0) \phi_1'(0) \\
& + z_2'''(\ell_1 + \ell_M + \ell_2) \phi_2(\ell_1 + \ell_M + \ell_2) \\
& - z_2'''(\ell_1 + \ell_M) \phi_2(\ell_1 + \ell_M) \\
& - z_2''(\ell_1 + \ell_M + \ell_2) \phi_2'(\ell_1 + \ell_M + \ell_2) \\
& + z_2''(\ell_1 + \ell_M) \phi_2'(\ell_1 + \ell_M)].
\end{aligned} \tag{4.62}$$

Regrouping further we obtain

$$\begin{aligned}
\langle \mathcal{D}_{\ell_0} z, \Phi \rangle_S & = \langle \gamma_1 z_1, \phi_1 \rangle_{L_2[0, \ell_1]} + \langle \gamma_1 z_2, \phi_2 \rangle_{L_2[\ell_1+\ell_M, \ell_1+\ell_M+\ell_2]} \\
& + \left\langle \frac{0.5 \rho_a v c k_2 k_3}{\ell_1} z_1, \phi_1 \right\rangle_{L_2[0, \ell_1]}
\end{aligned} \tag{4.63}$$

$$\begin{aligned}
& + \left\langle \frac{0.5\rho_a v c k_2 k_3}{\ell_2} z_2, \phi_2 \right\rangle_{L_2[\ell_1+\ell_M, \ell_1+\ell_M+\ell_2]} \\
& + \langle \gamma_2 I z_1'', \phi_1'' \rangle_{L_2[0, \ell_1]} + \langle \gamma_2 I z_2'', \phi_2'' \rangle_{L_2[\ell_1+\ell_M, \ell_1+\ell_M+\ell_2]} \\
& + \gamma_2 I (z_1'''(\ell_1)(\phi_1(\ell_1) - \phi_3) + z_2'''(\ell_1 + \ell_M)(\phi_3 - \phi_2(\ell_1 + \ell_M)) \\
& + z_1''(\ell_1)(\phi_4 - \phi'(\ell_1)) + z_2''(\ell_1 + \ell_M)(\phi_2'(\ell_1 + \ell_M) - \phi_4) \\
& - z_1'''(0)\phi_1(0) + z_1''(0)\phi_1'(0) \\
& + z_2'''(\ell_1 + \ell_M + \ell_2)\phi_2(\ell_1 + \ell_M + \ell_2) \\
& - z_2''(\ell_1 + \ell_M + \ell_2)\phi_2'(\ell_1 + \ell_M + \ell_2)).
\end{aligned}$$

Since $\Phi \in V$ substitutions are made into the boundary terms arising from the definition of the state z and the boundary conditions for displacement and slope at the mass location, resulting in

$$\begin{aligned}
\langle \mathcal{D}_{\ell_0} z, \Phi \rangle_S & = \langle \gamma_1 z_1, \phi_1 \rangle_{L_2[0, \ell_1]} + \langle \gamma_1 z_2, \phi_2 \rangle_{L_2[\ell_1+\ell_M, \ell_1+\ell_M+\ell_2]} \\
& + \left\langle \frac{0.5\rho_a v c k_2 k_3}{\ell_1} z_1, \phi_1 \right\rangle_{L_2[0, \ell_1]} \\
& + \left\langle \frac{0.5\rho_a v c k_2 k_3}{\ell_2} z_2, \phi_2 \right\rangle_{L_2[\ell_1+\ell_M, \ell_1+\ell_M+\ell_2]} \\
& + \langle \gamma_2 I z_1'', \phi_1'' \rangle_{L_2[0, \ell_1]} + \langle \gamma_2 I z_2'', \phi_2'' \rangle_{L_2[\ell_1+\ell_M, \ell_1+\ell_M+\ell_2]} \\
& - \gamma_2 I z_1'''(0)\phi_1(0) + \gamma_2 I z_1''(0)\phi_1'(0) \\
& + \gamma_2 I z_2'''(\ell_1 + \ell_M + \ell_2)\phi_2(\ell_1 + \ell_M + \ell_2) \\
& - \gamma_2 I z_2''(\ell_1 + \ell_M + \ell_2)\phi_2'(\ell_1 + \ell_M + \ell_2).
\end{aligned} \tag{4.64}$$

A weak formulation for the system is

$$\langle \ddot{z}(t), \Phi \rangle_S + \mathbf{d}(\dot{z}(t), \Phi) + \mathbf{a}(z(t), \Phi) = \langle \mathcal{B}u(t), \Phi \rangle_S, \tag{4.65}$$

where $u(t) = [u_L; u_R; 0; 0]^T$, $\mathcal{B} = \left[\frac{1}{\rho A - \frac{m_b}{\ell_1}} \mathcal{B}_L; \frac{1}{\rho A - \frac{m_b}{\ell_2}} \mathcal{B}_R; 0; 0 \right]^T$, and the sesquilinear forms $\mathbf{d}(z(t), \Phi)$ and $\mathbf{a}(z(t), \Phi)$ are defined to be

$$\begin{aligned} \mathbf{d}(z(t), \Phi) &= \left\langle \left(\gamma_1 + \frac{0.5\rho_a v c k_2 k_3}{\ell_1} \right) z_1, \phi_1 \right\rangle_{L_2[0, \ell_1]} \\ &\quad + \left\langle \left(\gamma_1 + \frac{0.5\rho_a v c k_2 k_3}{\ell_2} \right) z_2, \phi_2 \right\rangle_{L_2[\ell_1 + \ell_M, \ell_1 + \ell_M + \ell_2]} \\ &\quad + \langle \gamma_2 I z_1'', \phi_1'' \rangle_{L_2[0, \ell_1]} + \langle \gamma_2 I z_2'', \phi_2'' \rangle_{L_2[\ell_1 + \ell_M, \ell_1 + \ell_M + \ell_2]}, \end{aligned} \quad (4.66)$$

and

$$\mathbf{a}(z(t), \Phi) = \langle E I z_1'', \phi_1'' \rangle_{L_2[0, \ell_1]} + \langle E I z_2'', \phi_2'' \rangle_{L_2[\ell_1 + \ell_M, \ell_1 + \ell_M + \ell_2]}. \quad (4.67)$$

To show the model is well-posed, we consider the system

$$\langle \ddot{z}(t), \Phi \rangle_S + \tilde{\mathbf{d}}(\dot{z}(t), \Phi) + \tilde{\mathbf{a}}(z(t), \Phi) = \langle \mathcal{B}u(t), \Phi \rangle_S, \quad (4.68)$$

where the sesquilinear forms are defined as follows: $\tilde{\mathbf{d}}(z(t), \Phi) = \mathbf{d}(z(t), \Phi) + \langle \mathcal{A}_1 z, \phi \rangle_S$ and $\tilde{\mathbf{a}}(z(t), \Phi) = \mathbf{a}(z(t), \Phi) + \langle \mathcal{A}_1 z, \phi \rangle_S$.

Theorem 4.15. *The sesquilinear form $\tilde{\mathbf{a}}(\phi, \psi)$ satisfies (H1)-(H3) from Section 4.1.1.*

Proof. Symmetry holds due to the fact that $\tilde{\mathbf{a}}$ is defined via an inner product on a real Hilbert space. Continuity follows from an application of the Cauchy-Schwarz inequality,

$$\|\tilde{\mathbf{a}}(\phi, \psi)\| = \|\langle \phi, \psi \rangle_V\| \leq c \|\phi\|_V \|\psi\|_V \text{ for } c \geq 1$$

Coercivity is established by the following: Let $\lambda = 0$.

$$\begin{aligned}
\operatorname{Re} \tilde{\mathbf{a}}(\phi, \phi) &= \tilde{\mathbf{a}}(\phi, \phi) \\
&= \langle EI\phi_1'', \phi_1'' \rangle_{L_2[0, \ell_1]} + \langle EI\phi_2'', \phi_2'' \rangle_{L_2[\ell_1 + \ell_M, \ell_1 + \ell_M + \ell_2]} + \langle \mathcal{A}_1\phi, \phi \rangle_S \\
&\geq c \langle EI\phi_1'', \phi_1'' \rangle_{L_2[0, \ell_1]} + c \langle EI\phi_2'', \phi_2'' \rangle_{L_2[\ell_1 + \ell_M, \ell_1 + \ell_M + \ell_2]} + c \langle \mathcal{A}_1\phi, \phi \rangle_S \\
&= c \langle \phi, \phi \rangle_V \\
&= c \|\phi\|_V^2
\end{aligned} \tag{4.69}$$

for $0 < c \leq 1$. Therefore, $\tilde{\mathbf{a}}(\phi, \phi)$ is also elliptic in V . \square

An application of Theorem 4.11 shows that $\tilde{\mathcal{A}}$ has dense domain.

Theorem 4.16. *The sesquilinear form $\tilde{\mathbf{d}}(\phi, \psi)$ satisfies **(H4)**-**(H5)** from Section 4.1.1.*

Proof. Again continuity follows from the Cauchy-Schwarz inequality,

$$\begin{aligned}
\|\tilde{\mathbf{d}}(\phi, \psi)\| &= \left\| \left\langle \left(\gamma_1 + \frac{0.5\rho_a v c k_2 k_3}{\ell_1} \right) \phi_1, \psi_1 \right\rangle_{L_2[0, \ell_1]} \right. \\
&\quad + \left\langle \left(\gamma_1 + \frac{0.5\rho_a v c k_2 k_3}{\ell_2} \right) \phi_2, \psi_2 \right\rangle_{L_2[\ell_1 + \ell_M, \ell_1 + \ell_M + \ell_2]} \\
&\quad + \langle \gamma_2 I\phi_1'', \psi_1'' \rangle_{L_2[0, \ell_1]} + \langle \gamma_2 I\phi_2'', \psi_2'' \rangle_{L_2[\ell_1 + \ell_M, \ell_1 + \ell_M + \ell_2]} \\
&\quad \left. + \langle \mathcal{A}_1\phi, \psi \rangle_S \right\| \\
&= \left\| \left\langle \left(\gamma_1 + \frac{0.5\rho_a v c k_2 k_3}{\ell_1} \right) \phi_1, \psi_1 \right\rangle_{L_2[0, \ell_1]} \right. \\
&\quad + \left\langle \left(\gamma_1 + \frac{0.5\rho_a v c k_2 k_3}{\ell_2} \right) \phi_2, \psi_2 \right\rangle_{L_2[\ell_1 + \ell_M, \ell_1 + \ell_M + \ell_2]} \\
&\quad + \langle \gamma_2 I\phi_1'', \psi_1'' \rangle_{L_2[0, \ell_1]} + \langle \gamma_2 I\phi_2'', \psi_2'' \rangle_{L_2[\ell_1 + \ell_M, \ell_1 + \ell_M + \ell_2]} \\
&\quad + \left\langle \left(\rho A - \frac{m_b}{\ell_1} \right) \phi_1, \psi_1 \right\rangle_{L_2[0, \ell_1]} \\
&\quad + \left\langle \left(\rho A - \frac{m_b}{\ell_2} \right) \phi_2, \psi_2 \right\rangle_{L_2[\ell_1 + \ell_M, \ell_1 + \ell_M + \ell_2]} \\
&\quad \left. + m\phi_3\psi_3 + I_z\phi_4\psi_4 \right\|
\end{aligned} \tag{4.70}$$

$$\begin{aligned}
&= \left\| \left\langle \left(\gamma_1 + \frac{0.5\rho_a v c k_2 k_3}{\ell_1} + \rho A - \frac{m_b}{\ell_1} \right) \phi_1, \psi_1 \right\rangle_{L_2[0, \ell_1]} \right. \\
&\quad + \left\langle \left(\gamma_1 + \frac{0.5\rho_a v c k_2 k_3}{\ell_2} + \rho A - \frac{m_b}{\ell_2} \right) \phi_2, \psi_2 \right\rangle_{L_2[\ell_1 + \ell_M, \ell_1 + \ell_M + \ell_2]} \\
&\quad + \langle \gamma_2 I \phi_1'', \psi_1'' \rangle_{L_2[0, \ell_1]} + \langle \gamma_2 I \phi_2'', \psi_2'' \rangle_{L_2[\ell_1 + \ell_M, \ell_1 + \ell_M + \ell_2]} \\
&\quad \left. + m \phi_3 \psi_3 + I_z \phi_4 \psi_4 \right\| \\
&\leq c \left\| \langle EI \phi_1'', \psi_1'' \rangle_{L_2[0, \ell_1]} + \langle EI \phi_2'', \psi_2'' \rangle_{L_2[\ell_1 + \ell_M, \ell_1 + \ell_2 + \ell_M]} \right. \\
&\quad + \left\langle \left(\rho A - \frac{m_b}{\ell_1} \right) \phi_1, \psi_1 \right\rangle_{L_2[0, \ell_1]} \\
&\quad + \left\langle \left(\rho A - \frac{m_b}{\ell_2} \right) \phi_2, \psi_2 \right\rangle_{L_2[\ell_1 + \ell_M, \ell_1 + \ell_2 + \ell_M]} \\
&\quad \left. + m \phi_3 \psi_3 + I_z \phi_4 \psi_4 \right\| \\
&= c \left\| \langle EI \phi_1'', \psi_1'' \rangle_{L_2[0, \ell_1]} + \langle EI \phi_2'', \psi_2'' \rangle_{L_2[\ell_1 + \ell_M, \ell_1 + \ell_2 + \ell_M]} \right. \\
&\quad \left. + \langle \mathcal{A}_1 \phi, \psi \rangle_S \right\| \\
&= c \|\langle \phi, \psi \rangle_V\| \\
&\leq c \|\phi\|_V \|\psi\|_V,
\end{aligned}$$

for $c := \max \left\{ \frac{\gamma_2}{E}, \gamma_1 + \frac{0.5\rho_a v c k_2 k_3}{\ell_1} + \rho A - \frac{m_b}{\ell_1} \right\}$. Next we verify both coercivity and ellipticity. Let $\lambda = 0$.

$$\begin{aligned}
Re \tilde{\mathbf{d}}(\phi, \phi) &= \tilde{\mathbf{d}}(\phi, \phi) \\
&= \langle \gamma_1 \phi_1, \phi_1 \rangle_{L_2[0, \ell_1]} + \langle \gamma_1 \phi_2, \phi_2 \rangle_{L_2[\ell_1 + \ell_M, \ell_1 + \ell_M + \ell_2]} \\
&\quad + \left\langle \frac{0.5\rho_a v c k_2 k_3}{\ell_1} \phi_1, \phi_1 \right\rangle_{L_2[0, \ell_1]} \\
&\quad + \left\langle \frac{0.5\rho_a v c k_2 k_3}{\ell_2} \phi_2, \phi_2 \right\rangle_{L_2[\ell_1 + \ell_M, \ell_1 + \ell_M + \ell_2]} \\
&\quad + \langle \gamma_2 I \phi_1'', \phi_1'' \rangle_{L_2[0, \ell_1]} + \langle \gamma_2 I \phi_2'', \phi_2'' \rangle_{L_2[\ell_1 + \ell_M, \ell_1 + \ell_M + \ell_2]} \\
&\quad + \langle \mathcal{A}_1 \phi, \phi \rangle_S
\end{aligned} \tag{4.71}$$

$$\begin{aligned}
&\geq c \langle EI\phi_1'', \phi_1'' \rangle_{L_2[0, \ell_1]} + c \langle EI\phi_2'', \phi_2'' \rangle_{L_2[\ell_1 + \ell_M, \ell_1 + \ell_M + \ell_2]} + c \langle \mathcal{A}_1\phi, \phi \rangle_S \\
&= c \langle \phi, \phi \rangle_V \\
&= c \|\phi\|_V^2,
\end{aligned}$$

for $c = \frac{\gamma_2}{E}$. Therefore, $\tilde{\mathbf{d}}(\phi, \phi)$ is also elliptic in V . \square

By Theorem 4.4 Equation (4.68) is well-posed, and thus by Theorem 4.9 Equation (4.65) is well-posed. Furthermore, the first order system operator generates a C_0 -semigroup.

Finally, we consider the linear approximation of the BMB-PZT model described in Equation (3.20) and Equation (3.21). We refer to work done in [4] where it was shown that the inclusion of piezoceramic patches on a cantilevered beam is well-posed. Since the left hand side of the equations in the BMB-PZT model merely consist of altered parameter values from the original BMB model we can see that **(H1)**-**(H5)** would be readily satisfied for the BMB-PZT model by merely choosing appropriate values so that these hypotheses hold, as was done in the work above for the BMB model. For **(H6)** we refer to [4] which shows that for $V_1(\cdot) - V_2(\cdot) \in L_2[0, T]$ we have that $f \in L_2[(0, T), V^*]$ since the second derivatives $\chi'' \in V^*$. Therefore, we can infer that **(H6)** is satisfied and the BMB-PZT model is well-posed and generates a C_0 -semigroup.

CHAPTER 5

NUMERICAL RESULTS FOR THE BMB SYSTEM

5.1 Weak Formulation of the BMB System

In this section we employ the Galerkin finite element method in order to obtain a finite dimensional approximation of the BMB system.

5.1.1 Variational Form

Let H^2 denote the Hilbert space with at most two derivatives. The objective is to find a $[w_L(t, s_L), w_R(t, s_R)]^T \in V \subseteq S = H^2[0, \ell_1] \times H^2[\ell_1 + \ell_M, \ell_1 + \ell_M + \ell_2]$ so that multiplying Equation (3.8) and Equation (3.9) by test functions $\phi_L(s_L)$ and $\phi_R(s_R)$, respectively, yields

$$\begin{aligned} & \int_0^{\ell_1} [\rho A \ddot{w}_L(t, s_L) + \gamma_1 \dot{w}_L(t, s_L) + \gamma_2 I \dot{w}_L'''(t, s_L) + EI w_L''''(t, s_L)] \phi_L(s_L) ds_L \\ &= \int_0^{\ell_1} \left[b(s_L) u_L(t) + \frac{m_b g}{\ell_1} - \frac{0.5 \rho_a v^2 c}{\ell_1} C_\ell \right] \phi_L(s_L) ds_L, \end{aligned} \quad (5.1)$$

and

$$\begin{aligned} & \int_{\ell_1 + \ell_M}^{\ell_1 + \ell_M + \ell_2} [\rho A \ddot{w}_R(t, s_R) + \gamma_1 \dot{w}_R(t, s_R) + \gamma_2 I \dot{w}_R'''(t, s_R) + EI w_R''''(t, s_R)] \phi_R(s_R) ds_R \\ &= \int_{\ell_1 + \ell_M}^{\ell_1 + \ell_M + \ell_2} \left[b(s_R) u_R(t) + \frac{m_b g}{\ell_2} - \frac{0.5 \rho_a v^2 c}{\ell_2} C_\ell \right] \phi_R(s_R) ds_R \end{aligned} \quad (5.2)$$

for all $[\phi_L(s_L), \phi_R(s_R)]^T \in V = \{[\phi_L(\cdot), \phi_R(\cdot)]^T \in S : \phi_L(\ell_1) = \phi_R(\ell_1 + \ell_M), \phi_L'(\ell_1) = \phi_R'(\ell_1 + \ell_M)\}$. Applying integration by parts to Equation (5.1) and Equation (5.2)

results in the following

$$\begin{aligned}
& \int_0^{\ell_1} [\rho A \ddot{w}_L(t, s_L) \phi_L(s_L) + \gamma_1 \dot{w}_L(t, s_L) \phi_L(s_L) + \gamma_2 I \dot{w}_L''(t, s_L) \phi_L''(s_L) \\
& + EI w_L''(t, s_L) \phi_L''(s_L)] ds_L + \gamma_2 I \dot{w}_L'''(t, \ell_1) \phi_L(\ell_1) - \gamma_2 I \dot{w}_L'''(t, 0) \phi_L(0) \\
& - \gamma_2 I \dot{w}_L''(t, \ell_1) \phi_L'(\ell_1) + \gamma_2 I \dot{w}_L''(t, 0) \phi_L'(0) + EI w_L'''(t, \ell_1) \phi_L(\ell_1) \\
& - EI w_L'''(t, 0) \phi_L(0) - EI w_L''(t, \ell_1) \phi_L'(\ell_1) + EI w_L''(t, 0) \phi_L'(0) \\
& = \int_0^{\ell_1} \left[b(s_L) u_L(t) + \frac{m_b g}{\ell_1} - \frac{0.5 \rho_a v^2 c}{\ell_1} C_\ell \right] \phi_L(s_L) ds_L,
\end{aligned} \tag{5.3}$$

and

$$\begin{aligned}
& \int_{\ell_1 + \ell_M}^{\ell_1 + \ell_M + \ell_2} [\rho A \ddot{w}_R(t, s_R) \phi_R(s_R) + \gamma_1 \dot{w}_R(t, s_R) \phi_R(s_R) + \gamma_2 I \dot{w}_R''(t, s_R) \phi_R''(s_R) \\
& + EI w_R''(t, s_R) \phi_R''(s_R)] ds_R + \gamma_2 I \dot{w}_R'''(t, \ell_1 + \ell_M + \ell_2) \phi_R(\ell_1 + \ell_M + \ell_2) \\
& - \gamma_2 I \dot{w}_R'''(t, \ell_1 + \ell_M) \phi_R(\ell_1 + \ell_M) - \gamma_2 I \dot{w}_R''(t, \ell_1 + \ell_M + \ell_2) \phi_R'(\ell_1 + \ell_M + \ell_2) \\
& + \gamma_2 I \dot{w}_R''(t, \ell_1 + \ell_M) \phi_R'(\ell_1 + \ell_M) + EI w_R'''(t, \ell_1 + \ell_M + \ell_2) \phi_R(\ell_1 + \ell_M + \ell_2) \\
& - EI w_R'''(t, \ell_1 + \ell_M) \phi_R(\ell_1 + \ell_M) - EI w_R''(t, \ell_1 + \ell_M + \ell_2) \phi_R'(\ell_1 + \ell_M + \ell_2) \\
& + EI w_R''(t, \ell_1 + \ell_M) \phi_R'(\ell_1 + \ell_M) \\
& = \int_{\ell_1 + \ell_M}^{\ell_1 + \ell_M + \ell_2} \left[b(s_R) u_R(t) + \frac{m_b g}{\ell_2} - \frac{0.5 \rho_a v^2 c}{\ell_2} C_\ell \right] \phi_R(s_R) ds_R.
\end{aligned} \tag{5.4}$$

Summing Equation (5.3) and Equation (5.4) yields

$$\begin{aligned}
& \int_0^{\ell_1} [\rho A \ddot{w}_L(t, s_L) \phi_L(s_L) + \gamma_1 \dot{w}_L(t, s_L) \phi_L(s_L) + \gamma_2 I \dot{w}_L''(t, s_L) \phi_L''(s_L) \\
& + EI w_L''(t, s_L) \phi_L''(s_L)] ds_L \\
& + \int_{\ell_1 + \ell_M}^{\ell_1 + \ell_M + \ell_2} [\rho A \ddot{w}_R(t, s_R) \phi_R(s_R) + \gamma_1 \dot{w}_R(t, s_R) \phi_R(s_R) \\
& + \gamma_2 I \dot{w}_R''(t, s_R) \phi_R''(s_R) + EI w_R''(t, s_R) \phi_R''(s_R)] ds_R + \gamma_2 I \dot{w}_L'''(t, \ell_1) \phi_L(\ell_1) \\
& - \gamma_2 I \dot{w}_L'''(t, 0) \phi_L(0) - \gamma_2 I \dot{w}_L''(t, \ell_1) \phi_L'(\ell_1) + \gamma_2 I \dot{w}_L''(t, 0) \phi_L'(0) \\
& + EI w_L'''(t, \ell_1) \phi_L(\ell_1) - EI w_L'''(t, 0) \phi_L(0) \\
& - EI w_L''(t, \ell_1) \phi_L'(\ell_1) + EI w_L''(t, 0) \phi_L'(0)
\end{aligned} \tag{5.5}$$

$$\begin{aligned}
& +\gamma_2 I \dot{w}_R'''(t, \ell_1 + \ell_M + \ell_2) \phi_R(\ell_1 + \ell_M + \ell_2) - \gamma_2 I \dot{w}_R'''(t, \ell_1 + \ell_M) \phi_R(\ell_1 + \ell_M) \\
& -\gamma_2 I \dot{w}_R''(t, \ell_1 + \ell_M + \ell_2) \phi_R'(\ell_1 + \ell_M + \ell_2) + \gamma_2 I \dot{w}_R''(t, \ell_1 + \ell_M) \phi_R'(\ell_1 + \ell_M) \\
& +EI w_R'''(t, \ell_1 + \ell_M + \ell_2) \phi_R(\ell_1 + \ell_M + \ell_2) - EI w_R'''(t, \ell_1 + \ell_M) \phi_R(\ell_1 + \ell_M) \\
& -EI w_R''(t, \ell_1 + \ell_M + \ell_2) \phi_R'(\ell_1 + \ell_M + \ell_2) + EI w_R''(t, \ell_1 + \ell_M) \phi_R'(\ell_1 + \ell_M) \\
& = \int_0^{\ell_1} \left[b(s_L) u_L(t) + \frac{m_b g}{\ell_1} - \frac{0.5 \rho_a v^2 c}{\ell_1} C_\ell \right] \phi_L(s_L) ds_L \\
& + \int_{\ell_1 + \ell_M}^{\ell_1 + \ell_M + \ell_2} \left[b(s_R) u_R(t) + \frac{m_b g}{\ell_2} - \frac{0.5 \rho_a v^2 c}{\ell_2} C_\ell \right] \phi_R(s_R) ds_R.
\end{aligned}$$

Next natural boundary conditions (the first six boundary conditions presented in Table 3.1) are applied. The remaining two essential conditions are explicitly satisfied by elements in V and are not part of the weak form.

$$\begin{aligned}
& \int_0^{\ell_1} [\rho A \ddot{w}_L(t, s_L) \phi_L(s_L) + \gamma_1 \dot{w}_L(t, s_L) \phi_L(s_L) + \gamma_2 I \dot{w}_L''(t, s_L) \phi_L''(s_L) \\
& + EI w_L''(t, s_L) \phi_L''(s_L)] ds_L + \int_{\ell_1 + \ell_M}^{\ell_1 + \ell_M + \ell_2} [\rho A \ddot{w}_R(t, s_R) \phi_R(s_R) \\
& + \gamma_1 \dot{w}_R(t, s_R) \phi_R(s_R) + \gamma_2 I \dot{w}_R''(t, s_R) \phi_R''(s_R) \\
& + EI w_R''(t, s_R) \phi_R''(s_R)] ds_R + m \ddot{w}_L(t, \ell_1) \phi_L(\ell_1) + I_z \ddot{w}'(t, \ell_1) \phi_L'(\ell_1) \\
& = \int_0^{\ell_1} \left[b(s_L) u_L(t) + \frac{m_b g}{\ell_1} - \frac{0.5 \rho_a v^2 c}{\ell_1} C_\ell \right] \phi_L(s_L) ds_L \\
& + \int_{\ell_1 + \ell_M}^{\ell_1 + \ell_M + \ell_2} \left[b(s_R) u_R(t) + \frac{m_b g}{\ell_2} - \frac{0.5 \rho_a v^2 c}{\ell_2} C_\ell \right] \phi_R(s_R) ds_R
\end{aligned} \tag{5.6}$$

5.1.2 Discretization

A basis $\{e_i\}_i^N$ is chosen for the approximating space $V^N \subseteq V$, where N corresponds to the number of basis functions used in the finite element approximation. Cubic Hermite interpolating polynomials are used to approximate the displacements

of the left and right beams. The basis vectors take the form:

$$e_i^N = \begin{bmatrix} b_{L,i}^N(s_L) \\ b_{R,i}^N(s_R) \end{bmatrix}, \text{ for } i = 1, \dots, N. \quad (5.7)$$

That is, the state will be approximated as

$$\begin{bmatrix} w_L(t, s_L) \\ w_R(t, s_R) \end{bmatrix} \approx \begin{bmatrix} w_L^N(t, s_L) \\ w_R^N(t, s_R) \end{bmatrix} = \begin{bmatrix} \sum_{i=1}^N \alpha_i^N(t) b_{L,i}^N(s_L) \\ \sum_{i=1}^N \beta_i^N(t) b_{R,i}^N(s_R) \end{bmatrix}. \quad (5.8)$$

Substituting this state approximation into Equation (5.6), we obtain

$$\begin{aligned} & \int_0^{\ell_1} [\rho A \ddot{w}_L^N(t, s_L) \phi_L(s_L) + \gamma_1 \dot{w}_L^N(t, s_L) \phi_L(s_L) + \gamma_2 I (\dot{w}_L^N)''(t, s_L) \phi_L''(s_L) \\ & + EI (w_L^N)''(t, s_L) \phi_L''(s_L)] ds_L + \int_{\ell_1+\ell_M}^{\ell_1+\ell_M+\ell_2} [\rho A \ddot{w}_R^N(t, s_R) \phi_R(s_R) \\ & + \gamma_1 \dot{w}_R^N(t, s_R) \phi_R(s_R) + \gamma_2 I (\dot{w}_R^N)''(t, s_R) \phi_R''(s_R) \\ & + EI (w_R^N)''(t, s_R) \phi_R''(s_R)] ds_R + m \ddot{w}_L^N(t, \ell_1) \phi_L(\ell_1) + I_z (\ddot{w}_L^N)'(t, \ell_1) \phi_L'(\ell_1) \\ & = \int_0^{\ell_1} \left[b(s_L) u_L(t) + \frac{m_b g}{\ell_1} - \frac{0.5 \rho_a v^2 c}{\ell_1} C_\ell \right] \phi_L(s_L) ds_L \\ & + \int_{\ell_1+\ell_M}^{\ell_1+\ell_M+\ell_2} \left[b(s_R) u_R(t) + \frac{m_b g}{\ell_2} - \frac{0.5 \rho_a v^2 c}{\ell_2} C_\ell \right] \phi_R(s_R) ds_R. \end{aligned} \quad (5.9)$$

which implies

$$\begin{aligned} & \int_0^{\ell_1} \left[\rho A \sum_{i=1}^N \ddot{\alpha}_i^N(t) b_{L,i}^N(s_L) \phi_L(s_L) + \gamma_1 \sum_{i=1}^N \dot{\alpha}_i^N(t) b_{L,i}^N(s_L) \phi_L(s_L) \right. \\ & \left. + \gamma_2 I \sum_{i=1}^N \dot{\alpha}_i^N(t) b_{L,i}''(s_L) \phi_L''(s_L) + EI \sum_{i=1}^N \alpha_i^N(t) b_{L,i}''(s_L) \phi_L''(s_L) \right] ds_L \\ & + \int_{\ell_1+\ell_M}^{\ell_1+\ell_M+\ell_2} \left[\rho A \sum_{i=1}^N \ddot{\beta}_i^N(t) b_{R,i}^N(s_R) \phi_R(s_R) + \gamma_1 \sum_{i=1}^N \dot{\beta}_i^N(t) b_{R,i}^N(s_R) \phi_R(s_R) \right. \\ & \left. + \gamma_2 I \sum_{i=1}^N \dot{\beta}_i^N(t) b_{R,i}''(s_R) \phi_R''(s_R) + EI \sum_{i=1}^N \beta_i^N(t) b_{R,i}''(s_R) \phi_R''(s_R) \right] ds_R \\ & + m \sum_{i=1}^N \ddot{\alpha}_i^N(t) b_{L,i}^N(\ell_1) \phi_L(\ell_1) + I_z \sum_{i=1}^N \ddot{\alpha}_i^N(t) b_{L,i}'(\ell_1) \phi_L'(\ell_1) \end{aligned} \quad (5.10)$$

$$\begin{aligned}
&= \int_0^{\ell_1} \left[b(s_L)u_L(t) + \frac{m_b g}{\ell_1} - \frac{0.5\rho_a v^2 c}{\ell_1} C_\ell \right] \phi_L(s_L) ds_L \\
&+ \int_{\ell_1+\ell_M}^{\ell_1+\ell_M+\ell_2} \left[b(s_R)u_R(t) + \frac{m_b g}{\ell_2} - \frac{0.5\rho_a v^2 c}{\ell_2} C_\ell \right] \phi_R(s_R) ds_R.
\end{aligned}$$

Let the test functions range over the appropriate basis vectors, yielding the following:

$$\begin{aligned}
&\int_0^{\ell_1} \left[\rho A \sum_{i,j=1}^N \ddot{\alpha}_i^N(t) b_{L,i}(s_L) b_{L,j}(s_L) + \gamma_1 \sum_{i,j=1}^N \dot{\alpha}_i^N(t) b_{L,i}(s_L) b_{L,j}(s_L) \right. \\
&+ \gamma_2 I \sum_{i,j=1}^N \dot{\alpha}_i^N(t) b_{L,i}''(s_L) b_{L,j}''(s_L) + EI \sum_{i,j=1}^N \alpha_i^N(t) b_{L,i}''(s_L) b_{L,j}''(s_L) \left. \right] ds_L \\
&+ \int_{\ell_1+\ell_M}^{\ell_1+\ell_M+\ell_2} \left[\rho A \sum_{i,j=1}^N \ddot{\beta}_i^N(t) b_{R,i}(s_R) b_{R,j}(s_R) + \gamma_1 \sum_{i,j=1}^N \dot{\beta}_i^N(t) b_{R,i}(s_R) b_{R,j}(s_R) \right. \\
&+ \gamma_2 I \sum_{i,j=1}^N \dot{\beta}_i^N(t) b_{R,i}''(s_R) b_{R,j}''(s_R) + EI \sum_{i,j=1}^N \beta_i^N(t) b_{R,i}''(s_R) b_{R,j}''(s_R) \left. \right] ds_R \\
&+ m \sum_{i,j=1}^N \ddot{\alpha}_i^N(t) b_{L,i}(\ell_1) b_{L,j}(\ell_1) + I_z \sum_{i,j=1}^N \ddot{\alpha}_i^N(t) b_{L,i}'(\ell_1) b_{L,j}'(\ell_1) \\
&= \int_0^{\ell_1} \left[b(s_L)u_L(t) + \frac{m_b g}{\ell_1} - \frac{0.5\rho_a v^2 c}{\ell_1} C_\ell \right] b_{L,j}(s_L) ds_L \\
&+ \int_{\ell_1+\ell_M}^{\ell_1+\ell_M+\ell_2} \left[b(s_R)u_R(t) + \frac{m_b g}{\ell_2} - \frac{0.5\rho_a v^2 c}{\ell_2} C_\ell \right] b_{R,j}(s_R) ds_R,
\end{aligned} \tag{5.11}$$

which results in the following

$$\begin{aligned}
&\int_0^{\ell_1} \rho A b_{L,i}(s_L) b_{L,j}(s_L) ds_L \sum_{i,j=1}^N \ddot{\alpha}_i^N(t) \\
&+ \int_0^{\ell_1} \gamma_1 b_{L,i}(s_L) b_{L,j}(s_L) ds_L \sum_{i,j=1}^N \dot{\alpha}_i^N(t) \\
&+ \int_0^{\ell_1} \gamma_2 I b_{L,i}''(s_L) b_{L,j}''(s_L) ds_L \sum_{i,j=1}^N \dot{\alpha}_i^N(t) \\
&+ \int_0^{\ell_1} EI b_{L,i}''(s_L) b_{L,j}''(s_L) ds_L \sum_{i,j=1}^N \alpha_i^N(t) \\
&+ \int_{\ell_1+\ell_M}^{\ell_1+\ell_M+\ell_2} \rho A b_{R,i}(s_R) b_{R,j}(s_R) ds_R \sum_{i,j=1}^N \ddot{\beta}_i^N(t)
\end{aligned} \tag{5.12}$$

$$\begin{aligned}
& + \int_{\ell_1+\ell_M}^{\ell_1+\ell_M+\ell_2} \gamma_1 b_{R,i}(s_R) b_{R,j}(s_R) ds_R \sum_{i,j=1}^N \dot{\beta}_i^N(t) \\
& + \int_{\ell_1+\ell_M}^{\ell_1+\ell_M+\ell_2} \gamma_2 I b_{R,i}''(s_R) b_{R,j}''(s_R) ds_R \sum_{i,j=1}^N \dot{\beta}_i^N(t) \\
& + \int_{\ell_1+\ell_M}^{\ell_1+\ell_M+\ell_2} E I b_{R,i}''(s_R) b_{R,j}''(s_R) ds_R \sum_{i,j=1}^N \beta_i^N(t) \\
& + m b_{L,i}(\ell_1) b_{L,j}(\ell_1) \sum_{i,j=1}^N \ddot{\alpha}_i^N(t) + I_2 b'_{L,i}(\ell_1) b'_{L,j}(\ell_1) \sum_{i,j=1}^N \ddot{\alpha}_i^N(t) \\
& = \int_0^{\ell_1} \left[b(s_L) u_L(t) + \frac{m_b g}{\ell_1} - \frac{0.5 \rho_a v^2 c}{\ell_1} C_\ell \right] b_{L,j}(s_L) ds_L \\
& + \int_{\ell_1+\ell_M}^{\ell_1+\ell_M+\ell_2} \left[b(s_R) u_R(t) + \frac{m_b g}{\ell_2} - \frac{0.5 \rho_a v^2 c}{\ell_2} C_\ell \right] b_{R,j}(s_R) ds_R.
\end{aligned}$$

Or in a more condensed form, we have

$$\begin{aligned}
M_L \ddot{\alpha}(t) + M_R \ddot{\beta}(t) + D_L \dot{\alpha}(t) + D_R \dot{\beta}(t) + K_L \alpha(t) + K_R \beta(t) \\
= B_L u_L(t) + B_R u_R(t) + G_L + G_R + F_L + F_R,
\end{aligned} \tag{5.13}$$

where

$$\begin{aligned}
[M_L]_{i,j} &= \int_0^{\ell_1} \rho A b_{L,i}(s_L) b_{L,j}(s_L) ds_L + m b_{L,i}(\ell_1) b_{L,j}(\ell_1) + I_2 b'_{L,i}(\ell_1) b'_{L,j}(\ell_1), \\
[M_R]_{i,j} &= \int_{\ell_1+\ell_M}^{\ell_1+\ell_M+\ell_2} \rho A b_{R,i}(s_R) b_{R,j}(s_R) ds_R, \\
[D_L]_{i,j} &= \int_0^{\ell_1} \gamma_1 b_{L,i}(s_L) b_{L,j}(s_L) ds_L + \int_0^{\ell_1} \gamma_2 I b_{L,i}''(s_L) b_{L,j}''(s_L) ds_L, \\
[D_R]_{i,j} &= \int_{\ell_1+\ell_M}^{\ell_1+\ell_M+\ell_2} \gamma_1 b_{R,i}(s_R) b_{R,j}(s_R) ds_R \\
& + \int_{\ell_1+\ell_M}^{\ell_1+\ell_M+\ell_2} \gamma_2 I b_{R,i}''(s_R) b_{R,j}''(s_R) ds_R, \\
[K_L]_{i,j} &= \int_0^{\ell_1} E I b_{L,i}''(s_L) b_{L,j}''(s_L) ds_L, \\
[K_R]_{i,j} &= \int_{\ell_1+\ell_M}^{\ell_1+\ell_M+\ell_2} E I b_{R,i}''(s_R) b_{R,j}''(s_R) ds_R.
\end{aligned} \tag{5.14}$$

$$\begin{aligned}
[B_L]_j &= \int_0^{\ell_1} b(s_L)u_L(t)b_{L,j}(s_L) ds_L, \\
[B_R]_j &= \int_{\ell_1+\ell_M}^{\ell_1+\ell_M+\ell_2} b(s_R)u_R(t)b_{R,j}(s_R) ds_R, \\
[G_L]_j &= \int_0^{\ell_1} \frac{m_b g}{\ell_1} b_{L,j}(s_L) ds_L, \\
[G_R]_j &= \int_{\ell_1+\ell_M}^{\ell_1+\ell_M+\ell_2} \frac{m_b g}{\ell_2} b_{R,j}(s_R) ds_R. \\
[F_L]_j &= \int_0^{\ell_1} -\frac{0.5\rho_a v^2 c}{\ell_1} C_\ell b_{L,j}(s_L) ds_L, \\
[F_R]_j &= \int_{\ell_1+\ell_M}^{\ell_1+\ell_M+\ell_2} -\frac{0.5\rho_a v^2 c}{\ell_2} C_\ell b_{R,j}(s_R) ds_R.
\end{aligned}$$

Note that Equation (5.13) can be written as

$$\ddot{c}(t) = M^{-1}(-D\dot{c}(t) - Kc(t) + \bar{B} + \bar{G} + \bar{F}), \quad (5.15)$$

where

$$c(t) = \begin{bmatrix} \alpha(t) \\ \beta(t) \end{bmatrix} \Rightarrow \dot{c}(t) = \begin{bmatrix} \dot{\alpha}(t) \\ \dot{\beta}(t) \end{bmatrix} \Rightarrow \ddot{c}(t) = \begin{bmatrix} \ddot{\alpha}(t) \\ \ddot{\beta}(t) \end{bmatrix} \quad (5.16)$$

and

$$M = \begin{bmatrix} M_L & 0 \\ 0 & M_R \end{bmatrix}, \quad D = \begin{bmatrix} D_L & 0 \\ 0 & D_R \end{bmatrix}, \quad K = \begin{bmatrix} K_L & 0 \\ 0 & K_R \end{bmatrix}, \quad (5.17)$$

$$\bar{B} = \begin{bmatrix} B_L \\ B_R \end{bmatrix}, \quad \bar{G} = \begin{bmatrix} G_L \\ G_R \end{bmatrix}, \quad \bar{F} = \begin{bmatrix} F_L \\ F_R \end{bmatrix}.$$

Converting Equation (5.15) into a first order system results in

$$\dot{x}(t) = Ax(t) + Bu(t) + G + F(x(t)), \quad (5.18)$$

where

$$\begin{aligned}
 x(t) &= \begin{bmatrix} c(t) \\ \dot{c}(t) \end{bmatrix}, & A &= \begin{bmatrix} 0 & I \\ -M^{-1}K & -M^{-1}D \end{bmatrix} \\
 B &= \begin{bmatrix} 0 \\ M^{-1}\bar{B} \end{bmatrix}, & G &= \begin{bmatrix} 0 \\ M^{-1}\bar{G} \end{bmatrix}, & (5.19) \\
 F &= \begin{bmatrix} 0 \\ M^{-1}\bar{F}(x(t)) \end{bmatrix}.
 \end{aligned}$$

5.2 Target Tracking Results

Here we test the system's ability to transform its flexible wings from level flight into some prescribed morphed state. It is assumed that the controllers act over the entire beam structure with constant control input functions of the form

$$b(s_L) = b(s_R) = 30, \quad (5.20)$$

for $0 \leq s_L \leq \ell_1$ and $\ell_1 + \ell_M \leq s_R \leq \ell_1 + \ell_M + \ell_2$, and observations of the form

$$y(t) = 15w(t, s), \quad (5.21)$$

for $0 \leq s_L \leq \ell_1$ and $\ell_1 + \ell_M \leq s_R \leq \ell_1 + \ell_M + \ell_2$. In order to design control we employ a Galerkin finite element approximation on the linearly approximated BMB system described in Equation (3.15) and Equation (3.16) by applying the same approach from Section 5.1. This results in the following linearized discretized system

$$\dot{x}(t) = A_\ell x(t) + Bu(t), \quad (5.22)$$

where

$$A_\ell = \begin{bmatrix} 0 & I \\ -M_\ell^{-1}K & -M_\ell^{-1}D_\ell \end{bmatrix}. \quad (5.23)$$

with

$$M_\ell = \begin{bmatrix} M_{L_\ell} & 0 \\ 0 & M_{R_\ell} \end{bmatrix}, \quad D_\ell = \begin{bmatrix} D_{L_\ell} & 0 \\ 0 & D_{R_\ell} \end{bmatrix}, \quad (5.24)$$

and

$$\begin{aligned} [M_{L_\ell}]_{i,j} &= \int_0^{\ell_1} \rho A b_{L,i}(s_L) b_{L,j}(s_L) ds_L - \int_0^{\ell_1} m_b b_{L,i}(s_L) b_{L,j}(s_L) ds_L \\ &\quad + m b_{L,i}(\ell_1) b_{L,j}(\ell_1) + I_z b'_{L,i}(\ell_1) b'_{L,j}(\ell_1), \\ [M_{R_\ell}]_{i,j} &= \int_{\ell_1+\ell_M}^{\ell_1+\ell_M+\ell_2} \rho A b_{R,i}(s_R) b_{R,j}(s_R) ds_R - \int_{\ell_1+\ell_M}^{\ell_1+\ell_M+\ell_2} m_b b_{R,i}(s_R) b_{R,j}(s_R) ds_R, \\ [D_{L_\ell}]_{i,j} &= \int_0^{\ell_1} \gamma_1 b_{L,i}(s_L) b_{L,j}(s_L) ds_L + \int_0^{\ell_1} \gamma_2 I b''_{L,i}(s_L) b''_{L,j}(s_L) ds_L \\ &\quad + \int_0^{\ell_1} \xi b_{L,i}(s_L) b_{L,j}(s_L) ds_L, \\ [D_{R_\ell}]_{i,j} &= \int_{\ell_1+\ell_M}^{\ell_1+\ell_M+\ell_2} \gamma_1 b_{R,i}(s_R) b_{R,j}(s_R) ds_R + \int_{\ell_1+\ell_M}^{\ell_1+\ell_M+\ell_2} \gamma_2 I b''_{R,i}(s_R) b''_{R,j}(s_R) ds_R \\ &\quad + \int_{\ell_1+\ell_M}^{\ell_1+\ell_M+\ell_2} \xi b_{R,i}(s_R) b_{R,j}(s_R) ds_R. \end{aligned} \quad (5.25)$$

upon which control design is employed. Control matrices A_c , F_c , and K are then applied to the nonlinear system, yielding

$$\begin{aligned} \frac{d}{dt} \begin{bmatrix} x(t) \\ x_c(t) \end{bmatrix} &= \begin{bmatrix} A & -BK \\ F_c C & A_c \end{bmatrix} \begin{bmatrix} x(t) \\ x_c(t) \end{bmatrix} \\ &\quad + \begin{bmatrix} G \\ G \end{bmatrix} + \begin{bmatrix} F \\ F(\dot{x}_c(t)) \end{bmatrix} - \begin{bmatrix} u_{fw} \\ 0 \end{bmatrix}. \end{aligned} \quad (5.26)$$

Note this results in a nonlinear compensator. The control objective is to morph each beam from equilibrium to the desired position

$$w(t, s) = \frac{5s(s - \ell)(2s - \ell)^2}{8w_{\text{peak}}}, \quad (5.27)$$

and slope

$$w'(t, s) = \frac{5(2s - \ell)(8s^2 - 8s\ell + \ell^2)}{8w_{\text{peak}}}, \quad (5.28)$$

where $w_{\text{peak}} = 0.0762$ m. The desired target is represented graphically in Figure 5.1.

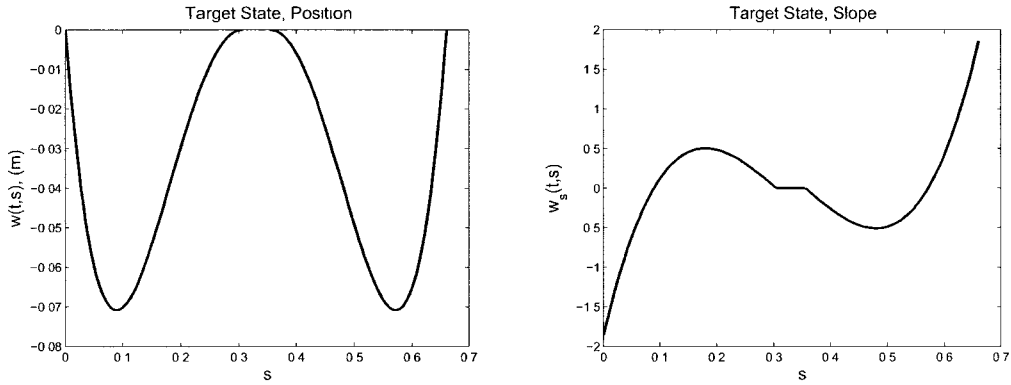


Figure 5.1: Desired State Target: Position (left), Slope (right)

To obtain a solution to the system, initial conditions are chosen as follows: $x(0) = [0; 0; -2; 0]$ ([displacement; slope; velocity; angular velocity]) and $x_c(0) = 0.75 * x(0)$. That is, to generate a nonzero state estimate, we choose the initial conditions for the observer equation to be 75% of the initial conditions for the state equation. A convergent finite element approximation using Hermite interpolating cubic polynomials of order $N = 30$ nodes for the spatial discretization of the BMB system is used to simulate Equation (5.18), and the parameter values for the BMB system are provided in Table 5.1.

Table 5.1: BMB System Parameters

| Parameter | Value | Units |
|-----------------------|------------------------|-------------------------|
| ℓ | 0.6096 | m |
| ℓ_M | 0.0508 | m |
| ρ | 980 | kg/m ³ |
| \hat{w} , width | 0.127 | m |
| h , height | 0.0254 | m |
| $a = \hat{w}h$ | 0.032 | m ² |
| E | 2.0×10^6 | N/m ² |
| $I = (\hat{w}h^3)/12$ | 1.734×10^{-7} | m ⁴ |
| m | 1.927 | kg |
| m_b | 1.927 | kg |
| γ_1 | 0.025 | kg/(m sec) |
| γ_2 | 1×10^2 | kg/(m ⁵ sec) |

Simulations were obtained using Matlab's ODE15s stiff system solver. For reference, the uncontrolled state plots of the nonlinear system are given in Figure 5.2. Controlled results are presented in Figures 5.3 and 5.4. To obtain stabilizing solutions to the algebraic Riccati equations, a Newton-Kleinman algorithm was used (see [12]). For the results presented here, it is assumed that measurements are available for the position and slope states. Numerical instabilities in solving finite dimensional approximations to the algebraic Riccati equations occurred when it was assumed that only velocity and angular velocity were available for measurement.

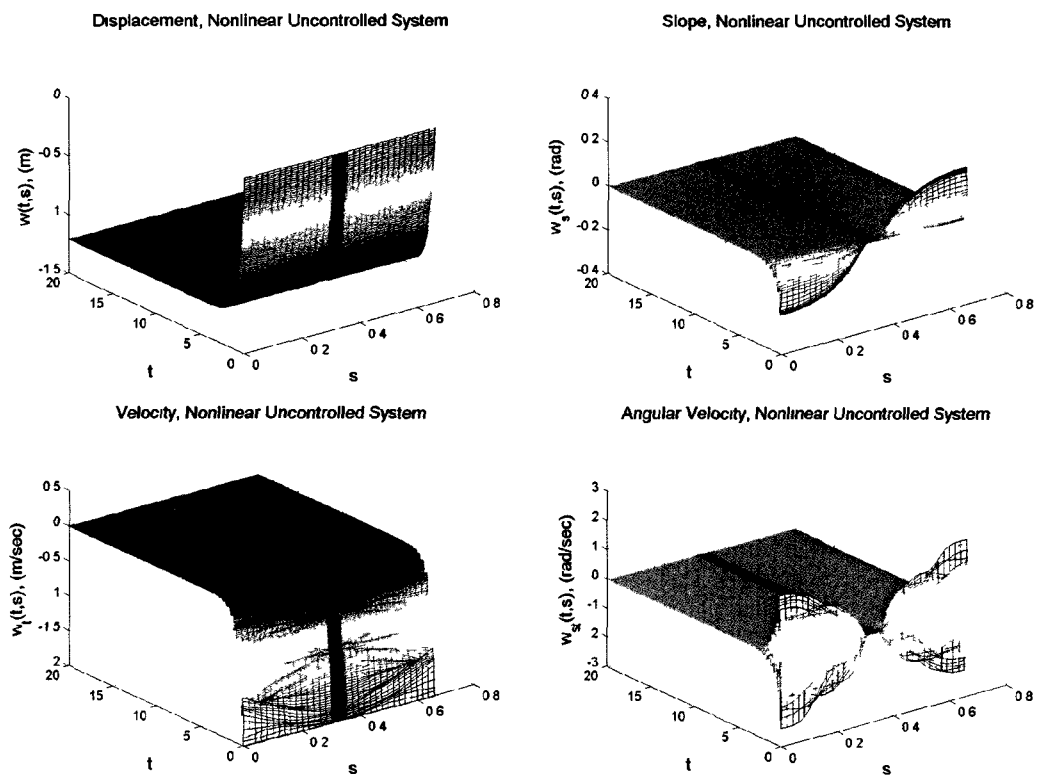


Figure 5.2: Uncontrolled System: Position (top left), Slope (top right), Velocity (bottom left), Angular Velocity, (bottom right)

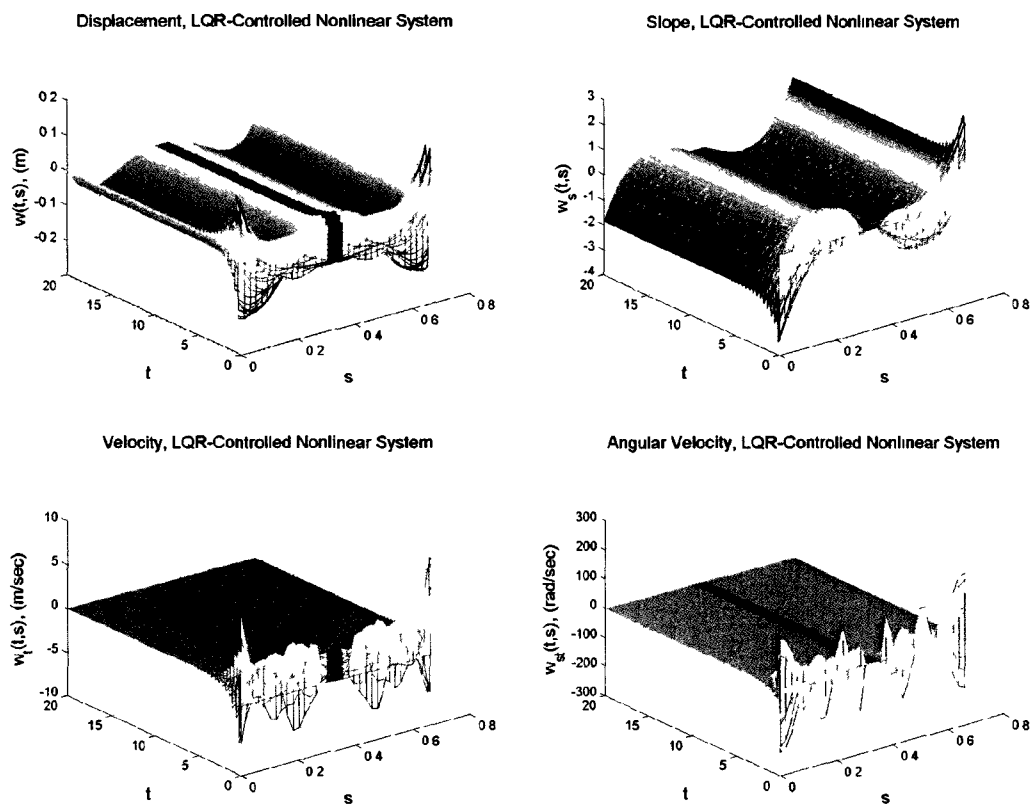


Figure 5.3: LQR Controlled System: Position (top left), Slope (top right), Velocity (bottom left), Angular Velocity (bottom right)

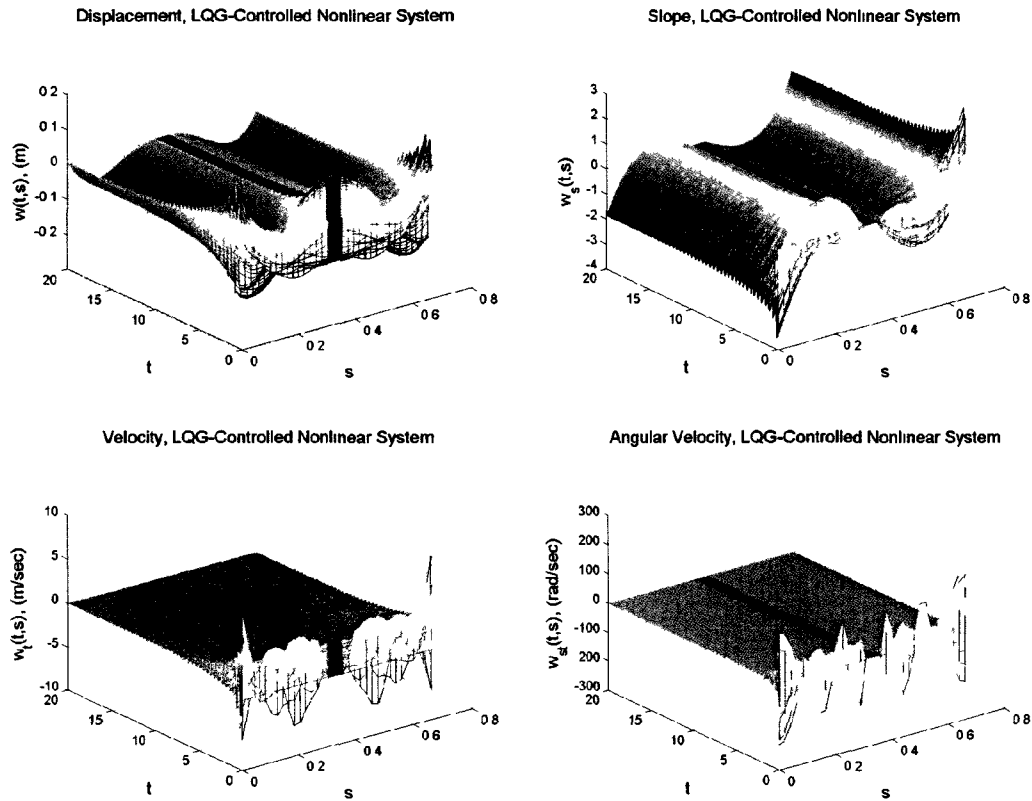


Figure 5.4: LQG Controlled System: Position (top left), Slope (top right), Velocity (bottom left), Angular Velocity (bottom right)

Initially, it was not known if the system would be able to track to the desired state in a reasonable amount of time without significant overshoot. After perturbing the parameters in Equation (3.10) so that lift and weight balance, and applying appropriate magnitudes for control effort by manipulating Equation (5.20), it can be seen that the system effectively reaches its target shape. As expected, the full state feedback results outperform those of the LQG-controlled system, although both systems reach unrealistically high magnitudes for angular velocity. Control effort results are shown in Figure 5.5.

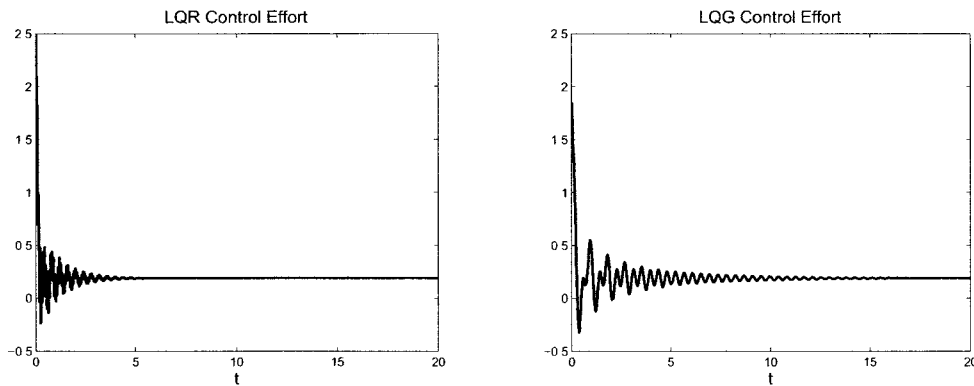


Figure 5.5: Control Effort: LQG (left), LQR (right)

5.3 Wing Morphing Trajectory Results

In this section we employ the same control design in Section 5.2, only here we test the system's ability to achieve a morphing trajectory over time. In order to alleviate overshoot in the LQG-controlled system constant control input functions are taken to be of the form

$$b(s_L) = b(s_R) = 1000, \quad (5.29)$$

for $0 \leq s_L \leq \ell_1$ and $\ell_1 + \ell_M \leq s_R \leq \ell_1 + \ell_M + \ell_2$, and observations of the form

$$y(t) = 650w(t, s), \quad (5.30)$$

for $0 \leq s_L \leq \ell_1$ and $\ell_1 + \ell_M \leq s_R \leq \ell_1 + \ell_M + \ell_2$. The control objective is to morph each beam (linearly in time) from equilibrium to twice the magnitude of Equation (5.27) in a five second time interval. The desired trajectories for each of the four states are represented graphically in Figure 5.6. To obtain a solution to the system, initial conditions are chosen as follows: $x(0) = [0; 0; 0; 0]$ ([displacement; slope; velocity; angular velocity]) and $x_c(0) = 0.75 * x(0)$. Again, a convergent finite element approximation using Hermite interpolating cubic polynomials of order $N = 30$ nodes

for the spatial discretization of the BMB system is used to simulate Equation (5.18), and the parameter values for the BMB system are provided in Table 5.1.

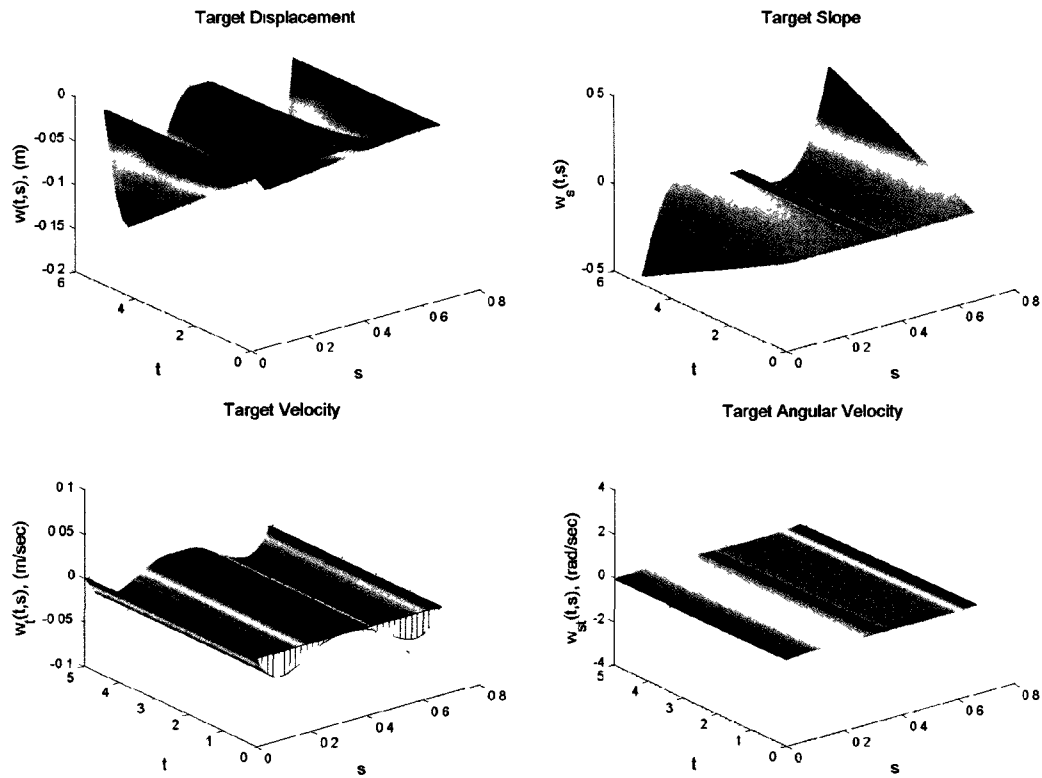


Figure 5.6: Target Trajectory: Position (top left), Slope (top right), Velocity (bottom left), Angular Velocity, (bottom right)

Controlled results are presented in Figures 5.7 and 5.8. For the results presented here, we again assume that measurements are available for the position and velocity states. Control effort results are shown in Figure 5.9.

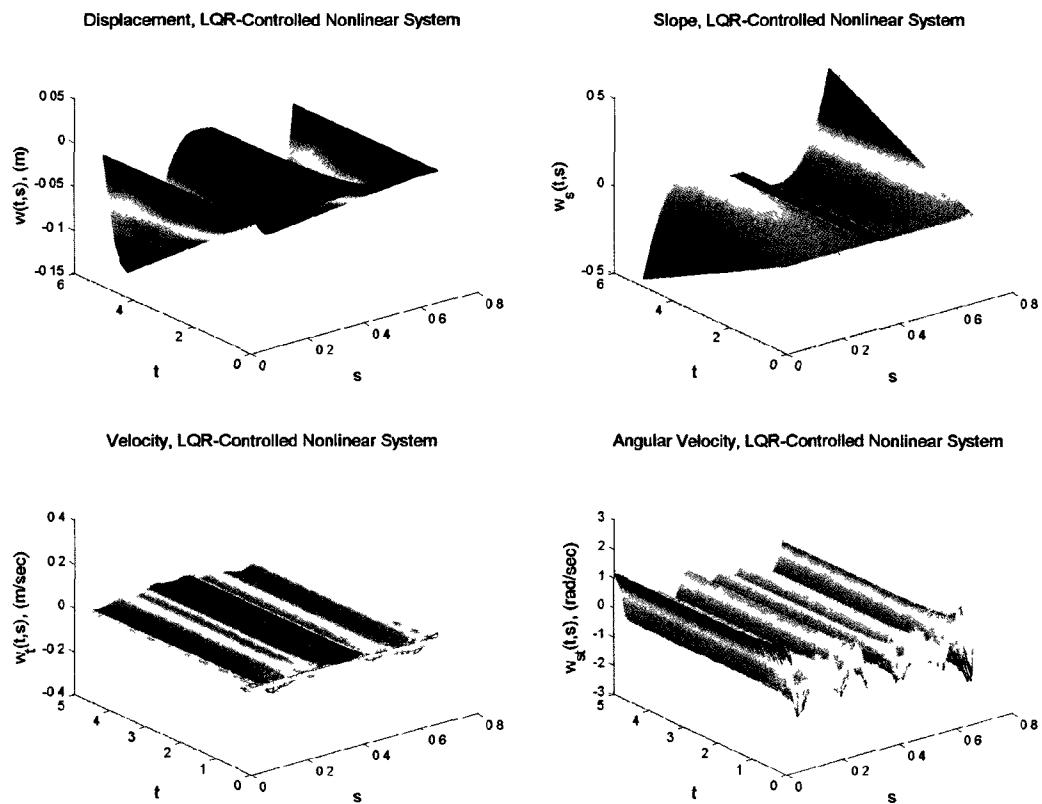


Figure 5.7: LQR Controlled Morphing Trajectory System: Position (top left), Slope (top right), Velocity (bottom left), Angular Velocity (bottom right)

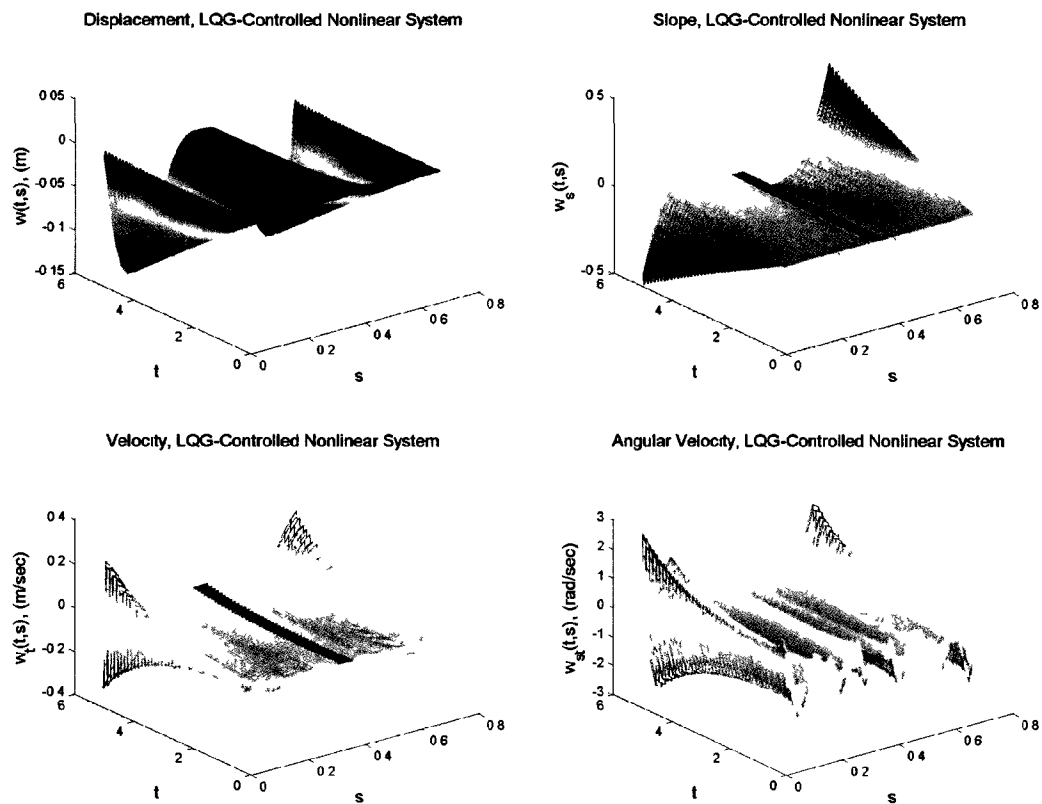


Figure 5.8: LQG Controlled Morphing Trajectory System: Position (top left), Slope (top right), Velocity (bottom left), Angular Velocity (bottom right)

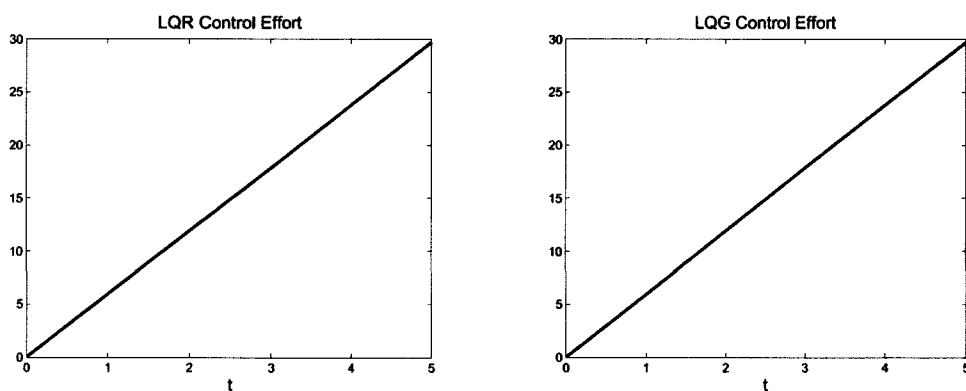


Figure 5.9: Control Effort, Morphing Trajectory: LQG (left), LQR (right)

The position and slope states morph quite efficiently for both the LQR and LQG controlled systems. The desired trajectory for the velocity and angular velocity

states is not achieved, although when comparing the LQR controlled results for the target tracking and the morphing trajectory we can see significant improvement regarding the magnitudes of the angular velocity state. One should note that velocity and angular velocity are not being measured in the LQG controlled system, and some improvement may be made if these states are available for measurement. Further, difficulties in obtaining stabilizing solutions to the algebraic Ricatti equations indicate that there may be Ricatti conditioning issues with this particular model, and point to the limitations of Linear Quadratic control on this nonlinear model. These results were compared with a nonlinear finite dimensional control mechanism, known as feedback linearization, in [10].

CHAPTER 6

NUMERICAL RESULTS FOR THE BMB-PZT MODEL

6.1 Weak Formulation of the BMB-PZT System

Here we present the weak formulation of the left beam of the BMB-PZT system.

The right beam follows similarly. We desire a solution $[w_L(t, s_L), w_R(t, s_R)]^T \in V \subseteq$

$S = H^2[0, \ell_1] \times H^2[\ell_1 + \ell_M, \ell_1 + \ell_M + \ell_2]$ such that

$$\begin{aligned}
 & \int_0^{\ell_1} [\rho A + 2c\rho_{pe}h_{pe}\chi_{pe}(s_L)] \ddot{w}_L(t, s_L)\phi_L(s_L) ds_L + \int_0^{\ell_1} \gamma_1 \dot{w}_L(t, s_L)\phi_L(s_L) ds_L \\
 & + \int_0^{\ell_1} \left[EI + \frac{2}{3}cE_{pe} \left(\frac{3}{4}h^2h_{pe} + \frac{3}{2}hh_{pe}^2 + h_{pe}^3 \right) \chi_{pe}(s_L) \right] w_L''''(t, s_L)\phi_L(s_L) ds_L \\
 & + \int_0^{\ell_1} \left[\gamma_2 I + \frac{2}{3}cC_{Dpe} \left(\frac{3}{4}h^2h_{pe} + \frac{3}{2}hh_{pe}^2 + h_{pe}^3 \right) \chi_{pe}(s_L) \right] \dot{w}_L''''(t, s_L)\phi_L(s_L) ds_L \\
 & = \int_0^{\ell_1} \frac{\partial^2}{\partial s^2} \left[-\frac{1}{2}E_{pe}cd_{31}(h + h_{pe})\chi_{pe}(s_L) \right] u(t)\phi_L(s_L) ds_L \\
 & + \int_0^{\ell_1} \frac{m_b g}{\ell_1} \phi_L(s_L) ds_L - \int_0^{\ell_1} \frac{0.5\rho_a v^2 c}{\ell_1} C_\ell \phi_L(s_L) ds_L,
 \end{aligned} \tag{6.1}$$

for all $[\phi_L(s_L), \phi_R(s_R)]^T \in V = \{[\phi_L(\cdot), \phi_R(\cdot)]^T \in S : \phi_L(\ell_1) = \phi_R(\ell_1 + \ell_M), \phi_L'(\ell_1) = \phi_R'(\ell_1 + \ell_M)\}$. We integrate the second, fourth, and fifth integrals in Equation (6.1)

by parts twice to get

$$\begin{aligned}
& \int_0^{\ell_1} [\rho A + 2c\rho_{pe}h_{pe}\chi_{pe}(s_L)] \ddot{w}_L(t, s_L)\phi_L(s_L) ds_L + \int_0^{\ell_1} \gamma_1 \dot{w}_L(t, s_L)\phi_L(s_L) ds_L \\
& + \int_0^{\ell_1} \left[EI + \frac{2}{3}cE_{pe} \left(\frac{3}{4}h^2h_{pe} + \frac{3}{2}hh_{pe}^2 + h_{pe}^3 \right) \chi_{pe}(s_L) \right] w_L''(t, s_L)\phi_L''(s_L) ds_L \\
& + \int_0^{\ell_1} \left[\gamma_2 I + \frac{2}{3}cC_{Dpe} \left(\frac{3}{4}h^2h_{pe} + \frac{3}{2}hh_{pe}^2 + h_{pe}^3 \right) \chi_{pe}(s_L) \right] \dot{w}_L''(t, s_L)\phi_L''(s_L) ds_L \\
& + \left[EI + \frac{2}{3}cE_{pe} \left(\frac{3}{4}h^2h_{pe} + \frac{3}{2}hh_{pe}^2 + h_{pe}^3 \right) \chi_{pe}(\ell_1) \right] [\phi_L(\ell_1)w_L'''(t, \ell_1) - \phi_L'(\ell_1)w_L''(t, \ell_1)] \\
& + \left[EI + \frac{2}{3}cE_{pe} \left(\frac{3}{4}h^2h_{pe} + \frac{3}{2}hh_{pe}^2 + h_{pe}^3 \right) \chi_{pe}(0) \right] [-\phi_L(0)w_L'''(t, 0) + \phi_L'(0)w_L''(t, 0)] \\
& + \left[\gamma_2 I + \frac{2}{3}cC_{Dpe} \left(\frac{3}{4}h^2h_{pe} + \frac{3}{2}hh_{pe}^2 + h_{pe}^3 \right) \chi_{pe}(\ell_1) \right] [\phi_L(\ell_1)\dot{w}_L'''(t, \ell_1) - \phi_L'(\ell_1)\dot{w}_L''(t, \ell_1)] \\
& + \left[\gamma_2 I + \frac{2}{3}cC_{Dpe} \left(\frac{3}{4}h^2h_{pe} + \frac{3}{2}hh_{pe}^2 + h_{pe}^3 \right) \chi_{pe}(0) \right] [-\phi_L(0)\dot{w}_L'''(t, 0) + \phi_L'(0)\dot{w}_L''(t, 0)] \\
& = \int_0^{\ell_1} \left[-\frac{1}{2}E_{pe}cd_{31}(h + h_{pe})\chi_{pe}(s_L) \right] u(t)\phi_L''(s_L) ds_L \\
& + \left[-\frac{1}{2}E_{pe}cd_{31}(h + h_{pe})\chi_{pe}(\ell_1) \right]' \phi_L(\ell_1) - \left[-\frac{1}{2}E_{pe}cd_{31}(h + h_{pe})\chi_{pe}(0) \right]' \phi_L(0) \\
& - \left[-\frac{1}{2}E_{pe}cd_{31}(h + h_{pe})\chi_{pe}(\ell_1) \right] \phi_L'(\ell_1) + \left[-\frac{1}{2}E_{pe}cd_{31}(h + h_{pe})\chi_{pe}(0) \right] \phi_L'(0) \\
& + \int_0^{\ell_1} \frac{m_b g}{\ell_1} \phi_L(s_L) ds_L - \int_0^{\ell_1} \frac{0.5\rho_a v^2 c}{\ell_1} C_t \phi_L(s_L) ds_L.
\end{aligned} \tag{6.2}$$

Since we have assumed that the piezoceramic patches are not located at the ends of the beams, $\chi_{pe}(\ell_1) = \chi_{pe}(0) = 0$ and Equation (6.2) reduces to

$$\begin{aligned}
& \int_0^{\ell_1} [\rho A + 2c\rho_{pe}h_{pe}\chi_{pe}(s_L)] \ddot{w}_L(t, s_L)\phi_L(s_L) ds_L + \int_0^{\ell_1} \gamma_1 \dot{w}_L(t, s_L)\phi_L(s_L) ds_L \\
& + \int_0^{\ell_1} \left[EI + \frac{2}{3}cE_{pe} \left(\frac{3}{4}h^2h_{pe} + \frac{3}{2}hh_{pe}^2 + h_{pe}^3 \right) \chi_{pe}(s_L) \right] w_L''(t, s_L)\phi_L''(s_L) ds_L \\
& + \int_0^{\ell_1} \left[\gamma_2 I + \frac{2}{3}cC_{Dpe} \left(\frac{3}{4}h^2h_{pe} + \frac{3}{2}hh_{pe}^2 + h_{pe}^3 \right) \chi_{pe}(s_L) \right] \dot{w}_L''(t, s_L)\phi_L''(s_L) ds_L \\
& + EI\phi_L(\ell_1)w_L'''(t, \ell_1) - EI\phi_L'(\ell_1)w_L''(t, \ell_1) - EI\phi_L(0)w_L'''(t, 0) + EI\phi_L'(0)w_L''(t, 0) \\
& + \gamma_2 I\phi_L(\ell_1)\dot{w}_L'''(t, \ell_1) - \gamma_2 I\phi_L'(\ell_1)\dot{w}_L''(t, \ell_1) - \gamma_2 I\phi_L(0)\dot{w}_L'''(t, 0) + \gamma_2 I\phi_L'(0)\dot{w}_L''(t, 0) \\
& = \int_0^{\ell_1} \left[-\frac{1}{2}E_{pe}cd_{31}(h + h_{pe})\chi_{pe}(s_L) \right] u(t)\phi_L''(s_L) ds_L + \int_0^{\ell_1} \frac{m_b g}{\ell_1} \phi_L(s_L) ds_L \\
& - \int_0^{\ell_1} \frac{0.5\rho_a v^2 c}{\ell_1} C_\ell \phi_L(s_L) ds_L.
\end{aligned} \tag{6.3}$$

Rearranging some terms, we have

$$\begin{aligned}
& \int_0^{\ell_1} [\rho A + 2c\rho_{pe}h_{pe}\chi_{pe}(s_L)] \ddot{w}_L(t, s_L)\phi_L(s_L) ds_L + \int_0^{\ell_1} \gamma_1 \dot{w}_L(t, s_L)\phi_L(s_L) ds_L \\
& + \int_0^{\ell_1} \left[EI + \frac{2}{3}cE_{pe} \left(\frac{3}{4}h^2h_{pe} + \frac{3}{2}hh_{pe}^2 + h_{pe}^3 \right) \chi_{pe}(s_L) \right] w_L''(t, s_L)\phi_L''(s_L) ds_L \\
& + \int_0^{\ell_1} \left[\gamma_2 I + \frac{2}{3}cC_{Dpe} \left(\frac{3}{4}h^2h_{pe} + \frac{3}{2}hh_{pe}^2 + h_{pe}^3 \right) \chi_{pe}(s_L) \right] \dot{w}_L''(t, s_L)\phi_L''(s_L) ds_L
\end{aligned} \tag{6.4}$$

$$\begin{aligned}
& +\phi_L(\ell_1) [EIw_L'''(t, \ell_1) + \gamma_2 I\dot{w}_L'''(t, \ell_1)] + \phi_L(0) [-EIw_L'''(t, 0) - \gamma_2 I\dot{w}_L'''(t, 0)] \\
& +\phi_L'(\ell_1) [-EIw_L''(t, \ell_1) - \gamma_2 I\dot{w}_L''(t, \ell_1)] + \phi_L'(0) [EIw_L''(t, 0) + \gamma_2 I\dot{w}_L''(t, 0)] \\
& = \int_0^{\ell_1} \left[-\frac{1}{2} E_{pe} c d_{31} (h + h_{pe}) \chi_{pe}(s_L) \right] u(t) \phi_L''(s_L) ds_L + \int_0^{\ell_1} \frac{m_b g}{\ell_1} \phi_L(s_L) ds_L \\
& - \int_0^{\ell_1} \frac{0.5 \rho_a v^2 c}{\ell_1} C_\ell \phi_L(s_L) ds_L.
\end{aligned}$$

Similarly the weak form of the right beam equation would be

$$\begin{aligned}
& \int_{\ell_1 + \ell_M}^{\ell_1 + \ell_M + \ell_2} [\rho A + 2c\rho_{pe} h_{pe} \chi_{pe}(s_R)] \ddot{w}_R(t, s_R) \phi_R(s_R) ds_R + \int_0^{\ell_1} \gamma_1 \dot{w}_R(t, s_R) \phi_R(s_R) ds_R \\
& + \int_{\ell_1 + \ell_M}^{\ell_1 + \ell_M + \ell_2} \left[EI + \frac{2}{3} c E_{pe} \left(\frac{3}{4} h^2 h_{pe} + \frac{3}{2} h h_{pe}^2 + h_{pe}^3 \right) \chi_{pe}(s_R) \right] w_R''(t, s_R) \phi_R''(s_R) ds_R \\
& + \int_{\ell_1 + \ell_M}^{\ell_1 + \ell_M + \ell_2} \left[\gamma_2 I + \frac{2}{3} c c_{Dpe} \left(\frac{3}{4} h^2 h_{pe} + \frac{3}{2} h h_{pe}^2 + h_{pe}^3 \right) \chi_{pe}(s_R) \right] \dot{w}_R''(t, s_R) \phi_R''(s_R) ds_R \\
& + \phi_R(\ell_1 + \ell_M + \ell_2) [EIw_R'''(t, \ell_1 + \ell_M + \ell_2) + \gamma_2 I\dot{w}_R'''(t, \ell_1 + \ell_M + \ell_2)] \\
& + \phi_R(\ell_1 + \ell_M) [-EIw_R'''(t, \ell_1 + \ell_M) - \gamma_2 I\dot{w}_R'''(t, \ell_1 + \ell_M)] \\
& + \phi_R'(\ell_1 + \ell_M + \ell_2) [-EIw_R''(t, \ell_1 + \ell_M + \ell_2) - \gamma_2 I\dot{w}_R''(t, \ell_1 + \ell_M + \ell_2)] \\
& + \phi_R'(\ell_1 + \ell_M) [EIw_R''(t, \ell_1 + \ell_M) + \gamma_2 I\dot{w}_R''(t, \ell_1 + \ell_M)] \\
& = \int_{\ell_1 + \ell_M}^{\ell_1 + \ell_M + \ell_2} \left[-\frac{1}{2} E_{pe} c d_{31} (h + h_{pe}) \chi_{pe}(s_R) \right] u(t) \phi_R''(s_R) ds_R
\end{aligned} \tag{6.5}$$

$$+ \int_{\ell_1+\ell_M}^{\ell_1+\ell_M+\ell_2} \frac{m_b g}{\ell_2} \phi_R(s_R) ds_R - \int_{\ell_1+\ell_M}^{\ell_1+\ell_M+\ell_2} \frac{0.5\rho_a v^2 c}{\ell_2} C_t \phi_R(s_R) ds_R.$$

We now apply the free end boundary conditions from Table 3.1, i.e. the first four. to Equation (6.4) and Equation (6.5), and we add the left and right beam weak forms, which yields

$$\begin{aligned} & \int_0^{\ell_1} [\rho A + 2c\rho_{pe}h_{pe}\chi_{pe}(s_L)] \ddot{w}_L(t, s_L) \phi_L(s_L) ds_L + \int_0^{\ell_1} \gamma_1 \dot{w}_L(t, s_L) \phi_L(s_L) ds_L \\ & + \int_0^{\ell_1} \left[EI + \frac{2}{3}cE_{pe} \left(\frac{3}{4}h^2h_{pe} + \frac{3}{2}hh_{pe}^2 + h_{pe}^3 \right) \chi_{pe}(s_L) \right] w_L''(t, s_L) \phi_L''(s_L) ds_L \\ & + \int_0^{\ell_1} \left[\gamma_2 I + \frac{2}{3}cC_{Dpe} \left(\frac{3}{4}h^2h_{pe} + \frac{3}{2}hh_{pe}^2 + h_{pe}^3 \right) \chi_{pe}(s_L) \right] \dot{w}_L''(t, s_L) \phi_L''(s_L) ds_L \\ & + \int_{\ell_1+\ell_M}^{\ell_1+\ell_M+\ell_2} [\rho A + 2c\rho_{pe}h_{pe}\chi_{pe}(s_R)] \ddot{w}_R(t, s_R) \phi_R(s_R) ds_R + \int_0^{\ell_1} \gamma_1 \dot{w}_R(t, s_R) \phi_R(s_R) ds_R \\ & + \int_{\ell_1+\ell_M}^{\ell_1+\ell_M+\ell_2} \left[EI + \frac{2}{3}cE_{pe} \left(\frac{3}{4}h^2h_{pe} + \frac{3}{2}hh_{pe}^2 + h_{pe}^3 \right) \chi_{pe}(s_R) \right] w_R''(t, s_R) \phi_R''(s_R) ds_R \\ & + \int_{\ell_1+\ell_M}^{\ell_1+\ell_M+\ell_2} \left[\gamma_2 I + \frac{2}{3}cC_{Dpe} \left(\frac{3}{4}h^2h_{pe} + \frac{3}{2}hh_{pe}^2 + h_{pe}^3 \right) \chi_{pe}(s_R) \right] \dot{w}_R''(t, s_R) \phi_R''(s_R) ds_R \\ & + \phi_L(\ell_1) [EIw_L'''(t, \ell_1) + \gamma_2 I \dot{w}_L'''(t, \ell_1)] + \phi_L'(\ell_1) [-EIw_L''(t, \ell_1) - \gamma_2 I \dot{w}_L''(t, \ell_1)] \\ & + \phi_R(\ell_1 + \ell_M) [-EIw_R'''(t, \ell_1 + \ell_M) - \gamma_2 I \dot{w}_R'''(t, \ell_1 + \ell_M)] \\ & + \phi_R'(\ell_1 + \ell_M) [EIw_R''(t, \ell_1 + \ell_M) + \gamma_2 I \dot{w}_R''(t, \ell_1 + \ell_M)] \end{aligned} \tag{6.6}$$

$$\begin{aligned}
&= \int_0^{\ell_1} \left[-\frac{1}{2} E_{pe} c d_{31} (h + h_{pe}) \chi_{pe}(s_L) \right] u(t) \phi_L''(s_L) ds_L + \int_0^{\ell_1} \frac{m_b g}{\ell_1} \phi_L(s_L) ds_L \\
&- \int_0^{\ell_1} \frac{0.5 \rho_a v^2 c}{\ell_1} C_\ell \phi_L(s_L) ds_L + \int_{\ell_1 + \ell_M}^{\ell_1 + \ell_M + \ell_2} \left[-\frac{1}{2} E_{pe} c d_{31} (h + h_{pe}) \chi_{pe}(s_R) \right] u(t) \phi_R''(s_R) ds_R \\
&+ \int_{\ell_1 + \ell_M}^{\ell_1 + \ell_M + \ell_2} \frac{m_b g}{\ell_2} \phi_R(s_R) ds_R - \int_{\ell_1 + \ell_M}^{\ell_1 + \ell_M + \ell_2} \frac{0.5 \rho_a v^2 c}{\ell_2} C_\ell \phi_R(s_R) ds_R.
\end{aligned}$$

Applying the boundary conditions which hold at the mass location, i.e. the last two conditions in Table 3.1, we have

$$\begin{aligned}
&\int_0^{\ell_1} [\rho A + 2c\rho_{pe}h_{pe}\chi_{pe}(s_L)] \ddot{w}_L(t, s_L) \phi_L(s_L) ds_L + \int_0^{\ell_1} \gamma_1 \dot{w}_L(t, s_L) \phi_L(s_L) ds_L \\
&+ \int_0^{\ell_1} \left[EI + \frac{2}{3} c E_{pe} \left(\frac{3}{4} h^2 h_{pe} + \frac{3}{2} h h_{pe}^2 + h_{pe}^3 \right) \chi_{pe}(s_L) \right] w_L''(t, s_L) \phi_L''(s_L) ds_L \\
&+ \int_0^{\ell_1} \left[\gamma_2 I + \frac{2}{3} c c_{Dpe} \left(\frac{3}{4} h^2 h_{pe} + \frac{3}{2} h h_{pe}^2 + h_{pe}^3 \right) \chi_{pe}(s_L) \right] \dot{w}_L''(t, s_L) \phi_L''(s_L) ds_L \\
&+ \int_{\ell_1 + \ell_M}^{\ell_1 + \ell_M + \ell_2} [\rho A + 2c\rho_{pe}h_{pe}\chi_{pe}(s_R)] \ddot{w}_R(t, s_R) \phi_R(s_R) ds_R \\
&+ \int_{\ell_1 + \ell_M}^{\ell_1 + \ell_M + \ell_2} \gamma_1 \dot{w}_R(t, s_R) \phi_R(s_R) ds_R \\
&+ \int_{\ell_1 + \ell_M}^{\ell_1 + \ell_M + \ell_2} \left[EI + \frac{2}{3} c E_{pe} \left(\frac{3}{4} h^2 h_{pe} + \frac{3}{2} h h_{pe}^2 + h_{pe}^3 \right) \chi_{pe}(s_R) \right] w_R''(t, s_R) \phi_R''(s_R) ds_R
\end{aligned} \tag{6.7}$$

$$\begin{aligned}
& + \int_{\ell_1+\ell_M}^{\ell_1+\ell_M+\ell_2} \left[\gamma_2 I + \frac{2}{3} c c_{Dpe} \left(\frac{3}{4} h^2 h_{pe} + \frac{3}{2} h h_{pe}^2 + h_{pe}^3 \right) \chi_{pe}(s_R) \right] \dot{w}_R''(t, s_R) \phi_R''(s_R) ds_R \\
& + m \ddot{w}_L(t, \ell_1) + I_2 \ddot{w}'_L(t, \ell_1) \\
& = \int_0^{\ell_1} \left[-\frac{1}{2} E_{pe} c d_{31} (h + h_{pe}) \chi_{pe}(s_L) \right] u(t) \phi_L''(s_L) ds_L + \int_0^{\ell_1} \frac{m_b g}{\ell_1} \phi_L(s_L) ds_L \\
& - \int_0^{\ell_1} \frac{0.5 \rho_a v^2 c}{\ell_1} C_\ell \phi_L(s_L) ds_L \\
& + \int_{\ell_1+\ell_M}^{\ell_1+\ell_M+\ell_2} \left[-\frac{1}{2} E_{pe} c d_{31} (h + h_{pe}) \chi_{pe}(s_R) \right] u(t) \phi_R''(s_R) ds_R \\
& + \int_{\ell_1+\ell_M}^{\ell_1+\ell_M+\ell_2} \frac{m_b g}{\ell_2} \phi_R(s_R) ds_R - \int_{\ell_1+\ell_M}^{\ell_1+\ell_M+\ell_2} \frac{0.5 \rho_a v^2 c}{\ell_2} C_\ell \phi_R(s_R) ds_R.
\end{aligned}$$

6.2 Discretization

A basis $\{e_i\}_i^N$ is chosen for the approximating space $V^N \subseteq V$, where N corresponds to the number of basis functions used in the finite element approximation. Cubic Hermite interpolating polynomials are used to approximate the displacements of the left and right beams. The basis vectors take the form:

$$e_i^N = \begin{bmatrix} b_{L,i}^N(s_L) \\ b_{R,i}^N(s_R) \end{bmatrix}, \text{ for } i = 1, \dots, N. \quad (6.8)$$

That is, the state will be approximated as

$$\begin{bmatrix} w_L(t, s_L) \\ w_R(t, s_R) \end{bmatrix} \approx \begin{bmatrix} w_L^N(t, s_L) \\ w_R^N(t, s_R) \end{bmatrix} = \begin{bmatrix} \sum_{i=1}^N \alpha_i^N(t) b_{L,i}(s_L) \\ \sum_{i=1}^N \beta_i^N(t) b_{R,i}(s_R) \end{bmatrix}. \quad (6.9)$$

Substituting the state approximation Equation (6.9) into Equation (6.7) yields the matrix equation

$$\begin{aligned} & M_L \ddot{\alpha}(t) + M_R \ddot{\beta}(t) + D_L \dot{\alpha}(t) + D_R \dot{\beta}(t) + K_L \alpha(t) + K_R \beta(t) \\ & = B_L u_L(t) + B_R u_R(t) + G_L + G_R + F_L + F_R, \end{aligned} \quad (6.10)$$

where

$$\begin{aligned} [M_L]_{i,j} &= \int_0^{\ell_1} [\rho A + 2c\rho_{pe}h_{pe}\chi_{pe}(s_L)] b_{L,i}(s_L)b_{L,j}(s_L) ds_L + mb_{L,i}(\ell_1)b_{L,j}(\ell_1) \\ & \quad + I_z b'_{L,i}(\ell_1)b'_{L,j}(\ell_1) \\ [M_R]_{i,j} &= \int_{\ell_1+\ell_M}^{\ell_1+\ell_M+\ell_2} [\rho A + 2c\rho_{pe}h_{pe}\chi_{pe}(s_R)] b_{R,i}(s_R)b_{R,j}(s_R) ds_R \\ [D_L]_{i,j} &= \int_0^{\ell_1} \gamma_1 b_{L,i}(s_L)b_{L,j}(s_L) ds_L + \\ & \quad \int_0^{\ell_1} \left[\gamma_2 I + \frac{2}{3} c c_{Dpe} \left(\frac{3}{4} h^2 h_{pe} + \frac{3}{2} h h_{pe}^2 + h_{pe}^3 \right) \chi_{pe}(s_L) \right] b''_{L,i}(s_L)b''_{L,j}(s_L) ds_L \\ [D_R]_{i,j} &= \int_{\ell_1+\ell_M}^{\ell_1+\ell_M+\ell_2} \gamma_1 b_{R,i}(s_R)b_{R,j}(s_R) ds_R \\ & \quad + \int_{\ell_1+\ell_M}^{\ell_1+\ell_M+\ell_2} \left[\gamma_2 I + \frac{2}{3} c c_{Dpe} \left(\frac{3}{4} h^2 h_{pe} \right. \right. \\ & \quad \left. \left. + \frac{3}{2} h h_{pe}^2 + h_{pe}^3 \right) \chi_{pe}(s_R) \right] b''_{R,i}(s_R)b''_{R,j}(s_R) ds_R \end{aligned} \quad (6.11)$$

$$[K_L]_{i,j} = \int_0^{\ell_1} \left[EI + \frac{2}{3}cE_{pe} \left(\frac{3}{4}h^2h_{pe} + \frac{3}{2}hh_{pe}^2 + h_{pe}^3 \right) \chi_{pe}(s_L) \right] b''_{L,i}(s_L)b''_{L,j}(s_L) ds_L$$

$$[K_R]_{i,j} = \int_{\ell_1+\ell_M}^{\ell_1+\ell_M+\ell_2} \left[EI + \frac{2}{3}cE_{pe} \left(\frac{3}{4}h^2h_{pe} + \frac{3}{2}hh_{pe}^2 + h_{pe}^3 \right) \chi_{pe}(s_R) \right] b''_{R,i}(s_R)b''_{R,j}(s_R) ds_R$$

$$[B_L]_j = \int_0^{\ell_1} \left[-\frac{1}{2}E_{pe}cd_{31}(h+h_{pe})\chi_{pe}(s_L) \right] u_L(t)b''_{L,j}(s_L) ds_L$$

$$[B_R]_j = \int_{\ell_1+\ell_M}^{\ell_1+\ell_M+\ell_2} \left[-\frac{1}{2}E_{pe}cd_{31}(h+h_{pe})\chi_{pe}(s_R) \right] u_R(t)b''_{R,j}(s_R) ds_R$$

$$[G_L]_j = \int_0^{\ell_1} \frac{m_b g}{\ell_1} b_{L,j}(s_L) ds_L,$$

$$[G_R]_j = \int_{\ell_1+\ell_M}^{\ell_1+\ell_M+\ell_2} \frac{m_b g}{\ell_2} b_{R,j}(s_R) ds_R$$

$$[F_L]_j = \int_0^{\ell_1} -\frac{0.5\rho_a v^2 c}{\ell_1} C_\ell b_{L,j}(s_L) ds_L,$$

$$[F_R]_j = \int_{\ell_1+\ell_M}^{\ell_1+\ell_M+\ell_2} -\frac{0.5\rho_a v^2 c}{\ell_2} C_\ell b_{R,j}(s_R) ds_R.$$

To simplify further, define

$$c(t) = \begin{bmatrix} \alpha(t) \\ \beta(t) \end{bmatrix} \Rightarrow \dot{c}(t) = \begin{bmatrix} \alpha(t) \\ \dot{\beta}(t) \end{bmatrix} \Rightarrow c(t) = \begin{bmatrix} \dot{\alpha}(t) \\ \ddot{\beta}(t) \end{bmatrix} \quad (6.12)$$

Substituting these relationships into Equation (6.10) yields

$$\begin{aligned} & \begin{bmatrix} M_L & 0 \\ 0 & M_R \end{bmatrix} \ddot{c}(t) + \begin{bmatrix} D_L & 0 \\ 0 & D_R \end{bmatrix} \dot{c}(t) + \begin{bmatrix} K_L & 0 \\ 0 & K_R \end{bmatrix} c(t) \\ & = \begin{bmatrix} B_L \\ B_R \end{bmatrix} + \begin{bmatrix} G_L \\ G_R \end{bmatrix} + \begin{bmatrix} F_L \\ F_R \end{bmatrix}, \end{aligned} \quad (6.13)$$

which can be re-written as

$$\ddot{c}(t) = M^{-1}(-D\dot{c}(t) - Kc(t) + \bar{B} + \bar{G} + \bar{F}), \quad (6.14)$$

where

$$M = \begin{bmatrix} M_L & 0 \\ 0 & M_R \end{bmatrix}, \quad D = \begin{bmatrix} D_L & 0 \\ 0 & D_R \end{bmatrix}, \quad K = \begin{bmatrix} K_L & 0 \\ 0 & K_R \end{bmatrix}. \quad (6.15)$$

$$\bar{B} = \begin{bmatrix} B_L \\ B_R \end{bmatrix}, \quad \bar{G} = \begin{bmatrix} G_L \\ G_R \end{bmatrix}, \quad \bar{F} = \begin{bmatrix} F_L \\ F_R \end{bmatrix}.$$

Converting Equation (6.14) into a first order system results in

$$\dot{x}(t) = Ax(t) + Bu(t) + G + F(x), \quad (6.16)$$

where

$$\begin{aligned}
 x(t) &= \begin{bmatrix} c(t) \\ \dot{c}(t) \end{bmatrix}, & A &= \begin{bmatrix} 0 & I \\ -M^{-1}K & -M^{-1}D \end{bmatrix} \\
 B &= \begin{bmatrix} 0 \\ M^{-1}\bar{B} \end{bmatrix}, & G &= \begin{bmatrix} 0 \\ M^{-1}\bar{G} \end{bmatrix}, & (6.17) \\
 F &= \begin{bmatrix} 0 \\ M^{-1}\bar{F}(x) \end{bmatrix}.
 \end{aligned}$$

6.3 Simulation

System parameters are provided in Table 6.1, and initial conditions are chosen as follows: $x(0) = [0; 0; -2; 0]$ ([displacement; slope; velocity; angular velocity]). Uncontrolled results are provided in Figure 6.1. Again, simulations were obtained using Matlab's ODE15s solver for stiff systems. A convergent finite element approximation using Hermite interpolating cubic polynomials of order $N = 30$ nodes for the spatial discretization of the BMB-PZT system is used to simulate Equation (6.16).

Table 6.1: BMB-PZT System Parameters

| Parameter | Value | Units |
|-----------------------|------------------------|-------------------------|
| $\ell_{1,2}$ | 0.6096 | m |
| ℓ_M | 0.0508 | m |
| ρ | 980 | kg/m ³ |
| \hat{w} , width | 0.127 | m |
| h , height | 0.0254 | m |
| $a = \hat{w}h$ | 0.032 | m ² |
| E | 2.0×10^6 | N/m ² |
| $I = (\hat{w}h^3)/12$ | 1.734×10^{-7} | m ⁴ |
| m | 1.927 | kg |
| m_b | 1.927 | kg |
| γ_1 | 0.025 | kg/(m sec) |
| γ_2 | 1×10^2 | kg/(m ⁵ sec) |
| ℓ_{pe} | 0.061 | m |
| E_{pe} | 3.47×10^{10} | N/m ² |
| ρ_{pe} | 4215.46 | kg/m ³ |
| c_{Dpe} | 10 | kg/(m ⁵ sec) |
| h_{pe} | 0.0008 | m |
| d_{31} | 0.0057 | m/volts |

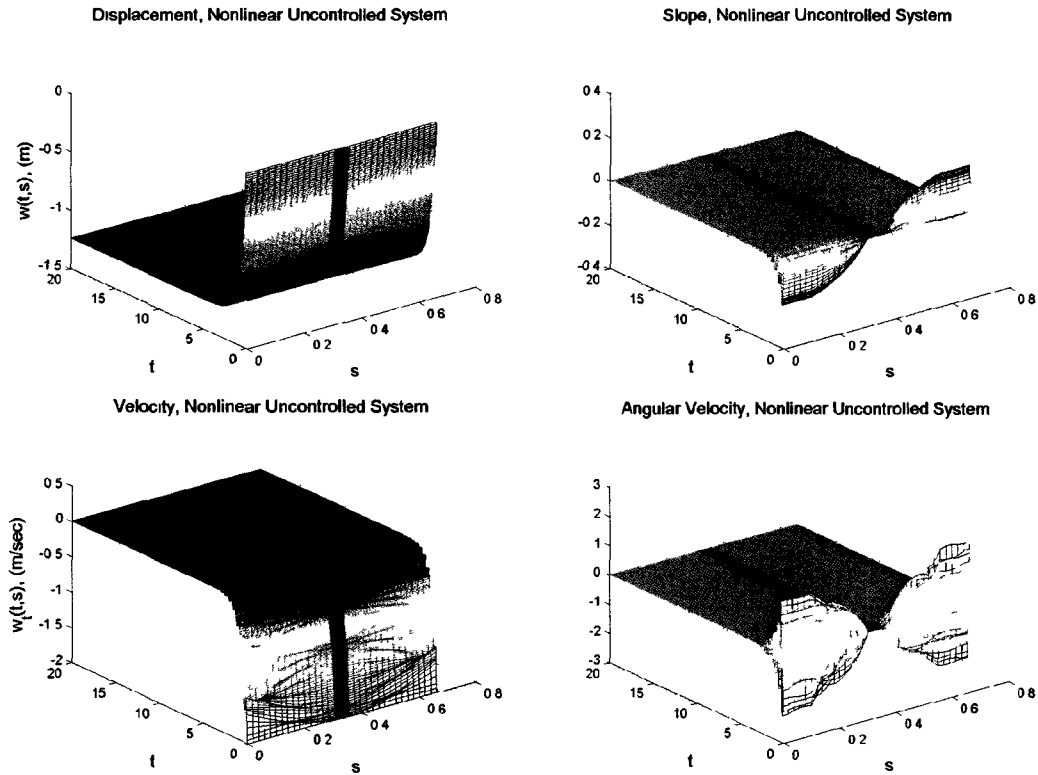


Figure 6.1: Uncontrolled BMB-PZT System: Position (top left), Slope (top right), Velocity (bottom left), Angular Velocity, (bottom right)

In [5] both the limitations of and necessity for using finite elements with piezoceramic patches was discussed. One disadvantage to the finite element approach is the fact that a computational representation of the patches must correspond with the grid. Therefore, in our code a patch begins at the nearest element which is approximately two inches from each of the free ends in these simulations. Furthermore, note that the finite element vectors B_L and B_R from Equation (6.11) contain two spatial derivatives. Hermite cubic splines are natural basis functions to apply to this model due to the continuity of displacement and slope conditions at the mass location, but enough smoothness exists at the nodes so that the control vectors B_L and B_R are continuous. Therefore, more work needs to be done to determine if other basis

functions (or a hybrid of basis functions) may be applied to this model so that control design may be employed.

CHAPTER 7

CONCLUSIONS

In this work two models are presented to represent the heave dynamics of a flexible wing MAV. The BMB system is described in Equation (3.8) and Equation (3.9), and the model is extended to include realistic actuation in the BMB-PZT system described in Equation (3.17) and Equation (3.19). Both of these systems are approximated by Hermite interpolating cubic polynomials with two displacement and two slope degrees of freedom for each beam element. A proof for well-posedness and the attainment of a C_0 -semigroup is provided for the BMB model and extended to the BMB-PZT model. Steady state linear quadratic tracking control was applied to the BMB system by obtaining a linear approximation of the nonlinear lift function, employing control design, and applying the control matrices to the nonlinear system. Two control objectives were analyzed: target state tracking and morphing trajectory over time. Both of these approaches resulted in a nonlinear controller for the BMB system.

Target state tracking results showed that the model effectively reached all four target states, although unrealistically high magnitudes were obtained for the angular velocity states. Morphing trajectory results indicated that the position and slope states morph quite efficiently for both the LQR and LQG controlled systems.

Improvement is made in the magnitudes for the angular velocity states of the LQR controlled system. However, both the velocity and angular velocity states (which were not assumed to be available for measurement) showed growth for the LQG controller.

Overall, results indicate that although tools from linear distributed parameter control theory can be successfully applied to this model there are limitations to linear control design, primarily difficulties in obtaining stabilizing solutions to algebraic Riccati equations. We also observe that although the boundary conditions applied to these models lend themselves to the use of Hermite cubic splines, discontinuities occur at the nodes when considering the second derivatives of these basis functions, which prevents implementation of control via piezoceramic actuators with these basis functions.

As a result, a natural extension of the theoretical work provided here would include stability analysis and verification of the existence of unique infinite dimensional Riccati solutions to the control problem. A rigorous theoretical analysis of the nonlinear model, including nonlinear semigroup theory, would help to gain further insight into the system. Additional future work includes investigation of an appropriate use of basis functions for the BMB-PZT model so that control can be modeled. Once control is implemented via realistic actuation, additional work from distributed parameter control theory would help to gain further insight into optimal morphing trajectories. We also seek to investigate the performance of other nonlinear controllers on this model, as done in [10]. Other modeling involves the inclusion of more realistic aerodynamics beyond that of heave dynamics, such as the model's ability to roll, pitch, and yaw. Finally, we seek to upgrade the system to a more realistic wing model. The

most natural step towards this two dimensional model may include modeling with one dimensional narrow plates and later the inclusion of two dimensional plates.

BIBLIOGRAPHY

- [1] <http://www.pi-usa.us/>.
- [2] R. Albertani, R. DeLoach, B. Stanford, J.P. Hubner, and P. Ifju. Wind tunnel testing and nonlinear modeling applied to powered micro air vehicles with flexible wings. *AIAA Journal of Aircraft*, 45(3), 2008.
- [3] W. Amrein. *Hilbert Space Methods in Quantum Mechanics*. Birkhauser Verlag, Basel, 2009.
- [4] H. T. Banks, R. C. Smith, and Y. Wang. *Smart Material Structures*. Masson and Wiley, Paris, 1996.
- [5] H. T. Banks, H.T. Tran, and R. C. H del Rosario. Proper orthogonal decomposition based control of transverse beam vibrations: Experimental implementation. *IEEE Transactions on Control Systems Technology*, 10(5):717–726, September 2002.
- [6] O. Bilgen, K.B. Kochersberger, D.J. Inman, and O.J. Ohanian III. Macro-fiber composite actuators for a swept wing unmanned aircraft. *The Aeronautical Journal*, 113(1144):385–395, 2009.
- [7] J. Burns. *Lecture notes on modern calculus of variations with applications to control theory, numerical methods, and differential equations*. 2000.
- [8] J. A. Burns and B. Batten King. A reduced basis approach to the design of low order feedback controllers for nonlinear continuous systems. *Journal of Vibration and Control*, 4:297–323, 1998.
- [9] A. Chakravarthy, K.A. Evans, and J. Evers. Sensitivities and functional gains for a flexible aircraft-inspired model. *Proceedings of the 2010 American Control Conference*, pages 4893–4898, 2010.
- [10] A. Chakravarthy, K.A. Evans, J. Evers, and L. Kuhn. Nonlinear controllers for wing morphing trajectories of a heave dynamics model. *Proceedings of the 2011 Conference on Decision and Control*. to appear.
- [11] R. F. Curtain and H. J. Zwart. *An Introduction to Infinite-Dimensional Linear Systems Theory*. Springer-Verlag, New York, 1995.
- [12] B. Datta. *Numerical Methods for Linear Control Systems*. Elsevier Academic Press, London, 2004.

- [13] M. Demuth and J. van Casteren. *Stochastic Spectral Theorey for Self-Adjoint Feller Operators*. EPFL Press, Spain, 2000.
- [14] B. Dickinson, J. Singler, and B. Batten. The detection of unsteady flow separation with bioinspired hair-cell sensors. *26th AIAA Aerodynamic Measurement Technology and Ground Testing Conference*, pages AIAA 2008-3937, 2008.
- [15] P. Dorato, C. Abdallah, and V. Cerone. *Linear-Quadratic Control, An Introduction*. Prentice Hall, Englewood Cliffs, 1995
- [16] J. S. Gibson. An analysis of optimal model regulation: convergence and stability. *SIAM J. Contr. Opt.*, 19:686-707, 1981.
- [17] J. S. Gibson and A. Adamian. Approximation theory for linear quadratic gaussian control of flexible structures. *SIAM J. Contr. Opt.*, 29:1-37, 1991.
- [18] Z. Liu R. Spies J. Burns, E. Cliff. On coupled transversal and axial motions of two beams with a joint. *Journal of Mathematical Analysis and Applications*, pages 182-196, 2008.
- [19] B. Batten King. *Modeling and Control of Multiple Component Structures*. PhD thesis, Clemson University, December 1991.
- [20] J. L. Lions. *Optimal Control of Systems Governed by Partial Differential Equations*. Springer-Verlag, Berlin, 1971.
- [21] A. Pazy. *Semigroups of Linear Operators and Applications to Partial Differential Equations*. Springer-Verlag, New York, 1983.
- [22] R. Showalter. *Hilbert Space Methods in Partial Differential Equations*. Dover Publications, Inc., New York, 2010.
- [23] W. Shyy, P.G. Ifju, and D. Viieru. Membrane wing-based micro air vehicles. *Applied Mechanics Reviews*, 58:283-301, 2005.
- [24] W. Shyy, P. Trizila, C. Kang, and H. Aono. Can tip vortices enhance lift of a flapping wing? *AIAA Journal*, 47:289-293, 2009.
- [25] A. Song, X. Tian, E. Israeli, R. Galvao, K. Bishop, S. Swartz, and K. Breuer. Aeromechanics of membrane wings, with implications for animal flight. *AIAA Journal*, 46(8):2096-2196, 2008.
- [26] M. Tadi. *An Optimal Control Problem for a Timoshenko Beam* PhD thesis, Virginia Polytechnic Institute and State University, August 1991.
- [27] X. Tian, J. Iriarte-Diaz, K. Middleton, R. Galvao, E. Israeli, A. Roemer, A. Sullivan. A. Song, S. Swartz. and K. Breuer. Direct measurements of the kinematics and dynamics of bat flight *Bioinspiration & Biomimetics*, 1.S10-S18, 2006.

- [28] Jr. W. Weaver, S. P. Timoshenko, and D. H. Young. *Vibration Problems in Engineering*. 5th ed., John-Wiley & Sons, 1990.
- [29] J. L. Walker. *Dynamical Systems and Evolution Equations*. Plenum Press, New York, 1980.
- [30] L. Zietsman, K. A. Evans, J. T. Brown, and R. A. Idowu. Riccati conditioning and sensitivity for a minmax controlled cable-mass system. *Proceedings of IEEE Conference on Decision and Control*, pages 4007–4011, 2008.